# THE EFFECT OF THE ACCUMULATION OF HEPATITIS B VIRUS e-ANTIGEN PRECURSOR ON CELL VIABILITY

Raquel Valongo Viana

Dissertation submitted to the Faculty of Health Sciences,
University of the Witwatersrand, Johannesburg,
in fulfillment of the requirements for the degree
of
Master of Science in Medicine

Johannesburg, 2005

# DECLARATION

I, Raquel Valongo Viana declare that this dissertation is my own work. It is being submitted for the degree of Master of Science in Medicine to the University of the Witwatersrand, Johannesburg. It has not been submitted before for any degree or examination at this or any other University.

*Raquel Valongo Viana*

09th of May, 2005

# DEDICATION

I dedicate my Master's dissertation to my parents, Eduardo and Alice Viana, without whom none of this would have been possible.

# PRESENTATIONS ARISING FROM THIS STUDY

- Viana R. The effect of the accumulation of hepatitis B virus e-antigen precursor on cell viability: Faculty of Health Sciences Research Day, University of the Witwatersrand; 2004 Aug 4; Johannesburg.

- Viana R. The effect of the accumulation of hepatitis B e-antigen precursor on cell viability. The Molecular Biology of Hepatitis B Viruses. 2004 International Hepatitis B Viruses Meeting; 2004 Oct 24-27; Woods Hole (Massachusetts, USA).

# ABSTRACT

The G1862T mutation in the bulge of the RNA encapsidation signal, in the precore region of hepatitis B virus, results in reduced expression of HBeAg and accumulation of the HBeAg precursor in the endoplasmic reticulum (ER)/Golgi apparatus of the cell. This accumulation can disturb the functioning of the ER and lead to the ER stress response that can affect various cellular pathways, in turn affecting cell viability. The aim of this study was to determine whether apoptosis or necrosis occurred when cultured Huh7 cells were transfected with a plasmid expressing the G1862T mutation. Plasmid constructs, with and without the G1862T mutation, were used to transfect cells. To differentiate between necrosis and apoptosis cells were stained with propidium iodide or YO-PRO-1®, respectively. These were analyzed quantitatively using flow cytometry and qualitatively using confocal microscopy. Confocal microscopy, using monoclonal anti-HBe and the Hoechst stain, was performed to ensure that apoptosis was present as a result of the accumulation of the G1862T mutant HBeAg precursor. Caspase profiling was carried out using a fluorogenic-based assay. When cells were transfected with wild-type plasmid, necrosis predominated over apoptosis. Apoptosis predominated when the cells were transfected with the G1862T mutant plasmid. The highest levels of apoptosis occurred at 72 hours post-transfection. Confocal microscopy revealed the co-localization of aggregates of mutant HBeAg precursor with apoptotic nuclei. Transfection with G1862T mutant plasmids resulted in significant differences in the expression of caspase 3, 8, and 9 relative to the wild-type, at 48 and 72 hours post-transfection. The accumulation of the G1862T mutant HBeAg precursor, in the ER/ Golgi compartment, leads to apoptosis and affects the levels of caspase expression.

# ACKNOWLEDGEMENTS

I would like to acknowledge and thank my supervisors Prof Anna Kramvis and Prof Michael C Kew for all they have done for me.

Thank you to the University of the Witwatersrand, the National Research Foundation and Poliomyelitis Research Foundation for their financial support during this study.

Thank you to Dr Eugenius M. Senaoana for his assistance with the statistical analysis and to Chien Yu Chen for her help during the study.

# TABLE OF CONTENTS

# LIST OF ABBREVIATIONS

**AAT :** α-1-antitrypsin

**AFU:** arbitrary fluorescence unit

**ainh:** apoptotic inducer plus an apoptotic inhibitor

**AMC:** 7-amino-4-methyl coumarin

**apop:** apoptotic inducer

**ATP:** adenosine triphosphate

**Asp:** aspartate

**β-gal:** β-galactosidase

**BiP:** immunoglobulin heavy chain-binding protein

**bps:** base pairs

**BVDV:** bovine viral diarrhea virus

**CASP:** caspase

**Cat B:** Cathepsin B

**cccDNA:** covalently closed circular DNA

**CHOP:** c/EBP homologous protein

**CMV:** cytomegalovirus

**COX:** cyclooxygenase

**CSV:** constitutive secretory vesicles

**Cyto *c*:** cytochrome *c*

**DAPI:** 4',6-diamidino-2-phenylindole

**DNA:** deoxyribonucleic acid

**ds:** double-stranded

**DEVD:** aspartate-glutamate-valine-aspartate

**ε:** epsilon

**EDTA:** ethylene diamine tetra-acetic acid di-sodium salt

**EE:** early endosomes

**eGFP:** enhanced green fluorescent protein

**EOR:** the endoplasmic reticulum overload response

**ER:** endoplasmic reticulum

**ERGIC:** the Endoplasmic Reticulum-Golgi intermediate compartment

**ERp72:** endoplasmic reticulum protein 72

**ERp60:** endoplasmic reticulum protein 60

**ERSDs:** ER storage diseases

**FADD:** the Fas associated death domain

**FS:** forward scatter

**GFP:** green fluorescent protein

**GRPs:** Glucose-regulated proteins

**GRP94:** glucose related protein 94

**GRP170:** glucose related protein 170

**HBcAg:** hepatitis B virus core protein

**HBeAg:** hepatitis B virus e antigen

**HBV:** hepatitis B virus

**HCC:** hepatocellular carcinoma

**hrs:** hours

**HSP 47:** heat shock protein 47

**Huh7:** Human hepatoma cell line

**IETD:** isoleucine-glutamate-threonine-aspartate

**ISG:** immature secretory granules

**LB:** Luria Bertoni

**LE:** late endosomes

**LEHD:** leucine-glutamate-histidine-aspartate

**Lyso:** lysosomes

**MHC:** major histocompatibility complex

**MPT:** mitochondrial permeability transition

**MSG:** mature secretory granules

**MT:** mitochondria

**NFκβ:** the nuclear transcription factor-κβ

**ORFs:** open reading frames

**PBS:** phosphate buffered saline

**pgRNA:** pregenomic RNA intermediate

**PI:** propidium iodide

**PROCASP:** procaspase

**RAP:** receptor associated protein

**ROS:** reactive oxygen species

**RPMI:** Roswell Park Memorial Institute

**SRP:** signal recognition particle

**SS:** side scatter

**TE:** Tris EDTA

**TBE:** Tris-Borate-EDTA

**TGN:** *trans*-Golgi network

**TNFα:** tumour necrosis factor-α

**UPR:** the unfolded protein response

**UV:** ultra violet

**VDVAD:** valine-aspartate-valine-alanine-aspartate

**wt:** wild-type

**YOPRO:** YO-PRO®-1

# LIST OF FIGURES

# LIST OF TABLES

# 1.0 INTRODUCTION

## 1.1 THE HEPATITIS B VIRUS (HBV)

More than two billion of the world's population have been exposed to the hepatitis B virus (HBV). Of these, approximately 387 million are currently chronically infected with the virus, with a further 10 million new carriers being identified each year [WHO, 2002]. These carriers could be at high risk for developing cirrhosis and hepatocellular carcinoma (HCC). The annual mortality from HBV infection is estimated at 1 million people. South Africa is a country with intermediate HBV endemicity with pockets of high endemicity occurring in rural areas [Dusheiko *et al*, 1989a; Dusheiko *et al*, 1989b].

HBV belongs to the family *Hepadnaviridae* and has a 3.2 kb partially double stranded deoxyribonucleic acid (DNA) genome, consisting of four partly overlapping open reading frames (ORFs). The preC/C ORF encodes the core protein (HBcAg) and e antigen (HBeAg), the preS/S ORF encodes the envelope proteins, the P ORF encodes the polymerase protein, and the X ORF encodes a transcriptional *trans*-activator protein [Tiollais *et al*, 1985; Ganem *et al*, 1987].

Upon entry into the cell, the circular partially double stranded DNA is released by the virus and converted into covalently closed circular DNA (cccDNA), which serves as a template for transcription by the host enzymes. HBV replicates by reverse transcription of a 3.5kb pregenomic RNA intermediate (pgRNA). Before being reverse transcribed, the pregenome is sequestered from the cytoplasm by being packaged, together with polymerase into subviral particles composed of core protein [Nassal *et al*, 1996]. For the

pgRNA to be encapsidated, its 5' end is folded into a stem-loop structure, known as the encapsidation signal or epsilon (ε) [Junker-Niepmann *et al*, 1998]. Epsilon (ε) is transcribed from the distal precore region and proximal core gene and consists of 70 nucleotides (positions 1846-1916 from *EcoR1* site). Inverted repeat sequences form a stable bi-partite stem-loop structure containing a six-nucleotide bulge, a six-nucleotide apical loop and a single unpaired uracil residue [Kramvis and Kew, 1998]. Once replication is complete mature viral nucleocapsids may take one of two possible pathways. The one involves the formation and secretion of new virions, whereas the other leads to further amplification of the viral genome. Mature nucleocapsids eventually bud out of the endoplasmic reticulum (ER) and Golgi apparatus and exit the cell by exocytosis (Figure 1).

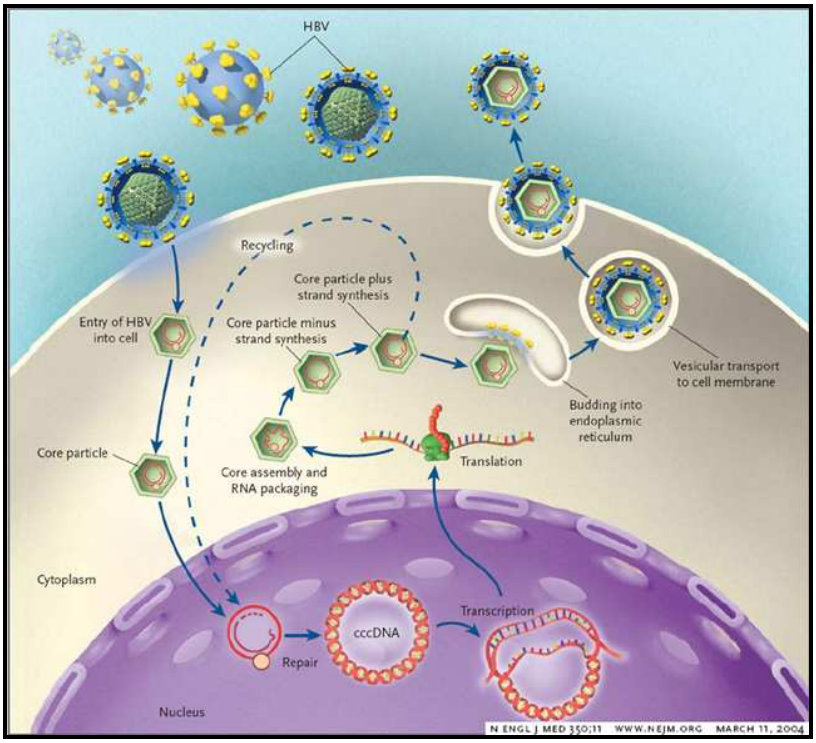


**Figure 1.** The lifecycle of HBV [Ganem *et al*, 2004]. This diagram represents the HBV lifecycle which entails viral entry into the hepatocyte, release of the circular partially double stranded DNA from the core particle into the nucleus, generation of cccDNA, formation and assembly of core particles which bud into the endoplasmic reticulum and exit the cells via vesicles.

HBV DNA encoding ε is part of the template that is translated into the precore/core fusion protein, which is in turn post-translationally modified to form HBeAg [Kramvis and Kew, 1998]. The precore/core fusion protein, the precursor of HBeAg, has a signal peptide at its amino end that targets it to the ER, where it is post-translationally modified. The first 19 amino acids of the precore region are cleaved and the remaining protein released into the lumen of the ER. Further proteolytic removal of the arginine-rich protamine-like carboxyl end results in the production of soluble HBeAg, which enters the serum [Aiba *et al*, 1997; Bruss and Gerlich, 1988; Ou *et al*, 1986].

Classically, the presence of HBeAg in the serum of HBV carriers is considered to be an indicator of active viral replication and high levels of infectivity. On the other hand, HBeAg negativity and HBeAg antibody positivity are indicators of decreased viral replication and resolution of inflammation [Hoofnagle *et al*, 1981]. An HBeAg negative phenotype, together with high viral replication, was initially observed in Europe and shown to be caused by a point mutation from guanine to alanine at nucleotide 1896, which converts codon 28 in the precore region from a tryptophan to a stop codon [Carman *et al*, 1989; Okamoto *et al*, 1990]. This mutation results in the truncation of the precore/core fusion protein, which is retained in the ER. Mature HBeAg is therefore not present in the serum.

A unique feature of southern African black carriers of the virus is that HBeAg expression is lost very early on during the course of infection [Dusheiko *et al*, 1985]. Although missense mutations are present predominantly in HBeAg-negative sera from South

African black carriers of HBV, the G1896A mutation was not found to be the reason for the HBeAg-negativity [Kramvis *et al*, 1997; Kramvis *et al*, 1998]. Genotype A of HBV predominates in South Africa and has a C at position 1858 of ε that precludes A at position 1896 [Kramvis and Kew, 1998]. However, another missense mutation, G1862T, was found in the precore region of South African black carriers. It has been detected in asymptomatic carriers and in patients with chronic active hepatitis [Carman *et al*, 1995; Horikita *et al*, 1994; Kramvis *et al*, 1997; Loriot *et al*, 1995; Santantonio *et al*, 1991; Tran *et al*, 1991], fulminant hepatitis [Hou *et al*, 2002; Laskus *et al*. 1993], cirrhosis [Valliammai *et al*, 1995] and HCC [Kramvis *et al,* 1998]. The G1862T mutation affects codon 17 and leads to the substitution of valine for phenylalanine. This change occurs near the signal peptide-cleavage site, which lies between residues 19 and 20. The presence of an aromatic residue at codon 17 of the signal peptidase recognition motif is ′forbidden′ [Bruss and Gerlich, 1988; Kramvis *et al*, 1997; von Heijne, 1984]. The removal of the first 19 amino acids of the precore/core fusion protein could therefore be prevented during its processing into HBeAg in the ER, resulting in HBeAg production being impaired [Hou *et al*, 2002; Kramvis *et al*, 1998]. This HBV variant is replication competent and therefore primer synthesis or reverse transcription are not affected by the variation in nucleotide sequence [Hou *et al*, 2002]. It is possible that the accumulation of the mutated precore/core fusion protein in the ER-Golgi compartment may be a mechanism contributing to the development of HCC by affecting apoptosis or necrosis of hepatocytes.

## 1.2 THE ENDOPLASMIC RETICULUM (ER)

All eukaryotic cells contain an ER, an inter-connected tubular membrane network continuous with the outer nuclear membrane. It is the site of synthesis of membranes and proteins that eventually form the organelles of the secretory and endocytic pathways, the plasma membrane, and the extracellular matrix. The lumen of the ER corresponds topologically to the cell exterior, and presents intracellularly, the conditions prevailing outside the cell [Rutishauser and Spiess, 2002].

### *1.2.1 PROTEIN PROCESSING*

One of the most important functions of the ER is to provide an environment to facilitate the proper folding and assembly of newly synthesized exportable proteins [Kim and Arvan, 1998]. The information necessary to target a protein to the ER is contained in its sequence [Blobel and Dobberstein, 1975]. A hydrophobic signal peptide, typically at the N-terminus, serves as an "address tag" to direct the growing polypeptide with its translating ribosome to the ER by interaction with the cytosolic signal recognition particle (SRP) and the SRP receptor in the ER membrane [Johnson and van Waes, 1999]. The nascent protein is threaded through an aqueous pore in the membrane, the translocon, formed by the heterotrimeric Sec61 complex. Co-translationally, i.e. while translocation is still ongoing, the nascent polypeptide is modified by translocon-associated proteins. The signal sequence is cleaved by signal peptidases, and N-glycans are added by oligosaccharyltransferases. Coupling of translation and translocation prevents premature protein folding and assures that the polypeptide is released directly into the exoplasmic environment with oxidizing conditions and high calcium concentration.

The ER contains mechanisms to monitor the fidelity of these early biosynthetic events in the protein export pathway. This has been called "ER quality control" [Hammond and Helenius, 1995], which involves machinery designed to try to prevent premature export of incompletely or improperly folded proteins from the ER, as well as machinery intended to initiate the removal of misfolded, incompetent proteins [Kopito, 1997]. These features of the ER have evolved to reduce potential harm posed by exportable proteins that are prone to aggregation and malfunction. Thus, ER quality control machinery is designed to differentiate normal and abnormal forms of a wide variety of exportable proteins, presumably by recognizing structural signals that are enriched in misfolded and incompletely folded molecules.

Chaperones, a family of conserved proteins found in bacteria, yeast, and higher eukaryotes, are involved in this quality control mechanism. These ER resident folding assistants associate with unfolded or misfolded substrates, preventing their aggregation and thus aiding them to achieve their native conformation, whereupon they detach [Hartl, 1996]. As long as folding is incomplete, the proteins are bound to chaperones and retained in the ER. Examples of classical ER chaperones include immunoglobulin heavy chain-binding protein (BiP), glucose related protein 94 (GRP94), endoplasmic reticulum protein 72 (ERp72), endoplasmic reticulum protein 60 (ER60), calreticulin, calnexin, glucose related protein 170 (GRP170), heat shock protein 47 (HSP 47), receptor associated protein (RAP), secretory propeptides and microsomal triglyceride transfer protein [Laboissiere *et al*, 1995; Munro and Pelham, 1986; Trombetta and Helenius, 2000]. They are expressed constitutively, but can also be induced by stress conditions

like heat shock or glucose starvation. The interaction of chaperones with newly synthesized proteins is neither specific nor exclusive, i.e. a particular chaperone interacts with a variety of different proteins, and different chaperones may bind to a nascent chain sequentially during the ongoing folding process [Rutishauser and Spiess, 2002].

The overall speed and efficiency of folding of exportable proteins is enhanced through a combination of interactions with another group of proteins resident in the ER, namely, folding catalysts. These are enzymes that also physically interact with substrate proteins, but in so doing lower the activation energy required for a discrete conformational change in an exportable protein. Catalysts that regulate folding include sugar processing enzymes, protein disulphide isomerase, peptidylprolyl isomerase, prolyl hydroxylase, lysyl hydroxylase, and glutamyl carboxylase [Kim and Arvan, 1998].

In order to cross or enter the ER membrane, newly synthesized plasma membrane proteins and secretory proteins must be in a highly unfolded state so that they can be targeted via their signal sequences and inserted into the phospholipid bilayer through a protein-conducting channel [Helenius *et al*, 1992]. After folding is accomplished, these proteins exit in transport vesicles, which bud from the ER and congregate at the ER-Golgi-intermediate compartment (ERGIC). They are delivered to the *cis*-side of the Golgi apparatus and then move, by vesicular transport or cisternal maturation, through the Golgi cisternae to the *trans*-Golgi network (TGN) [Kim and Arvan, 1998]. From here three different pathways are possible (Figure 2):

1) secretory granules of the regulated secretory pathway;

2) constitutive secretory vesicles to the cell surface;

3) vesicles to endosomes containing mannose-6-phosphate receptors and their cargo, lysosomal enzymes that have been tagged by a mannose-6-phosphate modification on N-glycans [Rutishauser and Spiess, 2002].

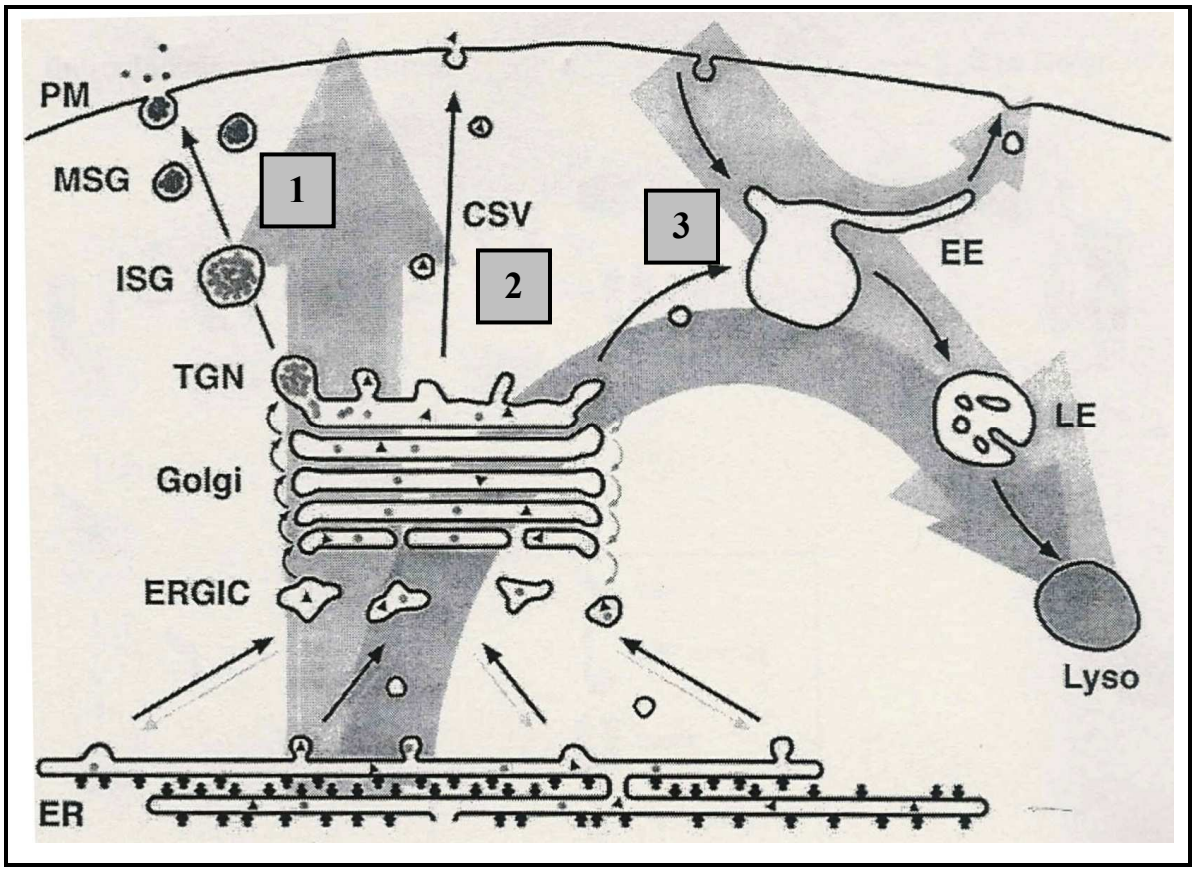


**Figure 2.** Secretory and endocytic pathways of eukaryotic cells [Kim and Arvan, 1998]. ERGIC: the ER-Golgi intermediate compartment; TGN: *trans*-Golgi network; ISG: immature secretory granules; MSG: mature secretory granules; CSV: constitutive secretory vesicles; EE: early endosomes; LE: late endosomes; Lyso: lysosomes.

Proteins that fail to fold and/or to oligomerize correctly are retained in the ER and are ultimately degraded. Degradation does not take place in the ER but in the cytosol. The protein is retro-translocated from the ER lumen to the cytosol through the same pore-forming protein complex that serves to translocate nascent chains into the ER [Pilon *et al*,

1997; Plemper and Wolf, 1999; Wiertz *et al*, 1996; Zhou and Schekman, 1999]. Interchain disulfide bonds are reduced and complexes dissociated before retro-translocation [Fagioli *et al*, 2001]. ER-associated degradation occurs using a large part of the machinery used for the degradation of cytosolic proteins [Ciechanover and Schwartz, 1998; Hershko *et al*, 2000]. First, multiple activated ubiquitin molecules are coupled to the protein substrate by specific ER-associated ubiquitin-conjugating enzymes. The polyubiquitinated protein is then hydrolyzed by the 26S proteolytic complex, a large multi-subunit structure composed of a 20S proteolytic core (proteasome) and two 19S regulator complexes. Besides mutant misfolded proteins, proteasomal substrates also include viral proteins that are processed to polypeptides for subsequent major histocompatibility complex (MHC)-associated presentation at the cell surface, and wild-type proteins that fail to fold properly because of translational or post-translational errors.

### *1.2.2 ER STRESS*

When the functions of the ER are disturbed, specific changes can occur in the cell's gene expression pattern. ER stress is defined functionally as an imbalance between the load of client proteins facing the ER and the organelle's ability to process this load [Ron, 2002]. ER stress may be caused by conditions that interfere with glycosylation or with protein folding, or by the accumulation of mutant proteins in the organelle. Overload of the ER with wild-type proteins also leads to ER stress and changes in calcium levels. A number of specific signaling pathways from the ER to the nucleus have been discovered, which help the cell to deal with ER stress, or drive it to cell death.

*1.2.2.1 The unfolded protein response (UPR)*

Glucose-regulated proteins (GRPs) are induced by glucose starvation [Lee, 2001]. The GRPs facilitate protein folding in the ER, reduce the number of misfolded proteins and thus alleviate ER stress. Because a common stimulus for the induction of GRPs is the presence of unfolded proteins in the ER [Kozutsumi *et al*, 1988], this pathway has been named the unfolded protein response (UPR). UPR can also be induced by the accumulation of correctly folded proteins, which cannot be processed.

*1.2.2.2 The ER overload response (EOR)*

This cellular response partly overlaps with, but is distinct from UPR. Certain, but not all of the conditions that evoke UPR will also trigger the endoplasmic reticulum overload response (EOR). In contrast to UPR, EOR activates the nuclear transcription factor κβ (NFκβ) [Pahl et al. 1997]. NFκβ is a mediator of inflammatory and immune responses. Target genes include those encoding β-interferon, interleukin-1 and -8, tumour necrosis factor-α (TNFα), MHC class I, or $\beta_2$-microglobulin [Pahl, 1999]. Transient expression of three unrelated viral proteins, influenza haemagglutinin [Pahl and Baeuerle, 1995], HBV middle surface protein [Meyer *et al*. 1992], and adenovirus E3/19K [Pahl *et al*, 1996], has been shown to activate NFκβ by an EOR. Because EOR can be triggered by high levels of wild-type (e.g. viral) or mutant proteins processed through or retained in the ER, it is believed that EOR has a role in a broad nonspecific antiviral host response [Pahl and Baeuerle, 1997; Pahl, 1999].

ER stress can also result in apoptosis via a number of pathways, which will be discussed in detail below.

## 1.3 CELL DEATH

### *1.3.1 APOPTOSIS VERSUS NECROSIS*

Apoptosis or programmed cell death is a genetically conserved process that maintains tissue homeostasis and is essential for both normal development and some pathological processes [Kerr *et al*, 1972]. It is a special form of cellular differentiation that leads to the orderly resorption of target cells without severe impairment of cellular metabolism [Jacobson *et al*, 1997]. Failure to negatively regulate apoptosis is connected to degenerative diseases, whereas failure to positively control apoptosis is linked to cancer and autoimmune diseases [Neuman, 2001].

Characteristic features of apoptosis include cell shrinkage and surface blebbing, degradation of various cellular proteins such as nuclear lamins and cytoskeletal components, nuclear chromatin condensation, absence of cytoplasmic membrane-bound apoptotic bodies, and phagocytosis in the final stage [Wyllie *et al*, 1984; Wyllie, 1987]. Only two independent markers are, however, used to define apoptosis. The morphological marker consists of condensation of chromatin, absence of cell membrane rupture, and cell fragmentation into small membrane-bound vesicles [Kerr *et al*, 1972; Jacobson *et al*, 1997]. The biochemical marker involves the endonuclease-activated

fragmentation of internucleosomal DNA to multiple 180 to 200 base pair fragments [Wyllie *et al*, 1980; Arends *et al*, 1990].

In tissue injury caused by viral infection apoptotic and necrotic features often coexist [Lemasters, 1999]. Necrotic cell death results from acute metabolic disruption with adenosine triphosphate (ATP) depletion, ion deregulation, mitochondrial and cellular swelling, and activation of degradative enzymes. This process culminates in the rupture of the plasma membrane and loss of intracellular proteins, metabolites and ions [Lemasters, 1999] (Figure 3).

Necrosis and apoptosis have long been viewed as morphologically and biochemically distinct forms of cell death. These, however, can occur simultaneously in tissues or cell cultures exposed to the same stimulus [Shimizu *et al*, 1996]. According to Lemasters (1999), "the term 'necrapoptosis' is used to describe the shared pathways leading to both forms of cell death. Necrapoptosis is a process that begins with a common death signal or toxic stress but that culminates in either cell lysis (necrotic cell death) or programmed cellular resorption (apoptosis), depending on other modifying factors. Pure apoptosis and pure necrosis represent extremes in the spectrum of necrapoptotic responses, but the more typical response of tissues and cells to injurious stresses and other death signals is a mixture of events associated with apoptotic and necrotic cell death" [Lemasters, 1999].

Derangements of apoptosis do occur and can have deleterious consequences, as exemplified by several human diseases including cancer, neurodegenerative disorders,

and acquired immunodeficiency syndrome [Thompson, 1995]. In the case of cancer, a neoplasm may form by an aberrant over-proliferation of cells. Conversely, a defect in the cell death machinery may promote a net increase in cell survival and thus disrupt overall homeostasis, leading to cancer.

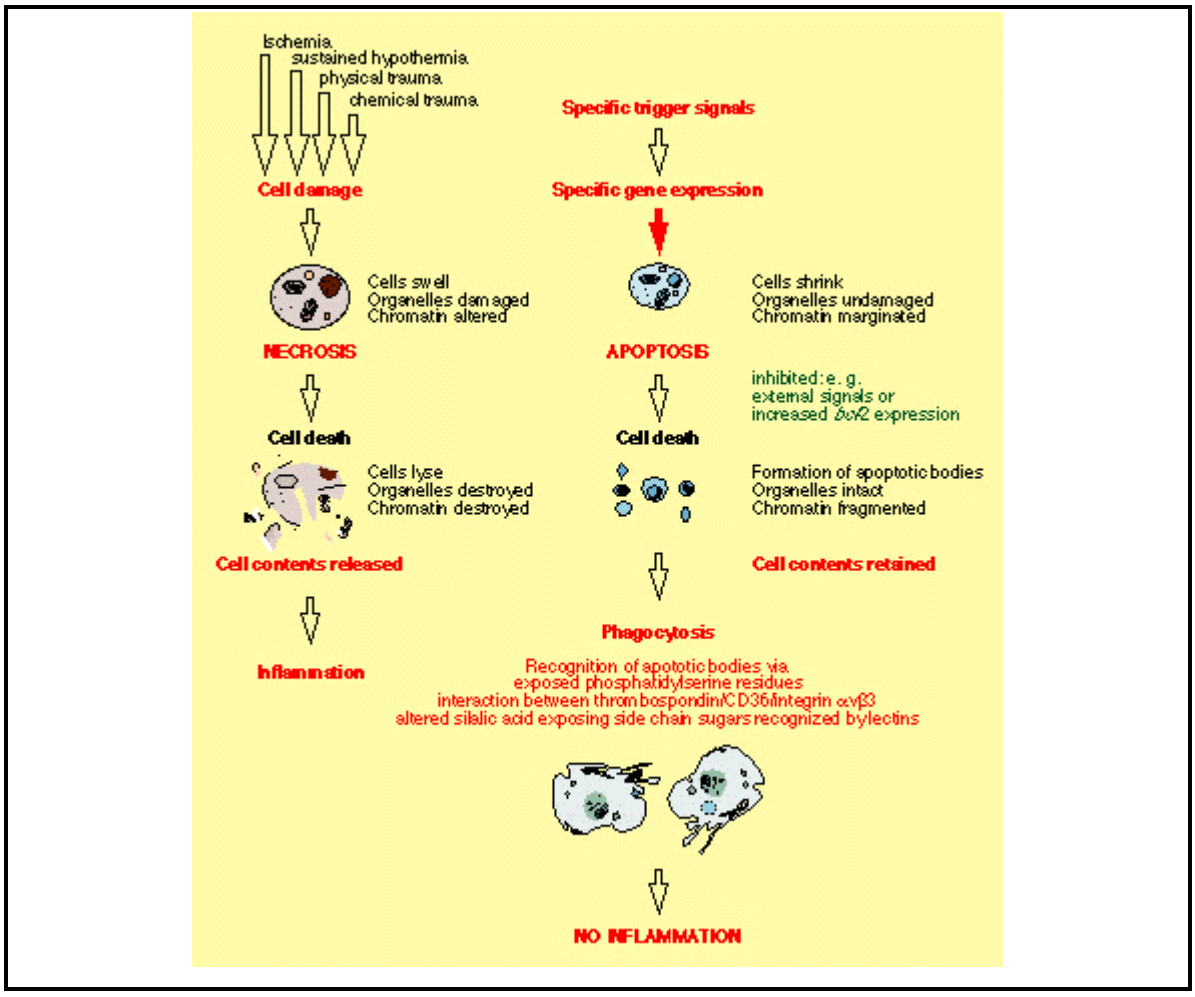


**Figure 3.** Comparison of cell death by apoptosis *versus* necrosis. (http://www.copewithcytokines.de/cope.cgi?000607) During necrotic cell death the cell contents are released and inflammation occurs. Apoptosis on the other hand results in the orderly resorption of the cell contents by other cells and therefore inflammation is averted.

The maintenance of homeostasis in organisms involves a combination of different pathways that relay specific signals from a stimulus to an effect. Information flow is mediated by specific post-translational proteolytic modifications of endogenous proteins,

mediated by a group of proteases, called caspases, present in the cytosol of all animals. These modifications alter the protein targets, directing their activities. The advantage of utilizing proteases for this purpose, rather than conventional signal transduction proteins such as protein kinases and phosphatases, is that they produce irreversible events and commit pathways unidirectionally.

### *1.3.2 CASPASES*

Caspases comprise a structurally-related group of homologous cysteine proteases belonging to the family of C14 in the Barrett and Rawlings classification [Barrett, 1997] and all cleave preferentially after aspartate (Asp) residues in a peptide substrate, a specificity that is very rare among other proteolytic enzymes. Caspases cleave a number of cellular proteins, and the process is one of limited proteolysis where a small number of cuts, usually only one, are made in interdomain regions. Sometimes cleavage results in activation of the protein, sometimes in inactivation, but never in degradation because their primary specificity for Asp distinguishes the caspases as among the most specific endopeptidases [Alnemri, 1997]. Caspases are indispensable for promoting the intracellular pathways to programmed cell death throughout the animal kingdom, and in mammals they have also adapted to activate pro-inflammatory cytokines [Thornberry, 1998].

One can recognize distinct groups of caspases from their domain structure, substrate specificity, and sequence relatedness. A useful distinction, however, between the caspases is based on their position in the cytokine activation or apoptotic signaling

pathways. Caspases 1, 2, 4, 5, and 11 are involved in cytokine activation; *initiator* caspases 2, 8, 9, 10, and 12 are responsible for the initiation of apoptotic pathways; whereas *effector* caspases 3, 6, and 7 are involved in the execution of apoptosis [Grutter, 2000]. Caspase 2 is seen both as a cytokine activator and apoptosis initiator depending on tissue type [Bergeron *et al*, 1998]. Caspase 2 expression however has not been analyzed in liver tissue or liver-derived cell lines. Thus, the placement of caspase 2 remains controversial, and the exact function, mode of activation, and regulation of caspase 2 remain unknown. Caspase 2 is therefore seen as both a cytokine activator and apoptosis initiator.

Several distinct triggers participate in the activation of effector caspases by first activating initiator caspases. Thus, a hierarchical relation is postulated to exist between the initiators and the effectors, with the former containing large N-terminal extensions necessary for the initiation phase. The effectors activate pro-apoptotic factors and cleave key proteins required for the maintenance of homeostasis, leading to apoptotic collapse and demise of the cell [Nicholson and Thornberry, 1997]. There are a number of caspase signaling pathways that are linked by mitochondrial permeability transition (MPT).

### *1.3.3 MITOCHONDRIAL PERMEABILITY TRANSITION (MPT)*

MPT is a pathophysiological mechanism shared by both necrosis and apoptosis. Signature changes of MPT include mitochondrial depolarization, uncoupling of oxidative phosphorylation, and mitochondrial swelling [Zoratti and Szabo, 1995]. Factors that promote MPT include $Ca^{2+}$, inorganic phosphate, reactive oxygen species (ROS), a

variety of oxidant chemicals, Bax, membrane depolarization, and cross linking of thiols in the pore complex, which increases pore conductance [Bernardi, 1992; Constantini *et al*, 1996; Gunter and Pfeiffer, 1990]. Factors that block the onset of the MPT consist of $Mg^{2+}$ (pH below 7), a variety of phospholipase inhibitors, immunosuppressive cyclic endecapeptide, and cyclosporin A [Lemasters, 1999].

The onset of MPT induces mitochondrial swelling, leading to outer mitochondrial membrane rupture resulting in the release of soluble mitochondrial factors, such as apoptosis inducing factor and cytochrome *c*, which activate caspases and initiate apoptotic nuclear changes. The commencement of MPT precedes and is required for caspase 3 activation, cytochrome *c* release and nuclear condensation [Bradham *et al*, 1998]. Progression to apoptosis or necrosis after MPT depends on the presence or absence of ATP, respectively [Eguchi *et al*, 1997; Leist *et al*, 1997; Nieminen *et al*, 1994]. When the onset of MPT is rapid and cellular ATP levels drop dramatically, necrosis ensues. If progression of the MPT is slower, or if other sources of ATP generation are available, then profound ATP depletion is avoided, allowing apoptotic signaling to proceed (Figure 4). Later, if ATP levels finally decrease, secondary necrosis occurs [Leist *et al*, 1997; Lemasters, 1999].

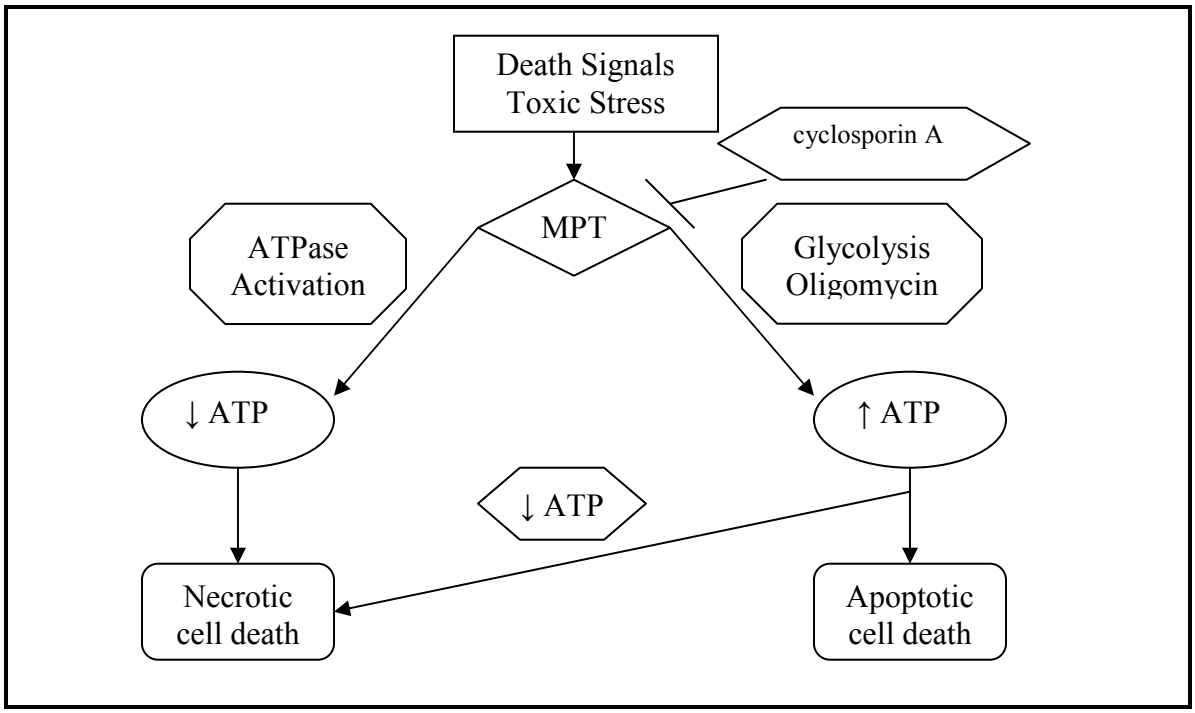


**Figure 4.** Role of MPT and ATP in necrosis and apoptosis [Lemasters, 1999].
Necrotic cell death takes place with the depletion of ATP by the MPT. When the MPT occurs without severe ATP depletion apoptosis develops instead. If ATP depletion develops during the progression of apoptosis, necrotic cell death will intervene to produce secondary necrosis.

### *1.3.4 APOPTOTIC PATHWAYS*

Apoptosis can be induced by a number of pathways, which interact to amplify weak apoptotic signals and to shorten cellular execution time. The most important and relevant pathways include ligand-dependent death receptor oligomerization, mediated by TNFα and Fas, and stress mediated events involving the ER. MPT is important in both ligand- and ER stress-induced apoptosis. Hepatocyte apoptosis induced by death domain ligands, such as TNFα and Fas, have been implicated in viral hepatitis and HCC [Galle and Krammer, 1998; Gonzales-Amaro *et al*, 1994].

*1.3.4.1* *Ligand-induced apoptosis*

TNFα is a pleiotropic cytokine that can signal for proliferation, stress, inflammation and cell death [Wallach *et al*, 1997]. TNFα and Fas recruit similar pathways including the Fas associated death domain (FADD), the activation of caspase 3 and caspase 8, MPT and cytochrome *c* release. The Fas signaling pathway for apoptosis however is more rapid [Clement and Stamenkovic, 1994; Hatano *et al*, 2000]. MPT is an essential component in the signaling pathway for TNFα-induced apoptosis [Lemasters, 1999] (Figure 5) whereas in Fas-mediated apoptosis, it accelerates apoptosis but is not obligatory for it to occur [Hatano *et al*, 2000].

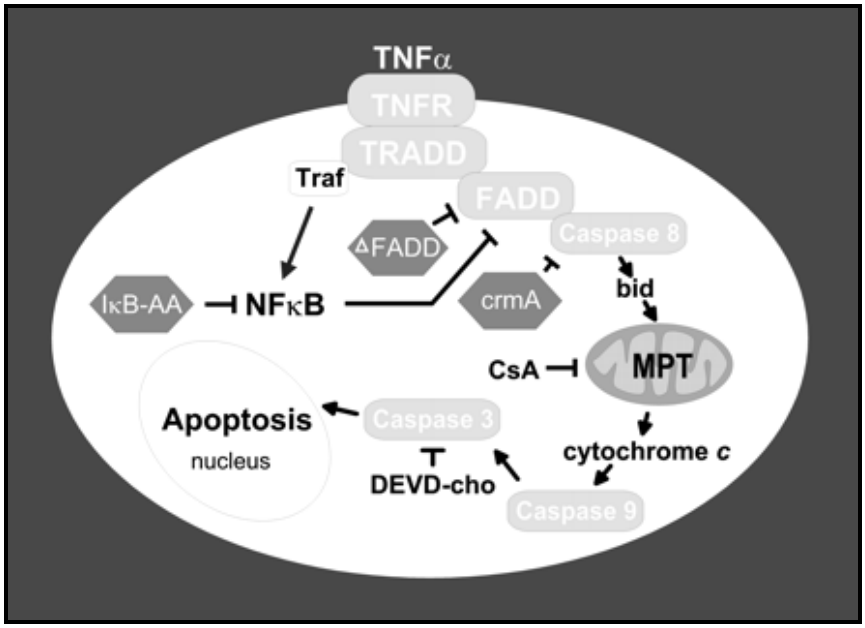


**Figure 5.** Scheme of the molecular events in tumor necrosis factor-α (TNFα)-induced apoptosis [Lemasters, 1999]. TNFα binding to its receptor (TNFR) activates caspase 8 via the adapter proteins, TRADD and FADD. Bid is cleaved and translocated to the mitochondria. Onset of the MPT leads to cytochrome *c* release followed by a cascade of caspase 9 and caspase 3 activation, resulting in apoptosis. Signaling through another adapter protein, Traf, activates the nuclear transcription factor, NFκB, which leads to antiapoptotic gene expression acting upstream of mitochondria. Expression of an IκB super-repressor, IκB-AA, inhibits the activation of NFκB and is permissive for TNFα-induced apoptosis. Expression of ΔFADD, a truncated FADD, blocks apoptotic signaling upstream of the MPT. Expression of crmA inhibits the upstream caspase 8 and blocks the MPT after TNFα addition, whereas inhibition of downstream caspase 3 with DEVD-cho prevents apoptosis but not the onset of the MPT.

Two distinct pathways for Fas-mediated apoptosis exist in different cell types. Type I cells demonstrate caspase 3 and caspase 8 activation independent of MPT and Bcl2. Type II cells, such as hepatocytes, demonstrate relatively late activation of caspase 3 and caspase 8, which is dependent on MPT and Bcl2 [Scaffidi *et al*, 1998]. Bcl2 maintains mitochondrial polarization by enhancing proton efflux in the presence of uncouplers [Shimizu *et al*, 1998]. Bcl-$_{XL}$, an antiapoptotic Bcl2 family member, regulates mitochondrial volume homeostasis, preventing the swelling associated with MPT [Vander Heiden, 1997]. Overexpression of Bcl2 or Bcl-$_{XL}$ blocks caspase 3 and caspase 8 activation, as well as Fas- and TNFα- mediated apoptosis [Hatano *et al*, 2000] (Figure 6).

Both TNFα and Fas activate NF-κβ in primary hepatocytes, which in turn inhibits apoptosis [Hatano *et al*, 2000; Xu *et al*, 1998]. This is achieved through the prevention of MPT and its interference with the activation of upstream caspases through transcription of a caspase inhibitor [Bradham *et al*, 1998]. Distal caspases, however can inhibit NF-κβ and amplify MPT to promote apoptosis.

TNFα may trigger apoptosis through another pathway involving acidic vesicles and activation of acid sphingomyelinase enzyme, which generates ceramides and other lipid secondary messengers such as glycosphingolipids [Kronke, 1999]. Ceramides interact with isolated mitochondria, impairing mitochondrial respiration and stimulating ROS formation and onset of MPT [Garcia-Ruiz *et al*, 1997]. Disialoganglioside GD3, a

glycospingolipid, interacts with the mitochondria *in vitro* leading to MPT, cytochrome *c* release, and caspase activation [Garcia-Ruiz *et al*, 2000].

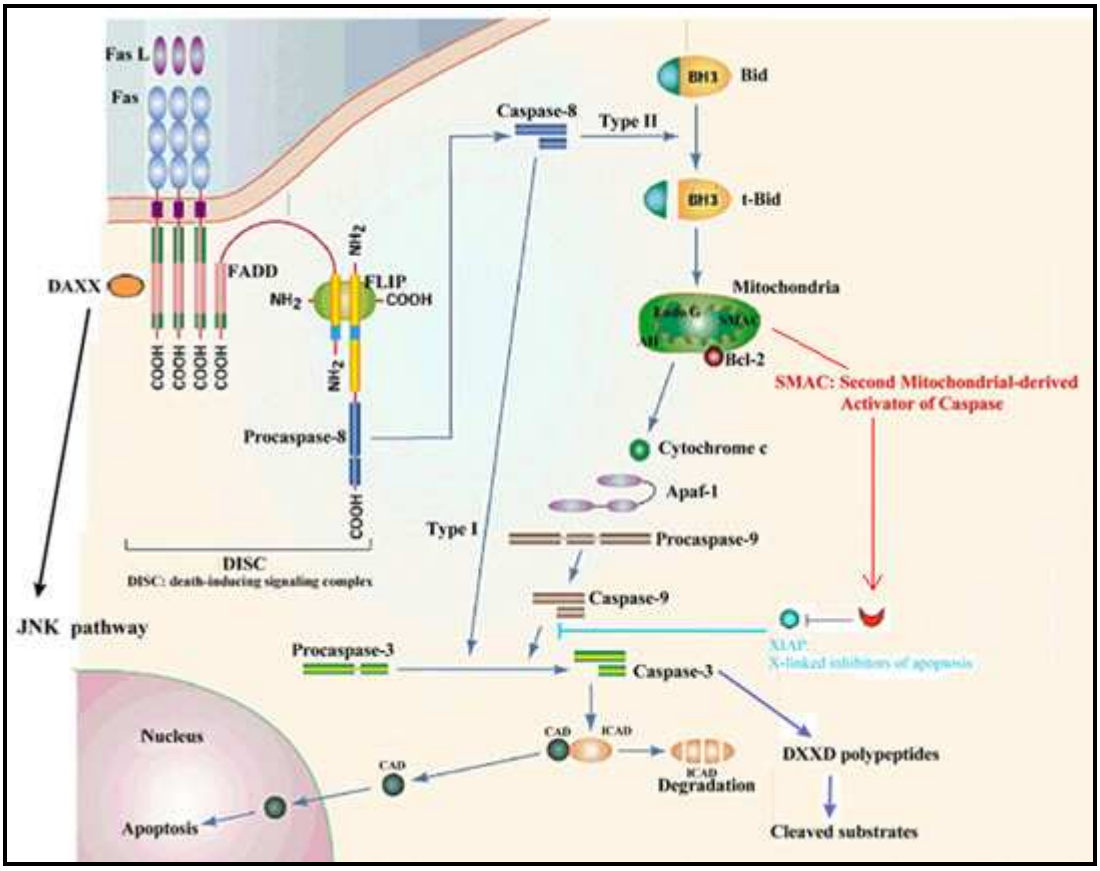


**Figure 6.** Fas pathways for Type I and II cells.
(http://www.infobiogen.fr/services/chromcancer/Deep/Fas-FasLigandID20039.html)
Following Fas-FasL ligation a complex of proteins associate with activated Fas. This death-inducing signaling complex (DISC) forms when the adaptor FADD recruits procaspase 8 which is then activated proteolytically and released from the DISC into the cytoplasm. Fas-mediated apoptosis in type I cells (lymphoid cells) is initiated by large amounts of caspase 8 followed by direct cleavage of procaspase 3. Activated caspase 3 then cleaves a variety of substrates leading to apoptosis. In contrast, in type II cells (hepatocytes) very little DISC and small amounts of caspase 8 are formed. The caspase cascade has to therefore be amplified by activating the apoptosome, the second initiator complex of apoptosis. Caspase 8 cleaves Bid and the truncated form inserts into the mitochondria resulting in the release of pro-apoptotic molecules such as cytochrome *c* and smac. Apoptosis protease-activating factor (Apaf-1) and procaspase 9 then combine with cytochrome *c* to form the apoptosome activating caspase 9, which in turn activates further downstream procaspase 3. Fas may also engage the JNK pathway via Death Domain associated protein (Daxx)-mediated activation.

Cathepsin B (Cat B), a lysosomal cysteine protease is another candidate for apoptosis via the acidic compartment [Guicciardi *et al*, 2000]. Cat B is synthesized as a proenzyme and transported into lysosomes, where it is processed and activated either by lysosomal proteases or by autoactivation [Mach *et al*. 1992]. Active caspase 2 or caspase 8 are then capable of causing the release of Cat B from purified lysosomes. Cat B is found upstream of the mitochondria in the Type II Fas pathway, as well as in this lysosomal pathway [Guicciardi *et al*, 2000] (Figure 7).

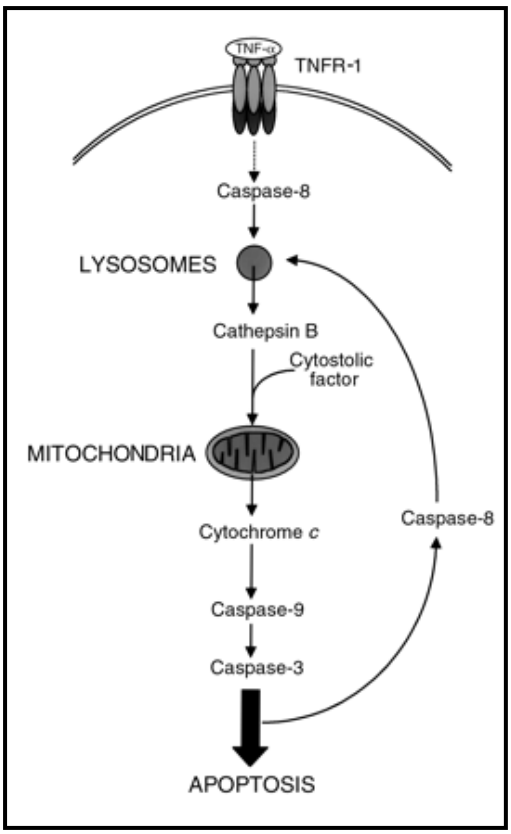


**Figure 7.** Model of TNFα signaling pathway through acidic compartment [Guicciardi *et al*, 2000]. Triggering of TNFR-1 leads to activation of a small amount of caspase 8 which is sufficient to induce the release of Cat B from the lysosomes. Active Cat B in turn promotes the release of cytochrome *c* from mitochondria by cleaving one or more still unidentified cytosolic substrates. Release of cytochrome *c* results in cleavage of caspase 9 and 3 followed by apoptosis. An amplification loop generates more caspase 8, inducing further release of Cat B from lysosomes.

*1.3.4.2 ER stress- induced apoptosis*

Apoptosis induced by ER stress can occur in a number of ways:

a) ER stress induces the nuclear transcription factor called c/EBP homologous protein (CHOP), which has been implicated in programmed cell death in response to impaired function of the ER [Wang *et al*, 1998; Zinszner *et al*, 1998].

b) Caspase 12, an ER stress response caspase, is localized in the ER membrane and is essential for this ER stress-induced apoptosis. The expression of caspase 12 can be induced by ER stress caused by the accumulation of excess proteins in the ER. ER stress also leads to translocation of cytosolic caspase 7 to the ER surface. Caspase 7 activates caspase 12, which then results in cell death [Rao *et al*, 2001].

c) The ER and mitochondria, either in parallel or in cooperation, control a number of electrochemical events that may be linked to the induction of apoptosis and come under the control of Bcl2 proteins such as Bax. Although the potential role of $Ca^{2+}$ in apoptosis remains unresolved, the ability of mitochondria to decode ER-transmitted oscillating $Ca^{2+}$ signals is one example in which the two organelles clearly cooperate to regulate metabolic events [Lam *et al*, 1994] (Figure 8).

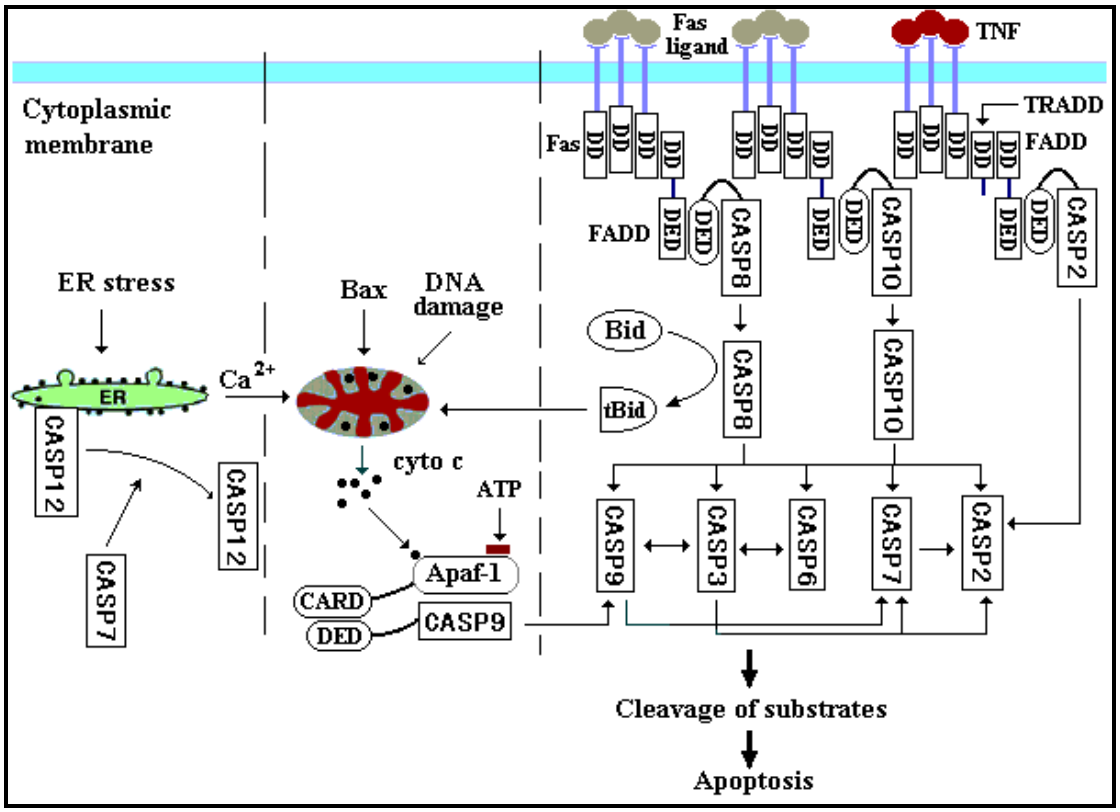


**Figure 8.** ER stress-induced apoptotic pathways (http://www.cmj.org/2wl/yuanchangqing2.htm). ER stress can directly affect the ER leading to the recruitment of caspase 7 and the translocation of caspase 12 from the ER membrane to the cytoplasm, where caspase 7 cleaves procaspase 12 into active caspase 12. ER stress also causes an imbalance in calcium ions leading to the activation of the MPT and release of cytochrome *c*. Cytochrome *c* in turn forms the apoptosome in combination with Apaf-1 and caspase 9 which results in a caspase cascade leading to cleavage of specific substrates and apoptosis. The previously discussed Fas and TNFα pathways also contribute to apoptosis.

## 1.4 RATIONALE OF THE STUDY

The G1862T mutation, which causes a valine to phenylalanine substitution in codon 17 of the precore/core open reading frame, occurs in 29% of HBV isolates from Southern African HCC patients [Kramvis *et al*, 1998]. Work carried out in our research unit has shown that this mutation interferes with the post-translational modification of the precore/core fusion protein and this can result in the retention of the mutant HBeAg in the ER and the impairment of the secretion of the mature HBeAg (Chien Yu Chen, personal communication). This could lead to ER stress resulting in necrosis or apoptosis [Rutishauser and Spiess, 2002].

The aim of the study was to determine whether apoptosis or necrosis occurs as a result of the accumulation of the mutant HBeAg in the ER and to investigate whether this accumulation affects caspase 2, 3, 8 and 9 expression levels.

# 2.0 MATERIALS AND METHODS

Figure 9 provides an overview of the methods used in the study.

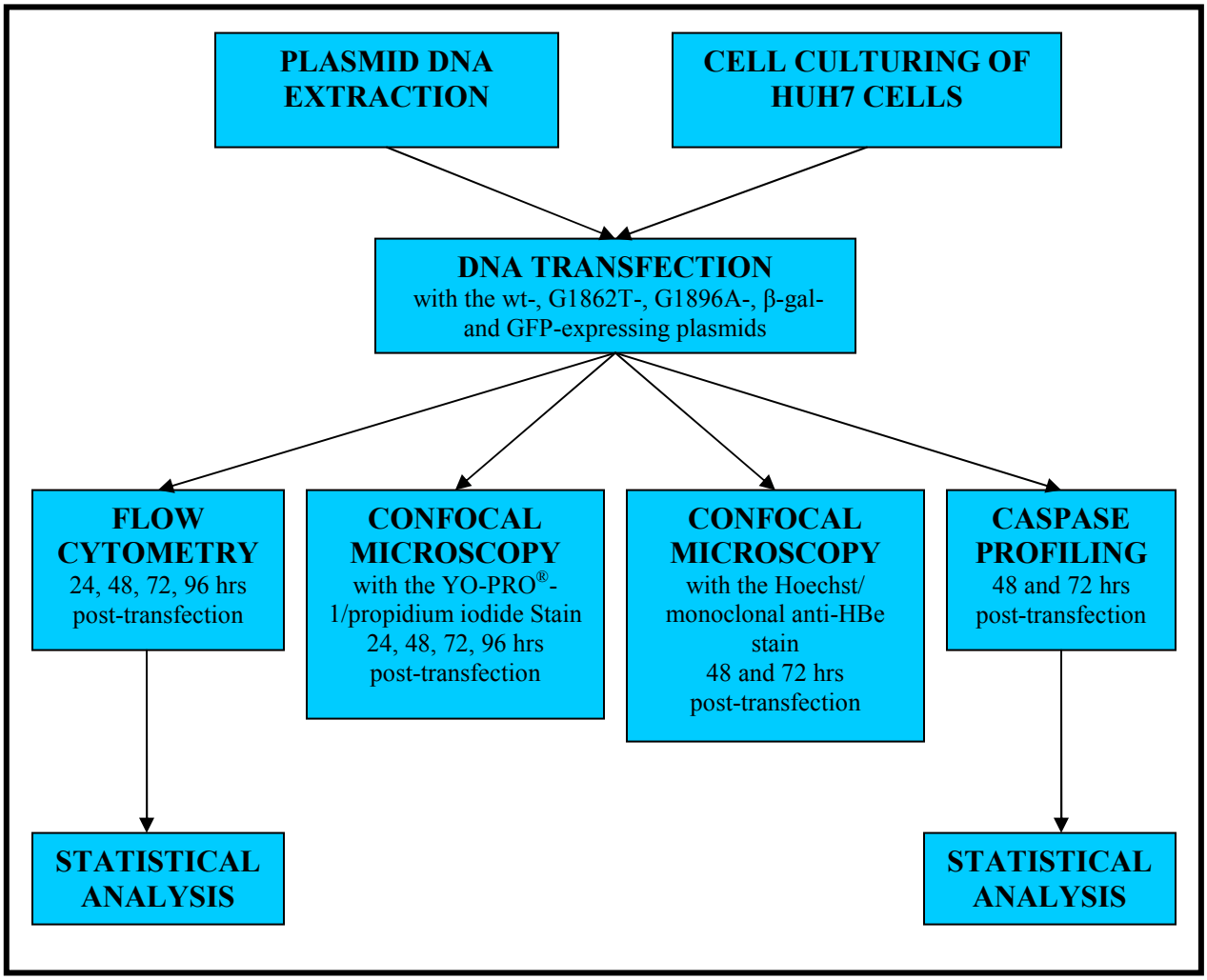


**Figure 9**. Flow diagram of methods utilized in the study.
Huh7: Human hepatoma cell line, wt: wild-type, β-gal: β-galactosidase, GFP: green fluorescent protein, hrs: hours.

## 2.1 PLASMIDS

Plasmids used for transfections include the pCRa-wild-type (wt), pCRa-1862T (G1862T) and pCRa-1896A (G1896A) all 5720 base pairs (bps) in size constructed and provided by Chien Yu Chen (Molecular Hepatology Research Unit, University of the Witwatersrand), as well as pWay21-eGFP (green fluorescent protein: GFP) 5814 bps and pMC1871 (β-galactosidase: β-gal) 7476 bps, both kindly provided by Dr Thomas Hughes (Montana State University). The wt plasmid contains the HBV wild-type precore/core gene insert. The G1862T and G1896A plasmids contain the same insert but possess a guanine to thymine and a guanine to alanine transversion at the relevant positions, respectively. The GFP plasmid contains the full enhanced green fluorescent protein (eGFP) gene while the β-gal plasmid contains the full β-galactosidase gene. All plasmids possess cytomegalovirus (CMV) promoters. The wt plasmid was the HBeAg-expressing control and the G1896A plasmid was the HBeAg- negative control. The β-gal plasmid was used to ensure that the changes observed were not as a result of the transfection itself. The GFP plasmid was used to verify that transfection efficiency was 70-75%, throughout all experiments.

In order to establish a primary culture of transformed bacteria, 5 ml Luria Bertoni (LB) broth (Appendix A1), supplemented with the appropriate antibiotic (10 mg/ml) to prevent contamination (Table 1), was inoculated by adding 50 µl of glycerol stocks of the bacterial cells containing the plasmids. This culture was incubated overnight at 37$^{o}$C in the Orbital Shaker Incubator LM-510 (YIH DER, Germany) at 150 rpm. The secondary culture was established by adding 1ml of the primary culture to 200 ml of LB broth

supplemented with the appropriate antibiotic (Table 1). This secondary culture was incubated overnight at 37$^{o}$C in the Orbital Shaker Incubator LM-510 (YIH DER, Germany) at 150 rpm. Plasmid DNA was extracted using the Endofree™ Plasmid Maxi Kit (Qiagen, USA) according to manufacturer's instructions and eluted into 400 µl Tris EDTA (TE) buffer, provided in the kit.

**Table 1**. Antibiotic and volume used for the growth of the various plasmids

| Plasmid | Antibiotic 10mg/ml | Volume used in the 5ml of 1$^{o}$ culture | Volume used in the 200ml of 2$^{o}$ culture |
|---|---|---|---|
| pCRa-wild-type | Kanamycin | 40 µl | 150 µl |
| pCRa-1862T | Kanamycin | 40 µl | 150 µl |
| pCRa-1896A | Kanamycin | 40 µl | 150 µl |
| pMC1871(β-gal) | Tetracycline | 25 µl | 500 µl |
| pWay21-eGFP | Ampicillin | 25 µl | 500 µl |

The extracted plasmid DNA was prepared for direct sequencing using the BigDye Terminator v3.0 Cycle Sequencing Ready Reaction Kit (Applied Biosystems, Foster City, USA), a pCR-vector-specific primer 5'-TAATACGACTCACTATAGGG-3' which binds at position 638-657 of the pCR-vector, and sequenced on a Spectrumedrix SCE2410 genetic analysis system with 24 capillaries (SpectruMedrix LLC in Pennsylvania, USA) to confirm the correct sequence. A 1:25 dilution of plasmid DNA was used to determine DNA concentration by measuring absorbance at 260nm on a GeneQuant Spectrophotometer (Amersham Pharmacia Biotech, USA) (Figure 10).

3 µg of DNA was diluted with 5 µl of 10X gel loading dye (Appendix A2) and electrophoresed on a 0.8% agarose gel in 1X Tris-Borate-EDTA (TBE) buffer (Appendix A3, A4) at 70 milliamps for 2 hours to evaluate DNA integrity and purity. The plasmid DNA was stored at 4°C until used.

$1_{A260}$U of dsDNA = 50 µg/µl

therefore

$$\text{dsDNA concentration (µg/µl)} = \frac{\text{A260 X dilution factor X 50 µg/µl}}{1000}$$

DNA yield (µg) = DNA concentration (µg/µl) X Volume of TE buffer for resuspension

**Figure 10**. Formulae used to determine DNA concentration. [ds: double-stranded.]

## 2.2 CELL CULTURE

Huh7 cells were maintained in supplemented Roswell Park Memorial Institute (RPMI) medium (Appendix A5) with 10% fetal calf serum (Gibco, UK). Every 2 or 3 days, when the 75 $cm^2$ flasks (Corning, USA) of cells were confluent, they were passaged. The conditioned medium was removed and filtered through a 0.2 µm minifilter (Sartorius MiniSart®, Germany) to remove cellular debris. The flask of cells was rinsed with 10 ml of phosphate buffered saline (PBS) (Gibco Invitrogen Corporation, UK), before 5 ml of 1X ethylene diamine tetra-acetic acid di-sodium salt (EDTA)/PBS solution (Appendix A6) was added and the flask incubated at 37°C for 10 minutes to detach the cells. The EDTA/PBS solution containing the detached cells was centrifuged at 300g on the Minor centrifuge (MSE, Germany) for 2 minutes and the supernatant discarded. The cell pellet was resuspended in 15 ml fresh medium, 5 ml of the filtered conditioned medium and 2

ml fetal calf serum. The cells were incubated at 37°C under an atmosphere of 95% air and 5% $CO_2$ for another 2 to 3 days or until confluent.

## 2.3 DNA TRANSFECTION

Huh7 cells were seeded 20 hours prior to transfection into either 60 mm plates (Corning, USA) for flow cytometry and caspase profiling or 8-well LAB-TEK® II chamber slides (Nalge Nunc International, USA) for confocal microscopy. Plates or wells with ± 70% confluency were transfected with the desired plasmid by cationic lipid-mediated transfection (Table 2).

**Table 2**: Volume of transfection reagents required for the two types of culture vessels

| Culture Vessel | Amount of DNA used | Volume of Opti-MEM I used | Volume of lipofectamine used |
|---|---|---|---|
| 60 mm plate | 30 µg | 500 µl (X2) | 5 µl |
| Well | 3 µg | 50 µl (X2) | 0.5 µl |

In order to homogenize the DNA, the appropriate volume of DNA was added to opti-MEM I dilution medium (Gibco, UK) to obtain the correct molecular weight (Table 2). In a separate tube, lipofectamine™ 2000 (Invitrogen, USA) was added to the second aliquot of opti-MEM I and left to stand at room temperature for 5 minutes. The contents of the two tubes were then combined and incubated at room temperature for 20 minutes with intermittent tapping of the tube to allow the DNA to be taken up by the lipids. The final mixture was split between two plates or wells so that each plasmid was transfected in duplicate. The cells were then incubated for 24, 48, 72 or 96 hours. Transfection efficiency was determined at each time interval by counting the number of GFP-

expressing cells after transfection with the GFP plasmid, with the Axiovert 25 microscope (CarlZeiss, USA).

## 2.4 FLOW CYTOMETRY

The conditioned culture medium was removed and retained. Cells were harvested 24, 48, 72 and 96 hours post-transfection using 3 ml 1X EDTA/PBS (Appendix A6). Cells were added to the retained conditioned medium, incubated for 10 minutes at 37$^{o}$C with 5% $CO_2$, and then centrifuged at 300g for 2 minutes. The supernatant was discarded and the cell pellet resuspended in 1 ml of fresh RPMI medium (Appendix A5).

The Vybrant™ Apoptosis Assay Kit #4 (Molecular Probes, USA) was used to quantitate the percentage of live, apoptotic and necrotic cells present in the various transfected cell groups. The green fluorescent YO-PRO®-1 dye was added to stain apoptotic cells while the red fluorescent propidium iodide dye was used to stain necrotic cells. 1 µl of each dye was added to each tube and the cells placed on ice for 30 minutes in the dark to allow for the dye uptake into the cells. Analysis was carried out by the EPICS® XL-MCL Flow Cytometer (Coulter, UK) using 488 nm excitation and measuring the fluorescence emission at 530 nm (FL1) and >575 nm (FL3) according to the parameters shown in Appendix B. Each experiment was carried out in triplicate.

A control for necrosis was prepared by placing a confluent 60 mm plate of Huh7 cells under an ultra violet (UV) 6 X 8 W, 312 nm tube, 96 W lamp (Syngene BTS-20M, Synoptics Ltd.) for one hour before staining and analyzing the cells. To generate an

apoptotic control the Apoptosis Inducer Set (Calbiochem, USA) was used. In order to determine the agent that produced the "optimal" level of apoptosis of Huh7 cells, various apoptotic inducers were tested at varying concentrations. The set included actinomycin D (10 mM), camptothecin (2 mM), cycloheximide (100 mM), dexamethasone (10 mM) and etopiside (100 mM). Actinomycin D is an anti-neoplastic antibiotic and inhibits RNA synthesis. Camptothecin and etoposide are inhibitors of nuclear topoisomerase. Cycloheximide is an active antibiotic against many yeast and fungi and inhibits protein synthesis. Dexamethasone is an active and highly stable glucocorticoid, which probably induces apoptosis by binding and activating the intracellular glucocorticoid receptor. After 24 and 48 hours the cells were harvested, stained and analyzed. The apoptosis inducer that produced the highest percentage of Huh7 apoptotic cells was used as the apoptotic control in subsequent experiments.

## 2.5 CONFOCAL MICROSCOPY

### *2.5.1 YO-PRO®-1/PROPIDIUM IODIDE STAIN*

Cells were analyzed using confocal microscopy 24, 48, 72 and 96 hours post-transfection to confirm the flow cytometry results. For each slide 1.2 µl of YO-PRO®-1 dye and 0.6 µl of propidium iodide dye was mixed with 1 ml of RPMI medium (Appendix A5), 125 µl of this mixture was added to each chamber of the slide. The slide was then placed on ice for 30 minutes in the dark. The slide was washed with PBS (Appendix A8) three times at room temperature allowing one minute per wash. FluoroSave anti-fading mounting media (Calbiochem, USA) was spread throughout the slide with a cover slip

and allowed to set for 20 minutes. The slides were analyzed immediately with the Axiovert 100M confocal microscope (Zeiss, Germany) using filters for fluorescein (FITC) (green YO-PRO®-1 fluorescence) and rhodamine (TRITC) (red propidium iodide fluorescence).

### *2.5.2 HOECHST/MONOCLONAL ANTI-HBe STAIN*

The Hoechst/monoclonal anti-HBe confocal stain was used to determine whether the mutant HBeAg co-localized with apoptotic nuclei. Cells were fixed 48 and 72 hours post-transfection with 4% paraformaldehyde/PBS (Appendix A7) for 10 minutes at room temperature. The slide was washed 3 times with PBS (Appendix A8) with gentle shaking for 5 minutes per wash. Triton X100/PBS (0.02% v/v) (Roche, Germany) (Appendix A9) was used to permeabilise the cells for 10 minutes at room temperature. The slide was washed again 3 times with PBS (Appendix A8) with gentle shaking for 5 minutes per wash. The cells were blocked using bovine serum albumin/PBS (1% w/v) (Roche, USA) (Appendix A10) for 1 hour at room temperature with gentle shaking. 150 µl of the primary antibody, mouse monoclonal e-antigen antibody (US Biological, USA) (Appendix A11), was added to the corners of each slide, spread throughout the slide and incubated overnight at 4$^{o}$C in a humid atmosphere. The slide was then washed in PBS three times with gentle shaking allowing 10 minutes per wash. 150 µl of the secondary antibody, Alexa Fluor 488 goat anti-mouse IgG (H+L) (Molecular Probes, USA) (Appendix A12),was added to the corners of each slide, spread with a cover slip and incubated for 1 hour at room temperature, in a dark and humid environment. The slide was then washed four times with PBS with gentle shaking for 10 minutes per wash. The

slide was counterstained with 5 µl of 10 ng/ml Hoechst 33258 (Molecular Probes, USA) and incubated in the dark at room temperature for 2 minutes to stain the nuclei of cells. The slide was washed three times in the dark with PBS and gentle shaking, allowing 5 minutes per wash. Once the excess PBS was shaken off, FluoroSave anti-fade mounting media (Calbiochem, USA) was added, spread with a cover slip and allowed to set for one hour in the dark. The ends of the slide were then sealed with Entellan (Merck, Germany) and analyzed on the Axiovert 100M confocal microscope (Zeiss, Germany) using filters for fluorescein (FITC) (green Alexa Flour fluorescence) and 4',6-diamidino-2-phenylindole (DAPI) (blue Hoechst 33258 fluorescence).

## 2.6 CASPASE PROFILING

The BD ApoAlert™ Caspase Assay Plate (BD Biosciences, USA) was used to quantitate the amount of caspase 3, 8, 9, and 2 in the cells and was carried out as per the manufacturer's instructions. Caspase 2 is a cytokine activator and apoptosis initiator that was not one of the targets of the study but was analyzed because it was included in the assay. Caspase 8 and 9 are initiator caspases while caspase 3 is an effector caspase, of apoptosis. The assay contains the fluorogenic substrates specific for different caspases immobilized in the wells of a 96-well Falcon plate (Figure 11).

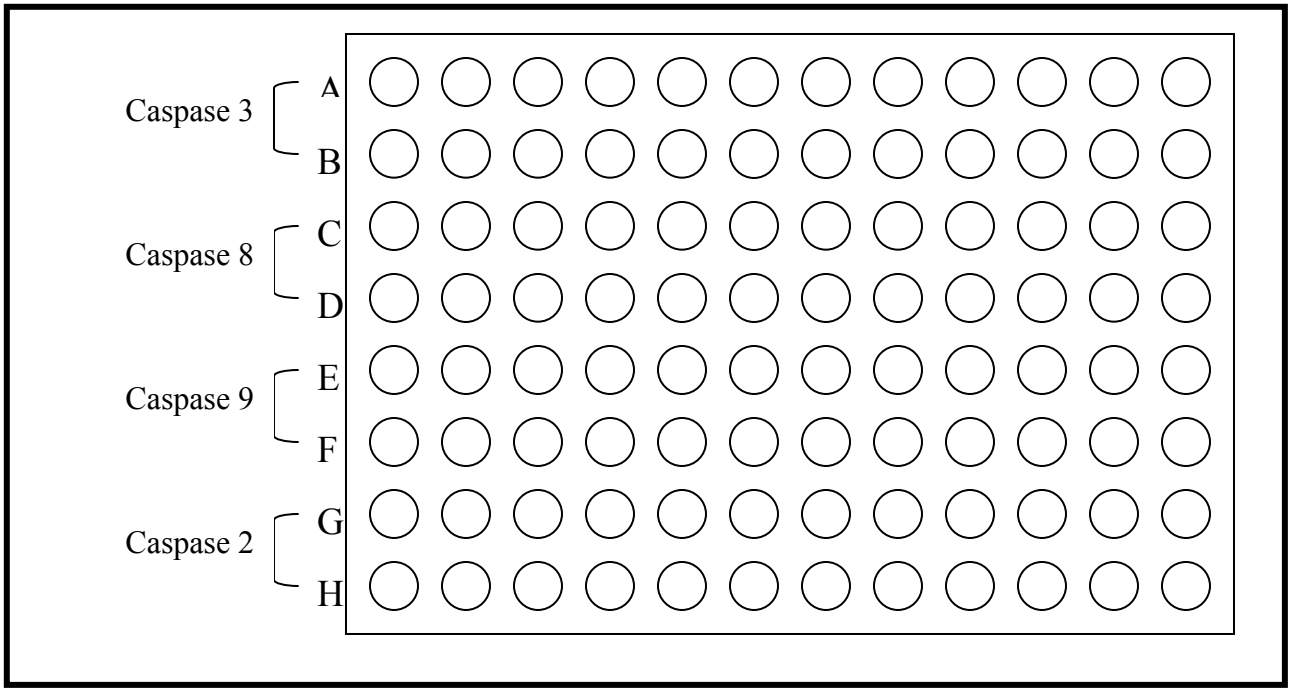


**Figure 11**. Diagram of the caspase profiling plate layout.

When the cell lysate containing the active caspase is applied to the wells, the caspase cleaves its substrate and a fluorescent product is released (Figure 12).

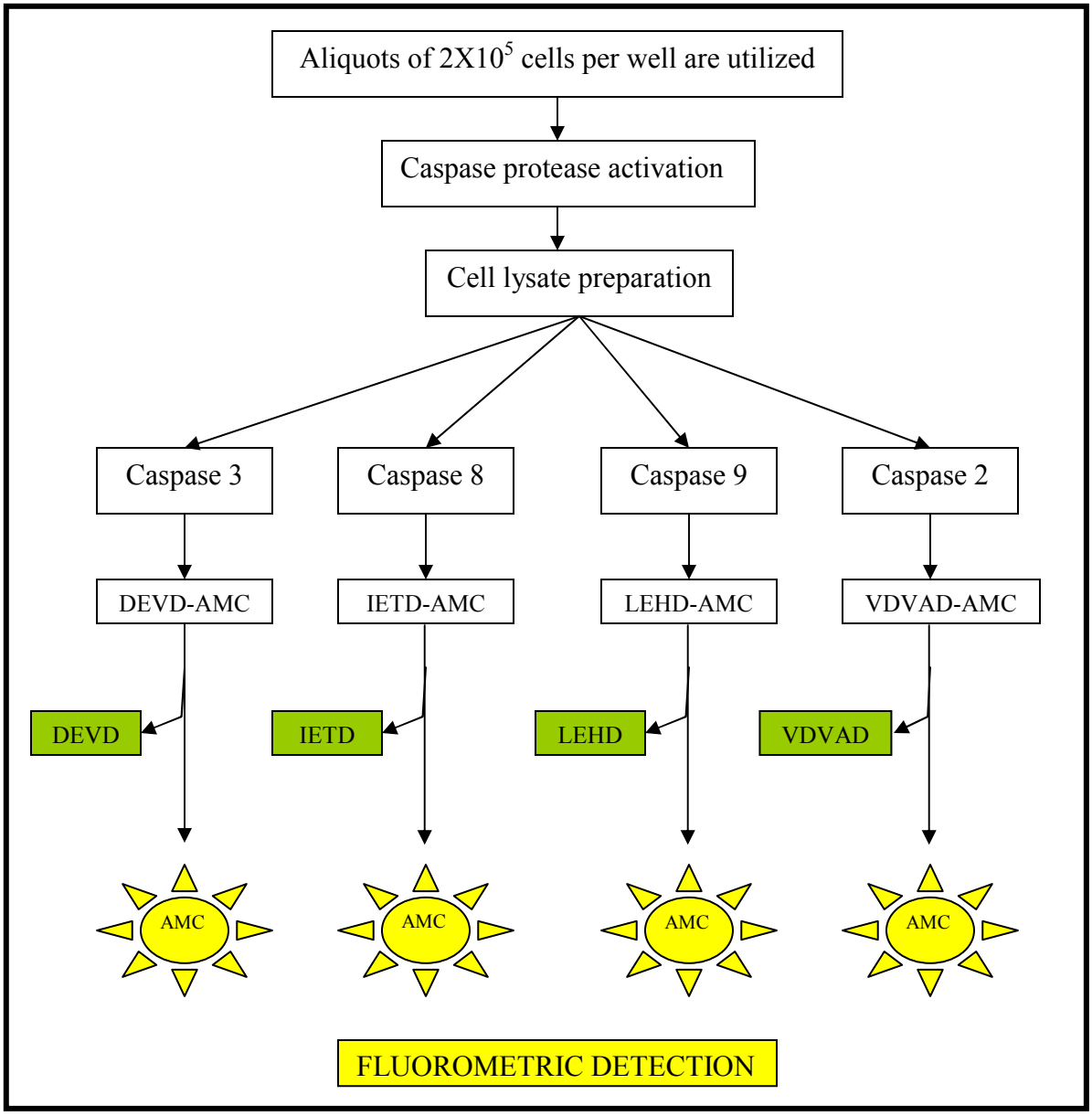


**Figure 12**. Flow diagram of the BD ApoAlert™ Caspase Assay. After protease activation, the activated caspases recognize their respective peptide substrates - DEVD (aspartate-glutamate-valine-aspartate), IETD (isoleucine-glutamate-threonine-aspartate), LEHD (leucine-glutamate-histidine-aspartate) and VDVAD (valine-aspartate-valine-alanine-aspartate) - which are covalently linked to the fluorogenic dye, 7-amino-4-methyl coumarin (AMC). Upon cleavage by the respective caspase the free dye can be detected.

Cells were harvested 48 and 72 hours post transfection using 3 ml of 1X EDTA/PBS (Appendix A6) and incubated for 10 minutes at 37°C with 5% $CO_2$ to allow the cells to detach. The conditioned medium and EDTA solution containing the cells were

centrifuged at 300g for 2 minutes at room temperature. The supernatant was discarded and the cell pellet resuspended in 1 ml of RPMI medium (Appendix A5). The number of cells in each tube was quantitated using 0.2% Trypan Blue Solution (Sigma, USA) and a haemocytometer. For each well of the caspase profiling plate $2X10^5$ cells were used (Figure 13).

| | | |
|---|---|---|
| $C = \tilde{N} \times 10^4$ | where | C = cells per ml<br>$\tilde{N}$ = cells counted within the middle square<br>$10^4$ = volume conversion factor for 1 $mm^2$ |

**Figure 13**. Formula used to quantitate the amount of cells present per tube.

Initially 25 μM cycloheximide was used to induce apoptosis. A higher level of apoptosis however occurred with 50 μM cycloheximide added 48 hours prior to the cells being harvested and this was used in subsequent experiments in the apoptosis control. The plate was analyzed using the CytoFlour® Multi-Well Plate Reader Series 4000 (PerSeptive Biosystems, USA) with excitation at 380 nm and emission at 460 nm.

## 2.7 STATISTICAL ANALYSIS

Statistical analysis was carried out on the flow cytometric and caspase profiling results using the Student t-test because $n<30$.

The data was normally distributed and the means compared - $H_o$: $\mu_1 - \mu_2 = 0$

$H_1$: $\mu_1 < \mu_2$; $\mu_2 < \mu_1$

Conclusions concerning the differences are drawn from the p-values. Two variables under consideration are said to be significantly different at 5% level of significance if the reported p-value is less than 0.05, otherwise the two variables are not significantly different.

# 3.0 RESULTS

## 3.1 PLASMID DNA INTEGRITY

Spectrophotometer readings at 260 nm and 280 nm were used to calculate DNA concentration, yield and purity. Because transfections require intact DNA without contamination (foreign DNA), the various plasmids were electrophoresed in 0.8% agarose gels (Figure 14). The wild-type, G1896A and β-gal plasmids were used as controls and the effect of the G1862T mutants on the various parameters was measured relative to these controls.

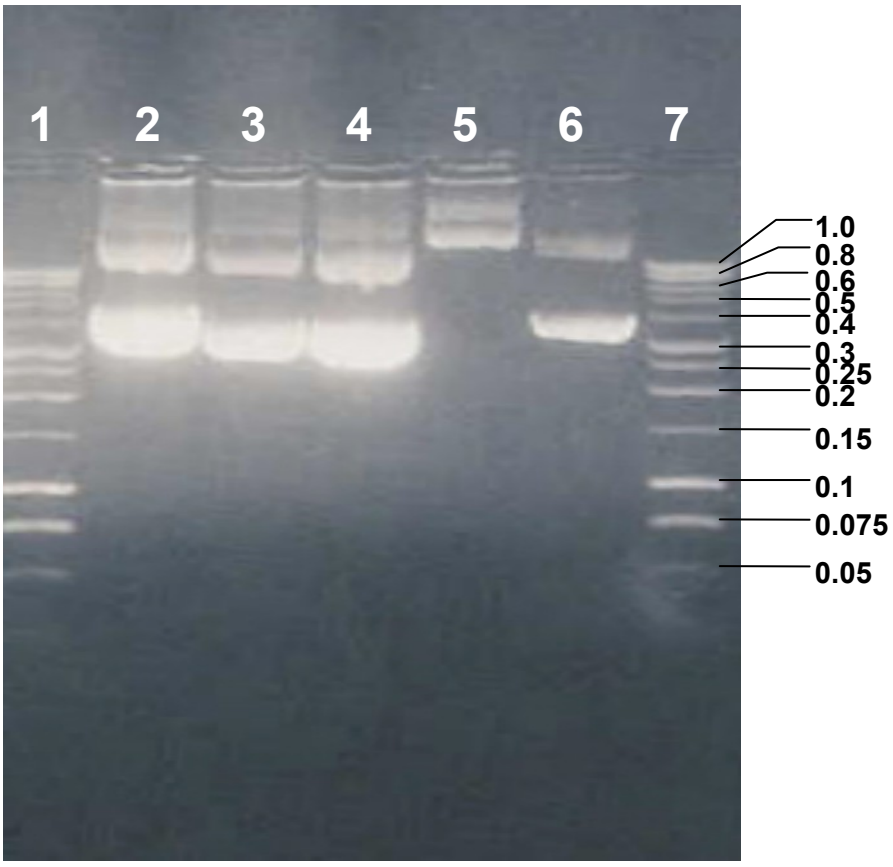


**Figure 14.** Ethidium bromide stained 0.8% agarose gel showing the resolution of the plasmid DNA used for transfection. Lanes 1 and 7 contain the molecular weight marker shown in kilo base pairs (Promega, USA); lane 2: pCRa-wild-type; lane 3: pCRa-1862T; lane 4: pCRa-1896A; lane 5: pMC1871 (β-gal); lane 6: pWay21-eGFP. The two bands present per plasmid depict the relaxed (larger) and supercoiled (smaller) forms of the plasmids.

## 3.2 OPTIMIZATION OF THE APOPTOTIC CONTROL FOR FLOW CYTOMETRY

In order to establish the correct gating for the flow cytometer, necrotic and apoptotic controls were needed. Huh7 cells were placed under a UV light for one hour to obtain a necrotic control (Figure 17a [2]). To acquire a suitable apoptotic control various apoptosis inducers were tested. Huh7 cells were incubated at different time intervals with varying concentrations of the apoptotic inducers. The cells were then stained with green fluorescent YO-PRO®-1 dye to detect apoptotic cells, and with propidium iodide to detect necrotic cells while the live cells do not take up any dye. Flow cytometric scatter patterns were then analyzed. The highest percentage of apoptotic cells were found after 24 hours incubation with the apoptotic inducer (Figure 15). Camptothecin, a nuclear topoisomerase inhibitor, caused the highest percentage (51%) of apoptotic cells (Figure 16a [2]) followed by cycloheximide (Figure 16a [3]), a protein synthesis inhibitor, and dexamethasone (Figure 16b [4]), a stable glucocorticoid, both of which caused similar percentages of apoptosis. Actinomycin D, a RNA synthesis inhibitor, resulted only in 12% apoptosis (Figure 16b [5]) while etopiside, a nuclear topoisomerase inhibitor, caused the lowest percentage (5%) of apoptotic cells (Figure 16b [6]). This was expected since etopiside utilizes the p53-apoptotic pathway and p53 is mutated in the Huh7 cell line therefore apoptosis is inhibited. Camptothecin was therefore used as the apoptotic control for flow cytometric analysis in subsequent experiments.

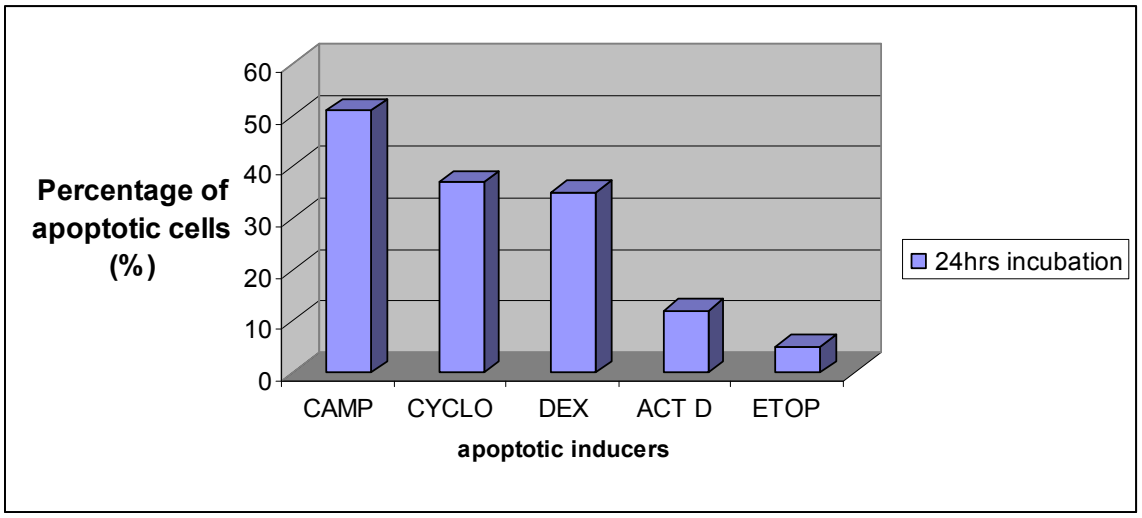


**Figure 15.** Comparison of the percentage of apoptotic cells present 24 hours after incubation with the various apoptotic inducers. CAMP: camptothecin, CYCLO: cycloheximide, DEX: dexamethasone, ACT D: actinomycin D, ETOP: etopiside.

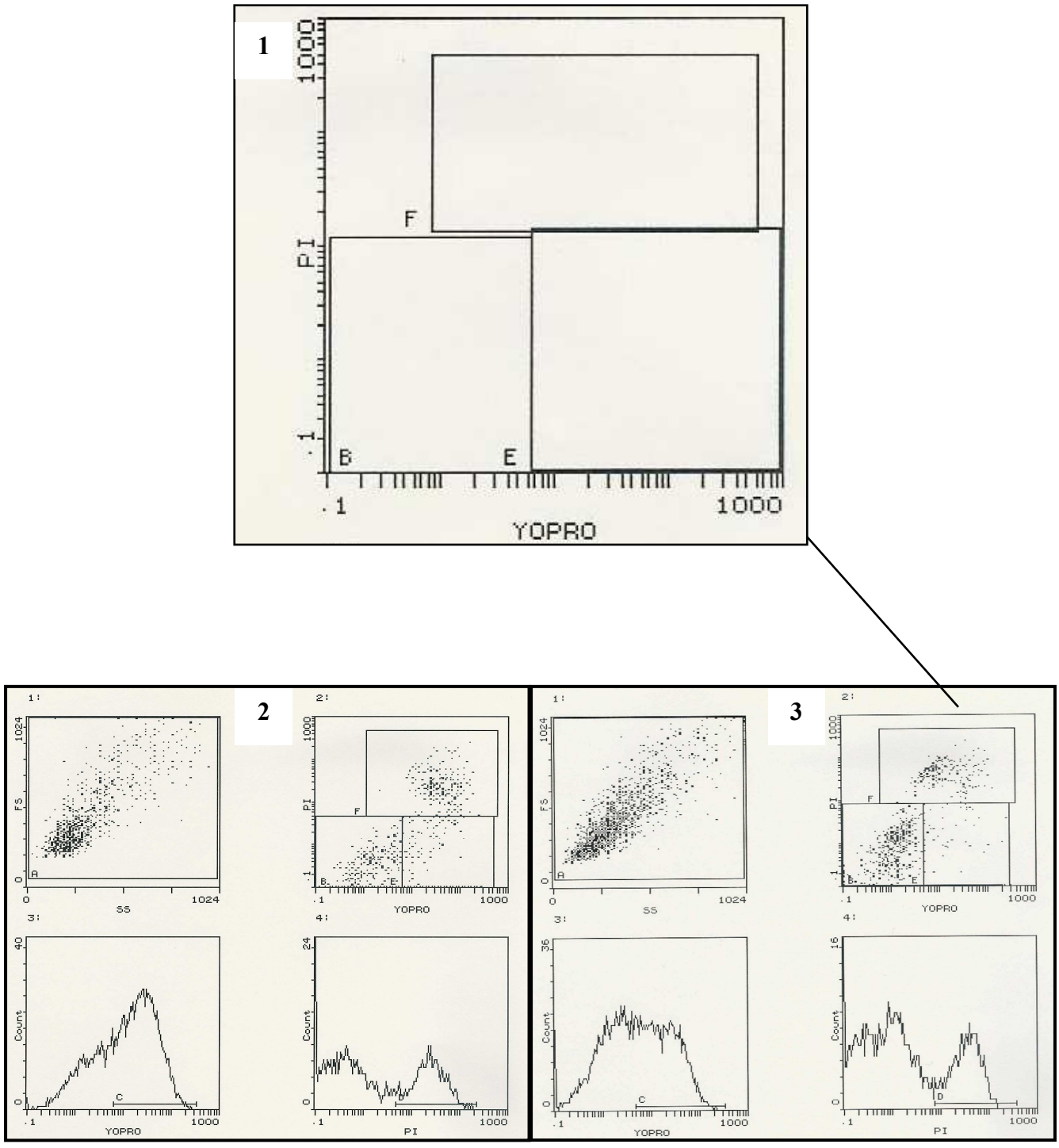


**Figure 16a.** Representative flow cytometric scatter analysis sheets for apoptosis inducers. Huh7 cells were stained with YO-PRO®-1 and propidium iodide before being analyzed on the flow cytometer. 1) Huh7 cells were scattered into one of three quadrants: The F quadrant contains late apoptotic/necrotic cells, the E quadrant contains apoptotic cells and the B quadrant live cells. 2) Camptothecin [8 μM] 3) Cycloheximide [25 μM].

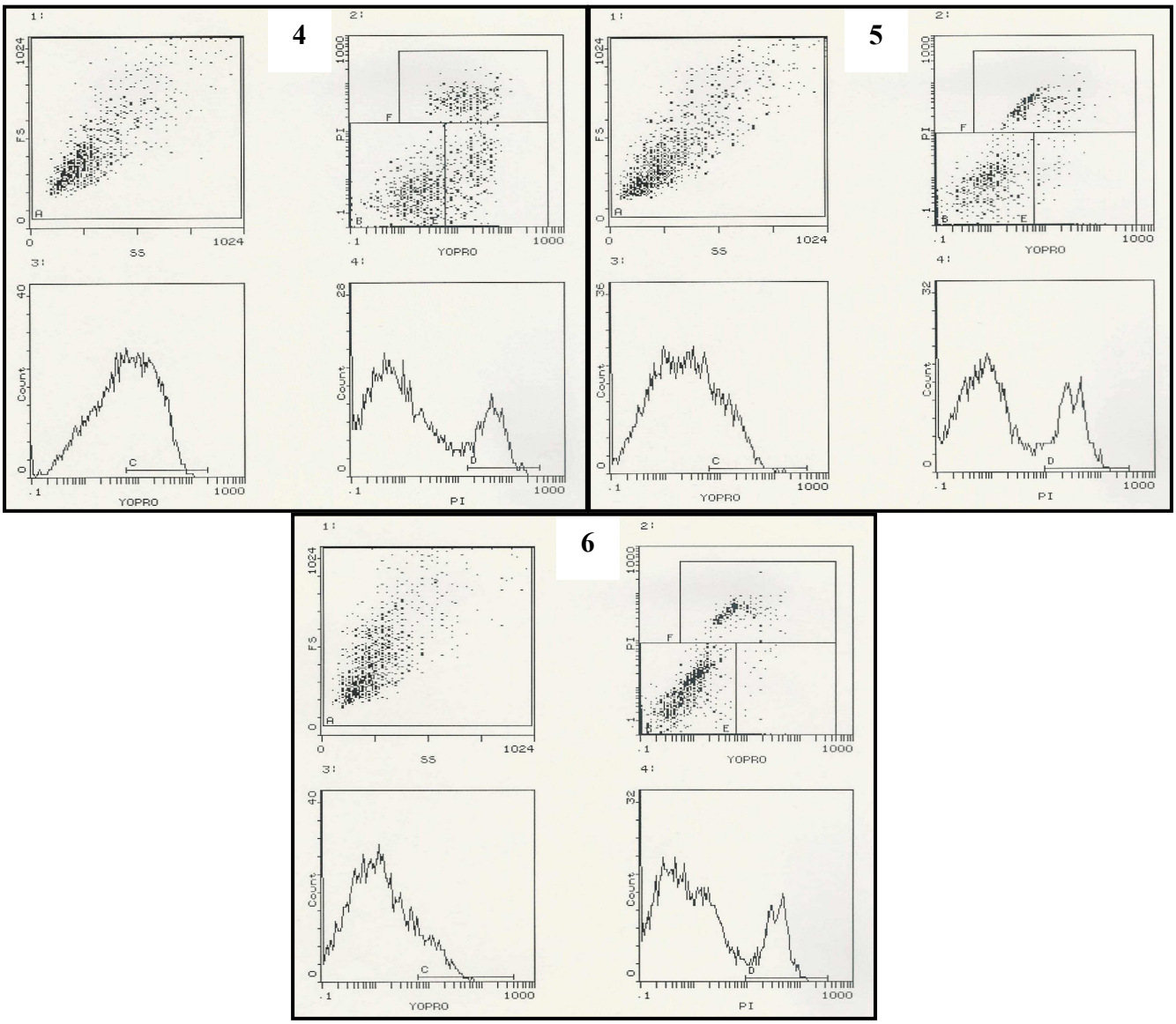


**Figure 16b.** Representative flow cytometric scatter analysis sheets for apoptosis inducers. Huh7 cells were stained with YO-PRO®-1 and propidium iodide before being analyzed on the flow cytometer. 1) Huh7 cells were scattered into one of three quadrants: The F quadrant contains late apoptotic/necrotic cells, the E quadrant contains apoptotic cells and the B quadrant live cells 4) Dexamethasone [10 μM] 5) Actinomycin D
[250 pM] 6) Etopiside [5 μM].

## 3.3 PERCENTAGE OF LIVE, APOPTOTIC AND NECROTIC CELLS POST-TRANSFECTION

Flow cytometric analysis was used to determine the effect of the various expression plasmids on cell viability. At 24, 48, 72 and 96 hours post-transfection apoptotic cells were stained with green fluorescent YO-PRO®-1 dye, necrotic cells with propidium iodide, whereas the live cells did not take up any dye. The Huh7 cells were then gated into live, apoptotic, or necrotic cells according to the fluorescence emitted (Figure 17a and b). Similar scatter plots were observed between the apoptotic control (Figure 17 [3]) and the G1862T mutant expressing cells (Figure 17 [5]). Each of the transfections was carried out in duplicate, with the means of multiple readings computed, and the entire experiment was repeated three times. Therefore three data sets (Appendix C) were statistically analyzed (Appendix D) using the Student t-test. The three data sets were not pooled because different passages of Huh7 cells were used and therefore each experiment is considered to be unique. Comparison was carried out within each experimental set between the experiment and the controls. Statistical analysis, by Dr Eugenius M. Senaoana (Statistics Department, University of the Witwatersrand) was carried out within each experiment. Although a significant difference of the percentage of apoptotic cells was only observed in set 3 at 72 hours post-transfection (Figure 18) between G1862T and the other transfection groups, when looking at the other two data sets the G1862T mutant group always showed the highest percentage of apoptotic cells at 72 hours post-transfection, although not at a significant level. These observations suggested that the G1862T mutation results in an increase in apoptosis 72 hours post-transfection compared to the wild-type and G1896A mutation.

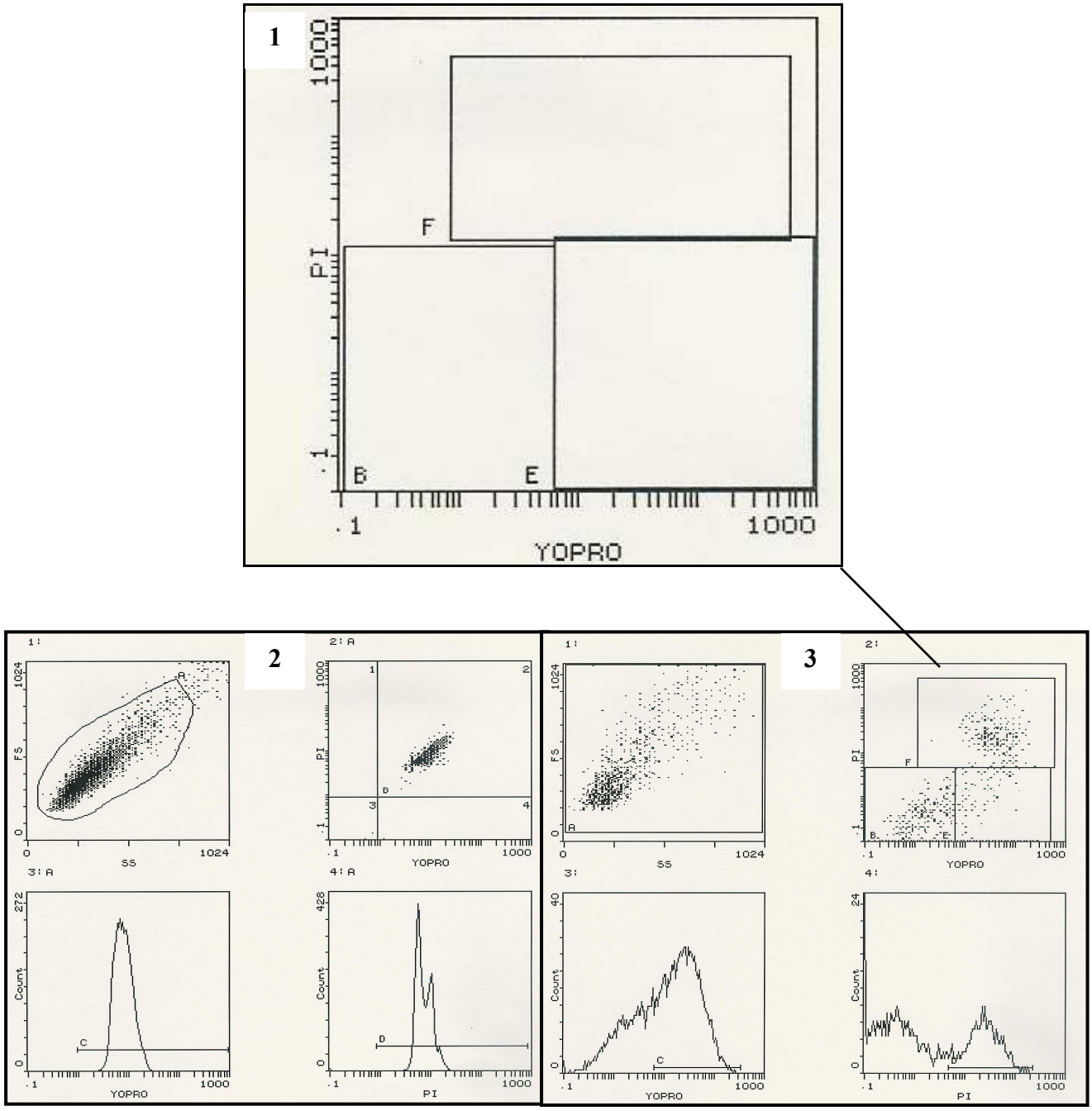


**Figure 17a.** Representative flow cytometric scatter analysis sheets. Huh7 cells were stained with YO-PRO®-1 and propidium iodide before being analyzed on the flow cytometer. 1) Huh7 cells were scattered into one of three quadrants: The F quadrant contains late apoptotic/necrotic cells, the E quadrant contains apoptotic cells and the B quadrant live cells. 2) Necrotic control (Huh7 cells exposed to UV light) (quadrant B2=F, B3=B and B4=E) 3) Apoptotic control (Camptothecin 8 μM).

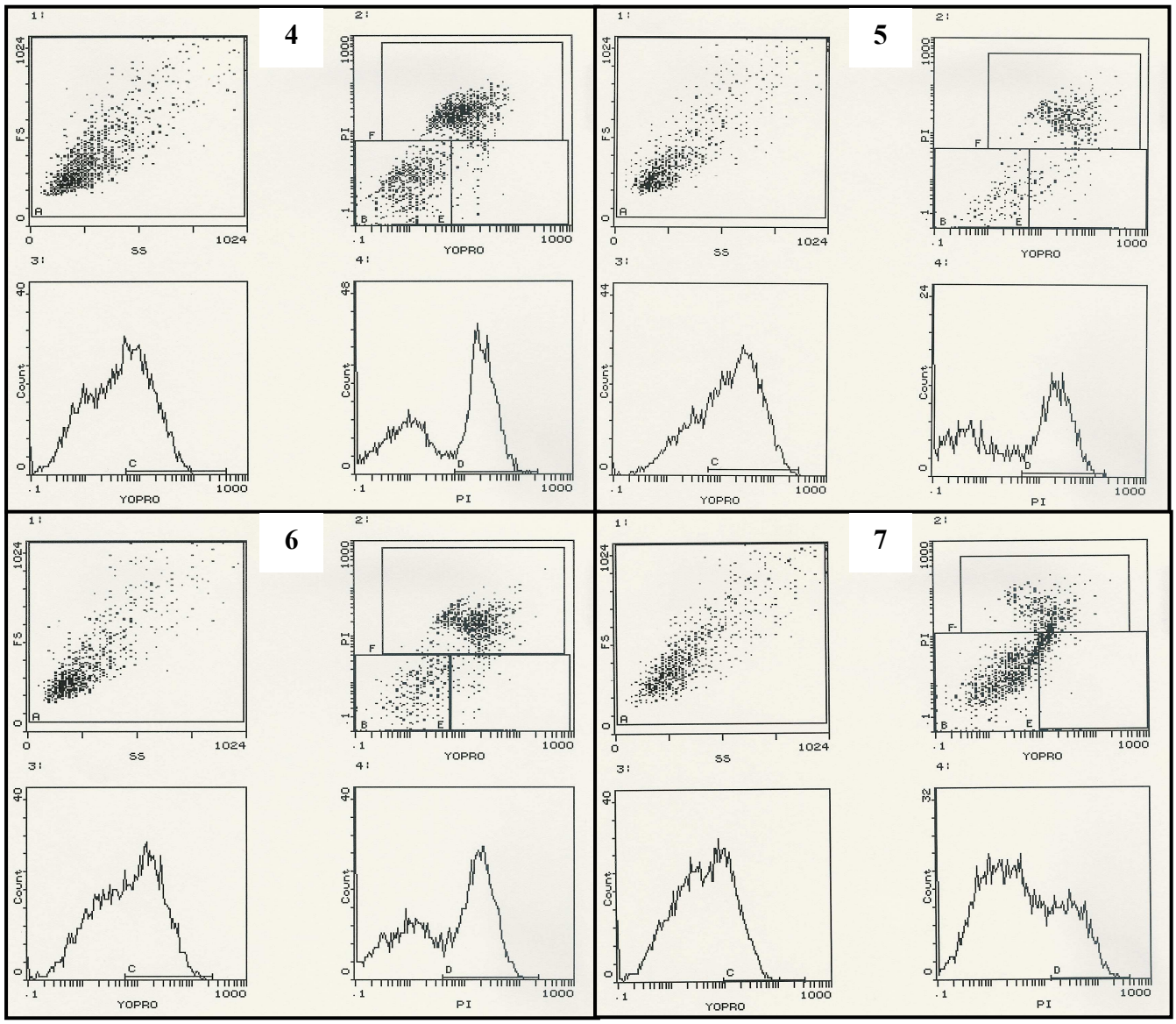


**Figure 17b.** Representative flow cytometric scatter analysis sheets. Huh7 cells were stained with YO-PRO®-1 and propidium iodide before being analyzed on the flow cytometer. 1) Huh7 cells were scattered into one of three quadrants: The F quadrant contains late apoptotic/necrotic cells, the E quadrant contains apoptotic cells and the B quadrant live cells 4) pCRa-wild-type expressing cells 5) pCRa-1862T expressing cells 6) pCRa-1896A expressing cells and 7) pMC1871 (β-gal) expressing cells.

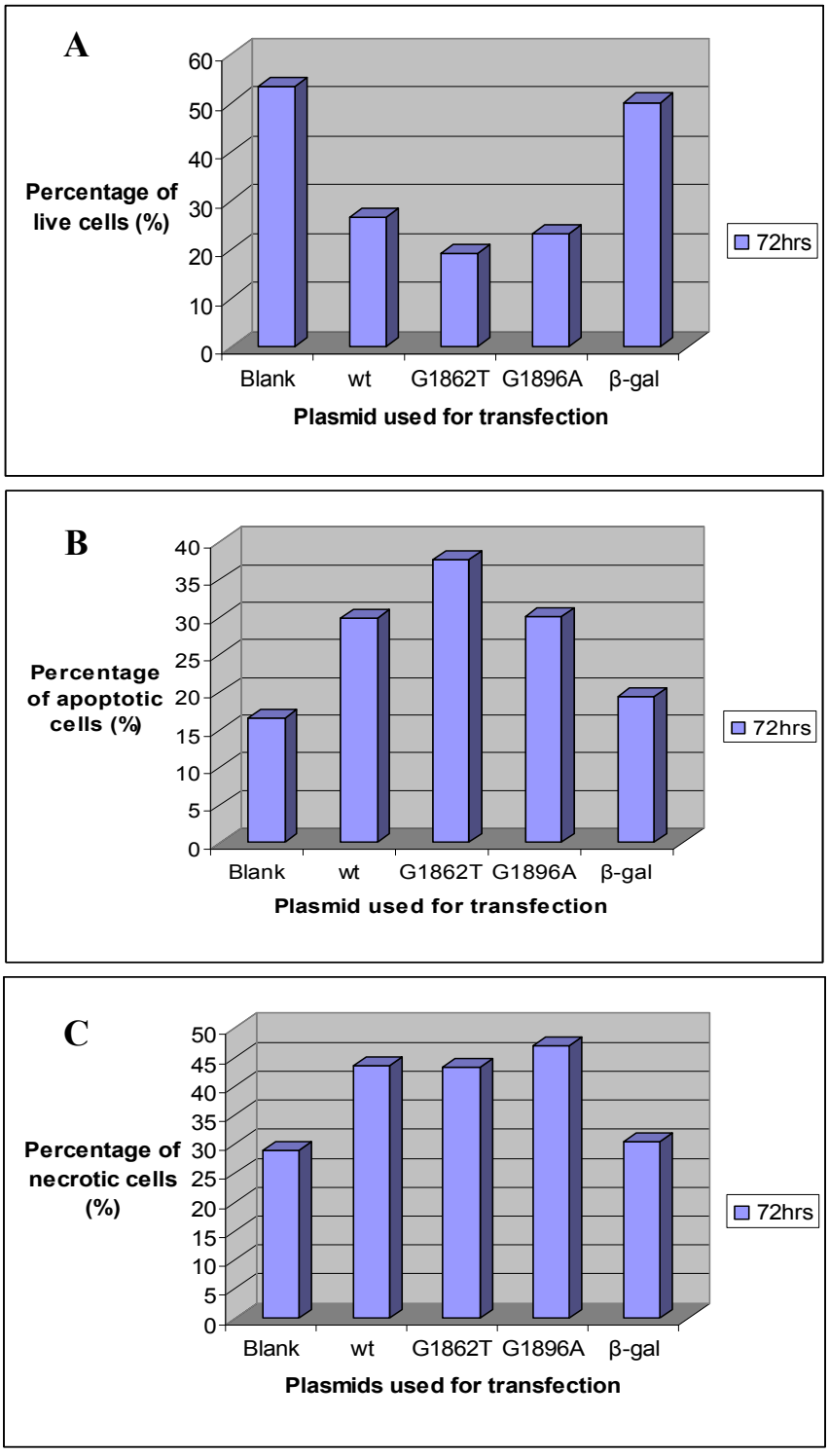


**Figure 18.** Representative flow cytometric results for data set #3 72 hours post-transfection. Comparison of the amount of live (A), apoptotic (B) and necrotic (C) cells.

In data set #3 the G1862T mutant showed the lowest percentage of live cells but highest percentage of apoptotic cells. The G1896A mutant shows the highest percentage of necrotic cells. The blank and β-gal groups show the highest percentage of live cells and the lowest percentage of apoptotic and necrotic cells. The wild-type has a higher percentage of necrotic cells than apoptotic or live cells (Figure 18).

## 3.4 APOPTOTIC/NECROTIC CONFOCAL CELL STAIN

Confocal microscopy was used to confirm the flow cytometric results. Huh7 cells transfected with the various plasmids were stained with YO-PRO®-1 and propidium iodide 24, 48, 72 and 96 hours post-transfection (Figure 19). The blank, which contained untransfected Huh7 cells, always contained a low percentage of apoptotic and necrotic cells. A similar trend was observed for the β-galactosidase control, except that the percentage of apoptotic and necrotic cells was somewhat higher. When comparing the wild-type, G1862T mutant, and G1896A mutant expressing cells obvious differences were evident at 72 hours post-transfection. There was a high percentage of apoptotic cells present in the G1862T expressing cells and a high percentage of necrotic cells when transfected with the wild-type plasmid. The G1896A mutant expressing cells showed a higher percentage of necrotic cells than the G1862T mutant expressing cells, but a lower percentage than the wild-type. At 96 hours post-transfection it was noted that the Huh7 cells began to change morphology and the transfection efficiency decreased, noted by the decrease in GFP-expressing cells.

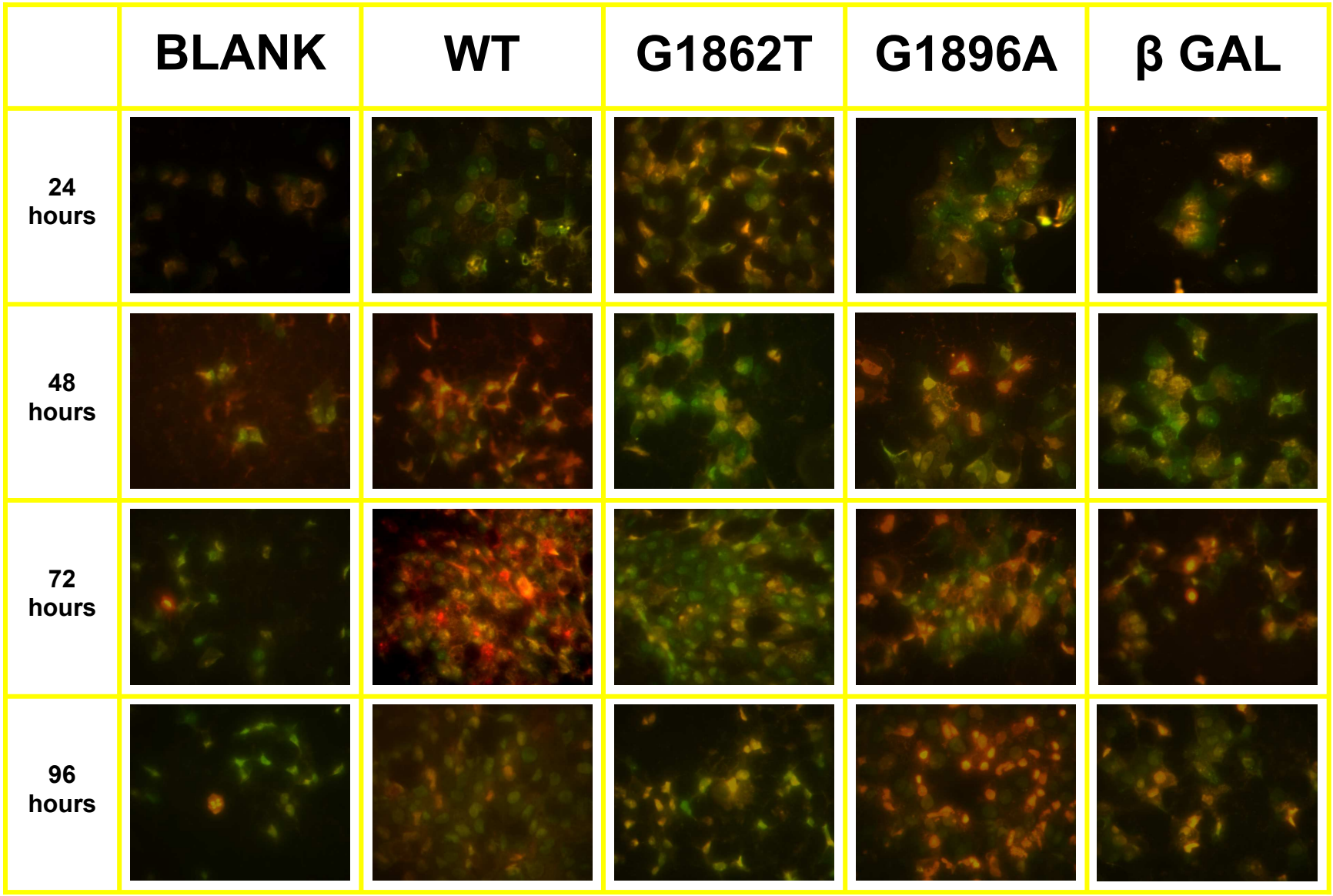


**Figure 19.** Confocal images of Huh7 cells transfected with various plasmids at 24, 48, 72 and 96 hours post-transfection. Apoptotic cells are stained green with YO-PRO®-1, necrotic cells red with propidium iodide, and cells in late apoptosis/early necrosis take up both dyes and are therefore stained yellow-brown (400X magnification). At 72 hours post-transfection a distinction is visible between the different transfection groups. The G1862T mutant shows a high level of apoptosis while the wild-type shows a high amount of necrosis.

## 3.5 ANALYSIS OF CELL MORPHOLOGY AND LOCALIZATION OF THE HBe-ANTIGEN

The Hoechst/monoclonal anti-HBe confocal stain was carried out to determine whether the precursor HBeAg produced by the G1862T expressing plasmid, co-localized with apoptotic nuclei (Figure 20a). The blank and β-galactosidase expressing cells did not produce the HBeAg and healthy nuclei were observed. The wild-type expressing cells showed a uniform distribution of the HBeAg and healthy nuclei. The G1896A mutant expressing cells displayed clumped HBeAg. However, at 72 hours post-transfection the majority of the HBeAg was very faint and was found adjacent to or just above the nuclei. Very few cells showed any HBeAg expression which suggests that the HBeAg precursor was being degraded. The G1862T mutant expressing cells showed a completely different pattern of HBeAg distribution compared to the rest of the groups. At 48 hours post-transfection the HBeAg began to accumulate in the central region surrounding the nucleus. By 72 hours post-transfection the HBeAg aggregate occupied the entire space of the cell resulting in the condensation of the nucleus and the formation of apoptotic nuclei (Figure 20b). This suggests that the apoptosis observed in the G1862T mutant expressing cells may be caused by the abnormal accumulation of the HBeAg precursor.

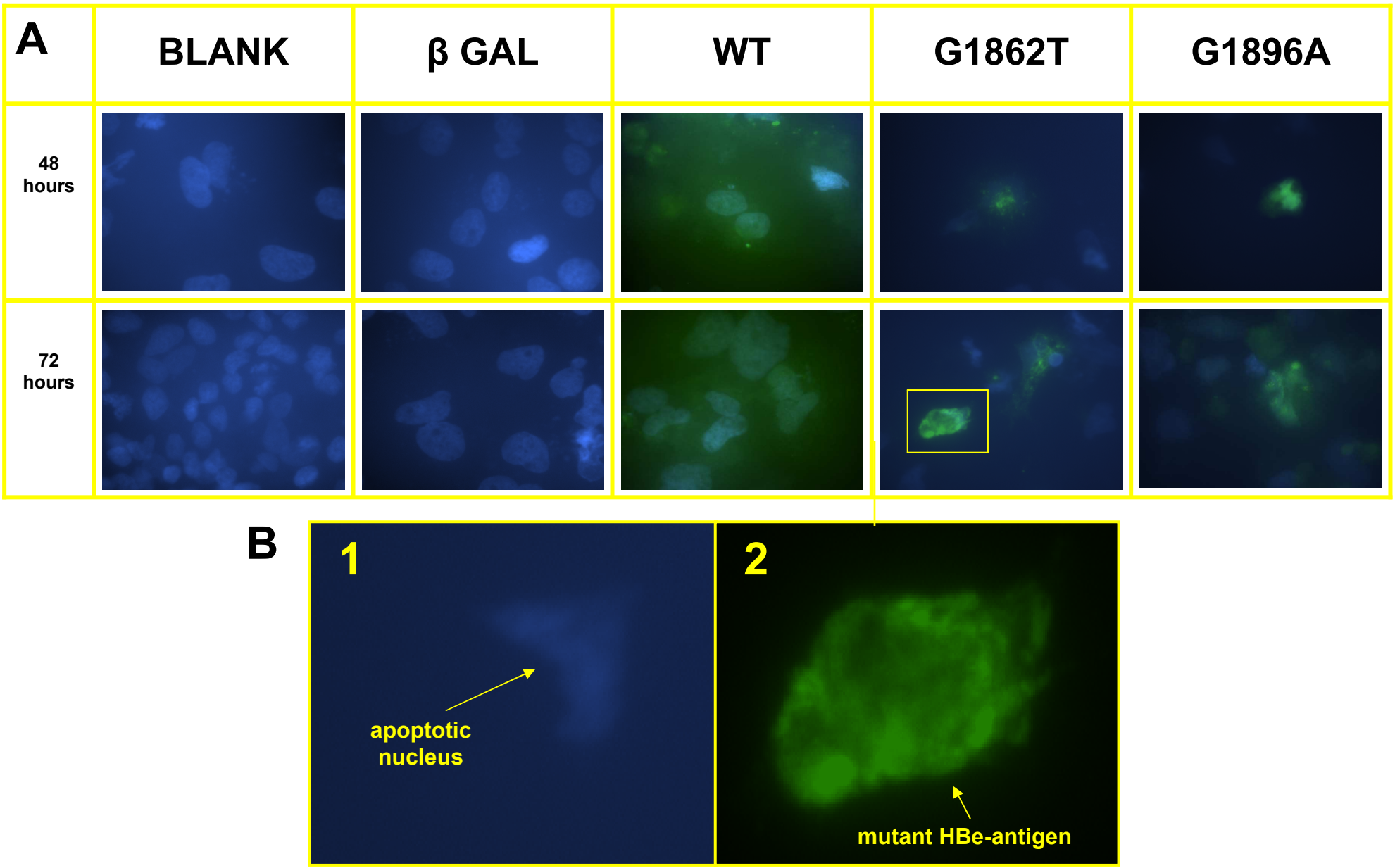


**Figure 20.** **A)** Hoechst/monoclonal anti-HBe confocal stain 48 and 72 hours post-transfection. Nuclei are stained blue with Hoechst 33258 and the HBe-antigen green with Alexa Fluor 488 (1000X magnification). **B)** Enlargement of the G1862T confocal image 72 hours post-transfection showing the apoptotic nucleus (1) and the accumulation of the mutant HBe-antigen (2).

## 3.6 CASPASE PROFILING

Having established that apoptosis was higher in the Huh7 cells transfected with the G1862T mutant relative to the other transfection control groups, caspase profiling was carried out. Caspase profiling was needed to determine which caspase cascade was involved in the apoptotic pathways activated by the accumulation of the HBeAg precursor, as a result of the G1862T mutation. Untransfected controls included: Huh7 cells alone, with an apoptotic inducer (apop), and with an apoptotic inducer plus an apoptotic inhibitor (ainh). Transfection controls include: HBV wild-type expressing cells, G1896A mutant expressing cells, and the β-galactosidase expressing cells. Each of the transfections was done in duplicate, and the entire experiment carried out in triplicate. Three data sets (Appendix E) were statistically analyzed (Appendix F) using the Student t-test. As mentioned in the flow cytometry section, the three data sets were not pooled because each passage of Huh7 cells used is unique and so the comparison has to be relative to the groups that use the same passage of Huh7 cells. The means and variance of multiple readings of two transfections per experiment were used to determine the statistical significance within the three data sets.

The apoptotic control showed the highest expression of caspase 2 at 48 and 72 hours post-transfection, and caspase 2 expression was reduced when the apoptosis inhibitor was included. No defined trend was observed in caspase 2 expression between wild-type, G1862T, and G1896A expressing cells in all three data sets (Appendix E1, Figure 26). Caspase 2 therefore does not appear to be involved in the apoptotic pathways initiated by the accumulation of HBeAg precursor as a result of the HBV G1862T mutation.

The results of the caspase profiling experiment for data set #3 are shown in Figure 21. There was no significant difference between the caspase 8 levels between 48 and 72 hours (Figure 21A). The apoptotic control had the highest readings, followed by the cells transfected with the mutant constructs G1862T and G1896A (Figure 21A). The transfection with the G1862T mutant resulted in a higher level of caspase 8 expression relative to the wild-type, this was significantly different in two of the three data sets.

At 48 hours post-transfection the Huh7 cells transfected with the G1862T mutants showed significantly higher caspase 9 expression levels relative to the wild-type (Figure 21B). This trend was seen in all three data sets. This pattern was also evident at 72 hours post-transfection.

Expression of caspase 3 was higher at 72 hours when compared to 48 hours post-transfection with the 1862T-transfected cells. The cells transfected with the G1862T plasmid construct expressed higher levels of caspase 3 relative to either the wild-type or G1896A mutant expressing cells (Figure 21C). These were significantly different at 48 hours in two of the three data sets and at 72 hours in all three data sets.

Initiator caspase 8 and 9 as well as effector caspase 3 may therefore be involved in the apoptotic pathways activated by the accumulation of the HBeAg precursor as a result of the HBV G1862T mutation.

The expression levels of all caspases never reached the levels of expression of the apoptotic control. In all three sets, the levels of caspase 8 and 9 peaked at 48 hours post-

transfection whereas the levels of caspase 3 peaked at 72 hours post-transfection. This may be reasonably expected because caspase 8 and 9 are initiator caspases whereas caspase 3 is an effector caspase. Moreover, the range of expression levels of caspase 3 [6286-12 479 AFU] were significantly higher than those of either caspase 8 [1769-2254 AFU] or caspase 9 [1292-1495 AFU].

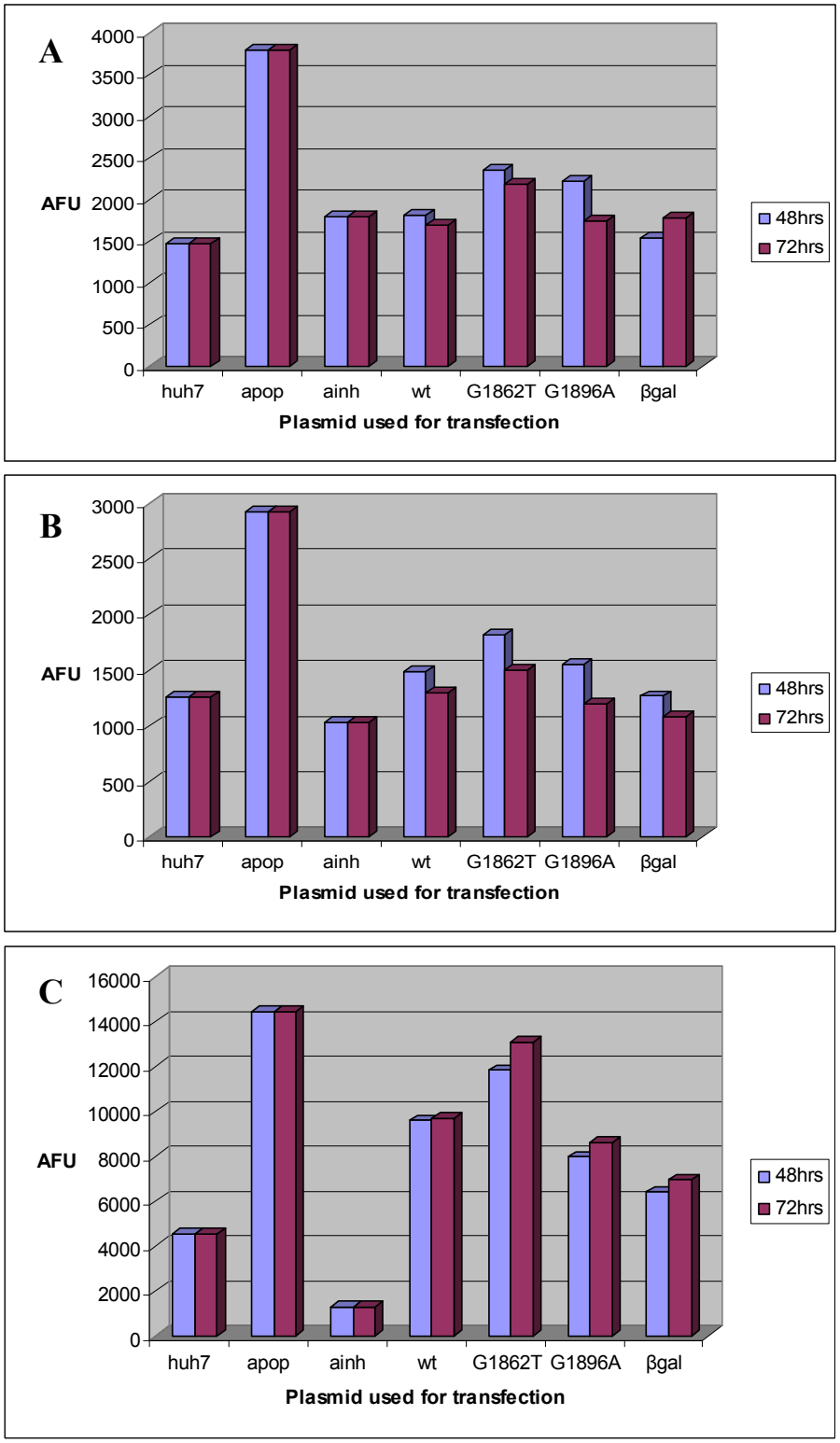


**Figure 21.** Representitive caspase profiling data set #3 showing the comparison of the amount of caspase 8 (A), caspase 9 (B) and caspase 3 (C) expression levels 48 and 72 hours post-transfection with the various plasmids. In all three histograms, the G1862T mutant possess the highest amount of caspase 8, 9, and 3 expression levels compared to the wild-type and G1896A mutant. AFU: arbitrary fluorescence unit.

# 4.0 DISCUSSION

HBeAg expression, in southern African Black carriers, is lost relatively early during the course of HBV infection, so that only about 5% remain HBeAg positive in adulthood [Dusheiko *et al*, 1985], as opposed to a rate of 40% or more found in the other major hyperendemic areas of the world, i.e. eastern and south-eastern Asia [Stevens and Szmuness, 1980]. The pre-core/core ORF of HBV encodes for the precore/core fusion protein, which is the precursor of HBeAg. This protein has a signal peptide at its amino end that targets it to the ER, where it is post-translationally modified [Ou *et al*, 1986]. The amino end is truncated at a fixed site, at amino acid 19, whereas the carboxyl end is cleaved at variable sites. The resulting HBeAg is water soluble and is secreted into the serum [Jean-Jean *et al*, 1989].

The most common missense mutation, in the precore region of HBV isolated from southern African black carriers of the virus occurs at position 1862. This mutation was found in 29% of patients with HCC [Kramvis *et al*, 1998] and in 24% of the asymptomatic carriers, predominantly in HBeAg-negative carriers [Kramvis *et al*, 1997]. A G to A or T mutation at position 1862 has also frequently been detected in Asian subgenotype A1 isolates, but not in any of 20 subgenotype A2 sequences [Sugauchi *et al*, 2004].

The 1862 mutation could conceivably affect HBeAg expression in two ways. Firstly, because this mutation is within the bulge of the encapsidation signal, it could affect the secondary structure of the bulge, thereby interfering with the initiation of reverse transcription [Fallows and Goff, 1995] and leading to low levels of HBV and hence low

levels of HBeAg expression. However, experiments carried out by Chien Yu Chen (Molecular Hepatology Research Unit, University of the Witwatersrand), have shown that viral replication was unaffected by this mutation (personal communication). Secondly, this G to T transversion at position 1862 of the precore region could affect HBeAg expression at the post-translational level by interfering with signal peptide cleavage [Hou *et al*, 2002]. The valine for phenylalanine phenotypic change introduced by this mutation at codon 17 is close to the signal peptide cleavage site, which is located at position 19 [Bruss and Gerlich, 1988]. Phenylalanine, is a forbidden amino acid at this position and may therefore abrogate signal peptide cleavage and lead to retention of the precursor in the cytoplasm [von Heijne, 1983; von Heijne, 1984]. Experiments carried out in our Unit, by Chien Yu Chen, have shown that the G1862T mutation causes the accumulation of an abnormal HBeAg precursor within the ERGIC of Huh7 cells. The aim of the present study was to determine whether this abnormal protein accumulation had any effect on the viability of Huh 7 cells.

The Hoechst/monoclonal anti-HBe confocal stain was used to examine HBeAg expression and localization in Huh 7 cells transfected with wild-type and mutant plasmid constructs (Figure 20a). Because HBeAg is secreted into the serum via the secretory and endocytic pathways of the cell, Huh7 cells expressing wild-type HBV showed a uniform distribution of the HBeAg throughout the cytoplasm of the cell. In cells expressing the G1896A mutant, which were used as the negative control, immunofluorescence was localized in the nuclei of the cells and diminished dramatically at 72 hours post-transfection when very few cells stained positively (Figure 20a). By introducing a premature stop codon this mutation results in the truncation of the precore/core fusion

protein which is retained in the ER. For this reason mature HBeAg is not secreted [Carman *et al*, 1989; Okamoto *et al*, 1990]. The decrease in the detection of the precursor of HBeAg in cells transfected with the G1896A mutant at 72 hours is the result of its degradation by the ER quality control machinery, which is triggered by the abnormal conformation of the truncated protein [Ciechanover and Schwartz, 1998; Hershko *et al*, 2000]. In agreement with the experiments performed by Chien Yu Chen, the G1862T expressing cells showed a distinctly different pattern of fluorescence compared to the controls. The abnormal HBeAg precursor produced by the G1862T mutant expressing cells was shown to aggregate within the peri-nuclear region of the cells causing the condensation of nuclei (Figure 20b). In contrast, untransfected and β-galactosidase expressing cells, which do not naturally express HBeAg, contained healthy nuclei. The condensation of the nuclei in cells transfected with the G1862T mutant is the first indication that the accumulation of the HBeAg precursor produced by the G1862T mutation may be triggering apoptosis.

Flow cytometry and confocal microscopy were used to determine whether apoptotic or necrotic cell death predominated as a result of the accumulation of the mutant HBeAg precursor. However, before the flow cytometry experiments could be performed, optimum controls for necrosis and apoptosis had to be established. The exposure of Huh7 cells to UV light for one hour resulted in necrosis, and these cells were then used as the control for necrosis (Figure 17a [2]). The following reagents: actinomycin D (10 mM), camptothecin (2 mM), cycloheximide (100 mM), dexamethasone (10 mM) and etopiside (100 mM), included in a commercially available apoptotic inducer set, were tested at varying concentrations in order to determine which one could "optimally"

induce apoptosis in Huh7 cells. Camptothecin (8 μM) was found to produce the highest percentage of apoptotic Huh7 cells (Figure 15) and was therefore used as the control for apoptosis in subsequent experiments. Camptothecin is an inhibitor of topoisomerases, which are nuclear enzymes that maintain and modulate DNA structure. Inhibitors of topoisomerases, like camptothecin, are widely used in clinical practice as antitumour drugs that interfere with transcription, induce DNA strand breaks, and trigger apoptosis preferentially in dividing cells [Hentze *et al*, 2004]. Exposure of Huh 7 cells to cycloheximide (25 μM), a protein synthesis inhibitor, or dexamethasone (10 μM), a stable glucocorticoid, produced similar percentages of apoptotic cells (Figure 15). Extremely low levels of apoptosis were observed following treatment of Huh7 cells with actinomycin D (250 pM), a transcriptional terminator that acts by binding to DNA, or with etopiside (5 μM), another nuclear topoisomerase inhibitor (Figure 15). The mechanism whereby these products cause apoptosis in Huh7 cells has not been fully evaluated. The reason that etopiside did not cause high levels of apoptosis is that, unlike camptothecin, etopiside has been shown to utilize a p53-dependent apoptotic pathway [Schultz *et al*, 2004]. Huh7 cells possess a mutated p53 [Lin *et al*, 1995] which may be the reason for lower levels of apoptosis being found in etopiside-treated Huh7 cells.

Huh7 is a human HCC cell line and therefore apoptosis and necrosis with their relevant pathways take place in these cells. For this reason the extent of apoptosis or necrosis was measured relative to the baseline levels found in untransfected cells or cells transfected with β-galactosidase. Using flow cytometry, the G1862T expressing cells revealed a higher level of apoptotic cells compared to the other transfection control groups at 72 hours post-transfection (Appendix C). This observation was confirmed visually, using

confocal microscopy of cells stained with the YOPRO®1/propidium iodide stain (Figure 19). The untransfected Huh7 and β-galactosidase expressing cells showed the lowest amounts of apoptosis and necrosis compared with the other transfection control groups. At 72 hours post-transfection, the cells expressing wild-type virus contained a high percentage of necrotic cells, perhaps caused by the productive HBV infection, whereas the cells transfected with G1862T mutant showed a significant percentage of apoptosis, presumably triggered by the accumulation of the mutant HBeAg precursor in the cytoplasm. The cells transfected with the G1896A mutant showed a mixture of both apoptosis and necrosis. As mentioned before, this may be a result of the truncated HBeAg being degraded and therefore not accumulating in the cell and not inducing ER stress [Ron, 2002] that can lead to apoptosis. Therefore, using both flow cytometry and confocal microscopy, it was shown that apoptosis was occurring in G1862T mutant expressing cells at higher levels than cells expressing wild-type or G1896A mutant virus. This is as a result of the accumulation of the HBeAg precursor in the ERGIC.

Caspase profiling, using a commercially available fluorogenic based assay was then carried out in order to determine which caspase cascade was involved in the apoptosis resulting from the accumulation of the mutant HBeAg precursor in the Huh 7 cells (Appendix E). The caspases analyzed were cytokine activator and apoptosis initiator, caspase 2, initiator caspases 8 and 9, as well as effector caspase 3. Caspase 2 did not appear to be involved in the apoptotic pathways initiated by the accumulation of the mutant HBeAg precursor (Appendix E1). This was expected because caspase 2 has not been found to be involved in ER stress-induced apoptosis and cytokine activation cannot be evaluated *in vitro*. Higher caspase 8, 9, and 3 expression levels were observed after transfection with the G1862T mutant plasmid construct (Appendix E2, E3, E4).

Therefore, these initiator caspases 8 and 9 and effector caspase 3 may be involved in the apoptotic pathways initiated by the accumulation of the HBeAg precursor in Huh 7 cells. Being an effector caspase, caspase 3 was found to peak at 72 hours post-transfection, later than the initiator caspases 8 and 9 that peaked at 48 hours post-transfection.

Therefore, ER stress caused by the accumulation of the mutant HBeAg precursor in Huh 7 cells appears to be activating several apoptotic pathways, involving caspases 8, 9 and 3 (Figure 22). Firstly, via the MPT pathway, ER stress may cause the ER to transmit oscillating $Ca^{2+}$ signals that the mitochondria decode, resulting in the activation of Apaf-1 and cytochrome *c* release and leading to caspase 9 expression. This in turn activates the effector caspases, including caspase 3, and culminates in apoptosis [Lam *et al*, 1994]. Secondly, ER stress can promote the translocation of effector caspase 7 from the cytosol to the ER surface [Rao *et al*, 2001], where it cleaves procaspase 12, found in the outer membrane of the ER, into caspase 12. Prolonged ER stress then facilitates the movement of active caspase 12 into the cytoplasm, where it interacts with caspase 9 and thus may set in motion the cytosolic component of the ER stress-induced apoptotic cascade [Jimbo *et al*, 2003, Morishima *et al*, 2002]. Thirdly, ER stress can activate initiator caspase 8, which is one of the main caspases involved in ER stress-mediated apoptosis. Caspase 8 can be directly activated by ER stress via Bap31, a polytopic integral membrane protein of the ER, which controls the transport of certain membrane proteins from the ER to the Golgi complex [Breckenridge *et al*, 2002]. Bid, a protein known to interact with both Bcl-2 and Bax, which block the release of cytochrome *c*, is processed by caspase 8 [Wang *et al*, 1996]. The C-terminal part of Bid translocates to the mitochondrial membrane and triggers MPT with cytochrome *c* release, activating caspase 9, which in

turn activates effector caspases, including caspase 3, leading to apoptosis [Li *et al*, 1998, Luo *et al*, 1998]. Caspase 8 can also activate caspase 9 via a cytochrome *c* independent-pathway. The effector caspase 3 is activated directly by both initiator caspases 8 and 9 [Herr *et al*, 2001, Jimbo *et al*, 2003].

Like HBV, other viruses including hepatitis C virus and bovine viral diarrhea virus (BVDV), utilize the host cell ER as an integral part of their life cycle and cause some level of ER stress. BVDV and related flaviviruses use the host ER as the primary site of envelope glycoprotein biogenesis, genomic replication, and particle assembly, which leads to the induction of an ER stress response involving an apoptotic cascade [Braakman *et al*, 1991; Jordan *et al*, 2002; Netherton *et al*, 2004; Tardif *et al*, 2002]. The apoptotic pathway involves downregulation of the antiapoptotic Bcl-2 protein, and induces caspase 12 expression with a decrease in intracellular glutathione levels [Jordan *et al*, 2002]. Similar findings exist for Japanese encephalitis virus infection, which causes the induction of the UPR, followed by expression of CHOP, p38 mitogen-activated protein kinase and caspase 12, culminating in apoptosis (Su *et al*, 2002).

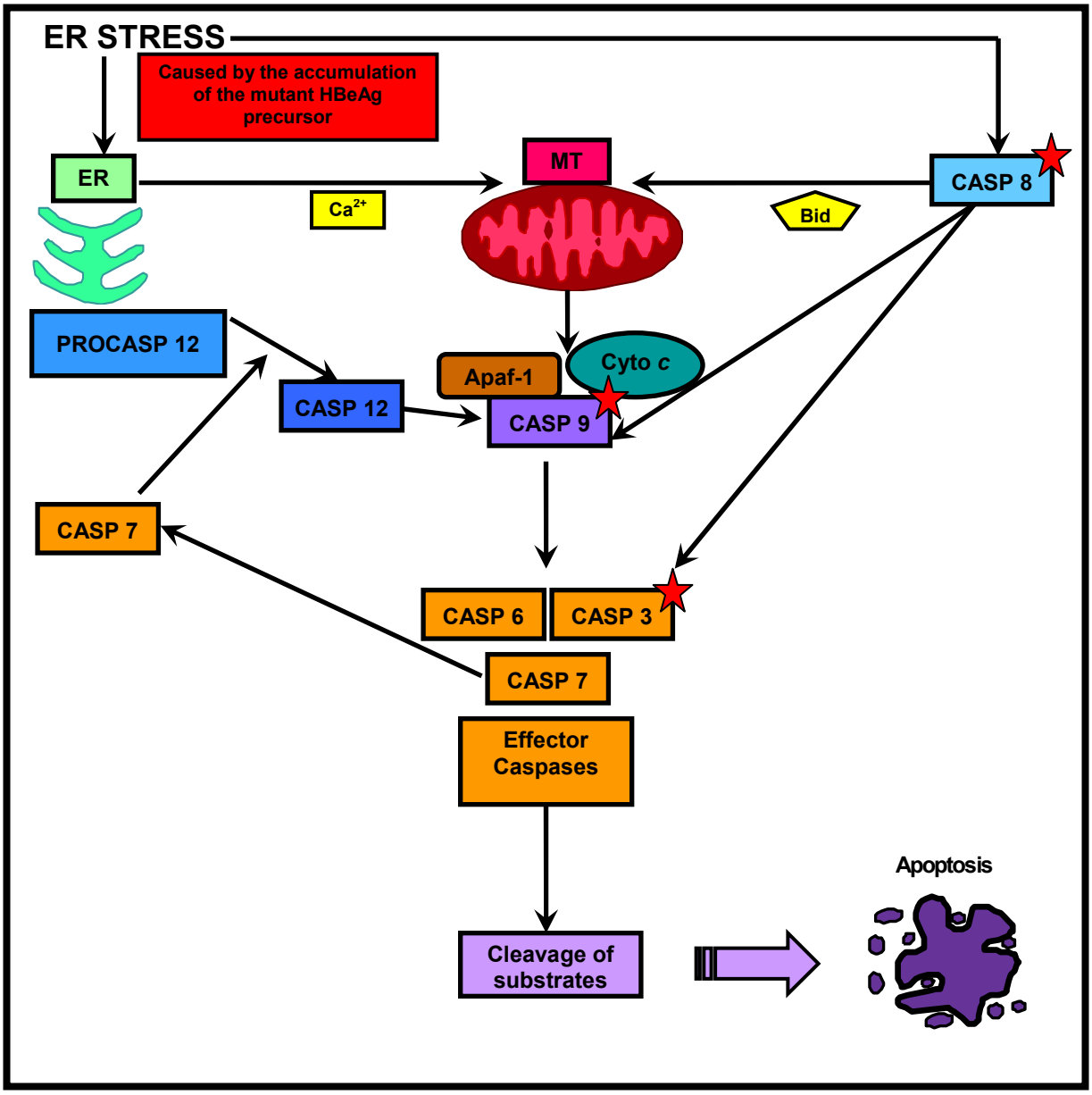


**Figure 22.** The possible apoptotic pathways initiated by ER stress caused by the accumulation of the mutant HBeAg precursor. ★ : expression of these caspases is affected in Huh7 cells transfected with the G1862T mutant. ER: endoplasmic reticulum, MT: mitochondria, PROCASP: procaspase, CASP: caspase, Cyto *c*: cytochrome *c*.

The accumulation of the mutant G1862T HBeAg may also lead to the induction of EOR. Efflux of $Ca^{2+}$ from the ER, such as that needed for mitochondria-derived apoptosis, is also required for EOR-mediated NFκβ activation [Pahl and Baeuerle, 1997]. Interestingly, NFκβ has been found to play an important role in hepatocarcinogenesis

[Arsura *et al*, 2003, Cavin *et al*, 2003]. It regulates the expression of cyclooxygenase (COX)-2 which directly correlates with NFκβ activity. Therefore in a state of ER stress NFκβ activity increases to cope with the accumulation of the abnormal protein causing the ER stress, thereby increasing COX-2 expression. Overexpression of COX-2 has been shown to be sufficient to induce tumourigenesis [Liu *et al*, 2001] and increased expression of COX-2 mRNA was observed in HCC tissue expressing mutant HBV large surface protein [Hung *et al*, 2004].

Many diseases are known to be caused by the accumulation of abnormal proteins in the ER. They are termed ER storage diseases (ERSDs). A well characterized ERSD resulting from accumulation of a toxic protein is α-1-antitrypsin (AAT) deficiency [Rutishauser and Spiess, 2002]. This condition occurs in ~1 in 1,800 live births and is the most common genetic liver disease in children [Teckman and Perlmutter, 1996]. AAT, an acute phase protein synthesized by the liver, is the most abundant serine protease inhibitor in plasma. The deficiency results from mutations that cause the protein to fold incorrectly [Callea *et al*, 1992] and thereby accumulate in the ER of the liver cell [Kim and Arvan, 1998], rather than being secreted into the bloodstream. Accumulation of the protein can lead to extensive hepatic damage, cirrhosis and HCC [Callea *et al*, 1992]. Using this disease as a precedent, it can be hypothesized that the accumulation of the mutant G1862T HBeAg, in the ERGIC of liver cells, could be a contributing factor to the development of HCC, in southern African black carriers of the virus.

# 5.0 CONCLUSION

The accumulation of the G1862T mutant HBeAg precursor in the endoplasmic reticulum/Golgi compartment, leads to apoptosis and an increase in caspases 8, 9 and 3, which are involved in several ER stress-induced apoptotic pathways. This may affect the liver cells at a physiological and pathological level. Further research is required to determine whether this may be a contributing factor in the development of HCC.

# APPENDIX A – LISTING OF SOLUTIONS

## *A1) LURIA BERTONI (LB) BROTH*

- 10 g/ℓ sodium chloride
- 10 g/ℓ tryptone
- 5 g/ℓ yeast extract
- Dissolve in 1 ℓ Sabax water

pH 7.4

- Autoclave for 20 minutes

## *A2) 10X GEL LOADING DYE*

- 50 % glycerol
- 0.25 % bromophenol blue
- 0.25 % xylene cyanol
- 0.1 M EDTA pH 8
- Make up with Sabax water

## *A3) 1X TRIS-BORATE-EDTA (TBE) BUFFER*

- 10.8 g of Tris-base
- 0.93 g of EDTA
- 5.5 g Boric acid
- Dissolve in 1 ℓ distilled water

### *A4) 0.8% AGAROSE GEL IN 1X TBE BUFFER*

- 100 ml 1 X TBE buffer
- 0.8 g of agarose
- 6 µl of 0.01 mg/µl ethidium bromide

### *A5) SUPPLEMENTED ROSWELL PARK MEMORIAL INSTITUTE (RPMI) MEDIUM*

- 10.4 g Powdered RPMI 1640 + L-Glutamine (Gibco Invitrogen Corporation, UK)
- 1.19 g Hepes
- 2 g $NaHCO_3$
- Dissolve in 1 ℓ of distilled water

} pH 7.12

- Add filtered supplements –
  - 0.5 ml $Na_2SeO_3$ ($3 \times 10^{-8}$ M)
  - 0.5 ml $FeSO_4.7H_2O$ ($1 \times 10^{-4}$ M)
  - 0.5 ml of solution 3 which contains:$(NH_4)_6MO_7O_2.4H_2O$ ($3 \times 10^{-9}$ M)/ $MnCl_2.4H_2O$ ($3 \times 10^{-10}$ M)/ $NH_4VO_3$ ($1 \times 10^{-8}$ M)
  - 50 µl Linoleic/Oleic acid BSA complex (L9655 from Sigma) ($3 \times 10^{-9}$ M)
  - 0.5 ml Ethanolamine ($3 \times 10^{-6}$ M)

### *A6) 1X ETHYLENE DIAMINE TETRA-ACETIC ACID DI-SODIUM SALT (EDTA)/PHOSPHATE BUFFERED SALINE (PBS)*

- 1 g EDTA (Saarchem, Merck Laboratory Supplies Pty Ltd, RSA)
- 100 ml PBS
- Filter sterilize

### *A.7) 4% PARAFORMALDEHYDE/PBS*

- Boil 100 ml of PBS (see A8)
- Stir in 4 g of paraformaldehyde
- Add drop by drop 1 M sodium hydroxide until the paraformaldehyde begins to dissolve
- pH solution to 7.4

### *A8) PHOSPHATE BUFFERED SALINE (PBS)*

- 0.2 g KCl
- 8 g NaCl
- 0.2 g $KH_2PO_4$
- 1.15 g $Na_2H_2PO_4$
- Dissolve in 1 ℓ distilled water

} pH 7.4

### *A.9) TRITON X100/PBS*

- 0.1 g Triton X100
- Dissolved in 100 ml of PBS (see A8)

### *A10) BOVINE SERUM ALBUMIN/PBS*

- 1 g bovine serum albumin
- Dissolved in 100 ml of PBS (see A8)

### *A11) MOUSE MNOCLONAL HBe-ANTIGEN ANTIBODY*

- 5 µg mouse monoclonal e-antigen antibody
- Dissolve in 100 µl of 1% Bovine serum albumin/PBS (see A10)

### *A12) ALEXA FLOUR 488 GOAT ANTI-MOUSE IgG*

- 2 µg Alexa Flour 488 goat anti-mouse IgG
- Dissolve in 100 µl of 1% Bovine serum albumin/PBS (see A10)

# APPENDIX B - FLOW CYTOMETRY PARAMETERS

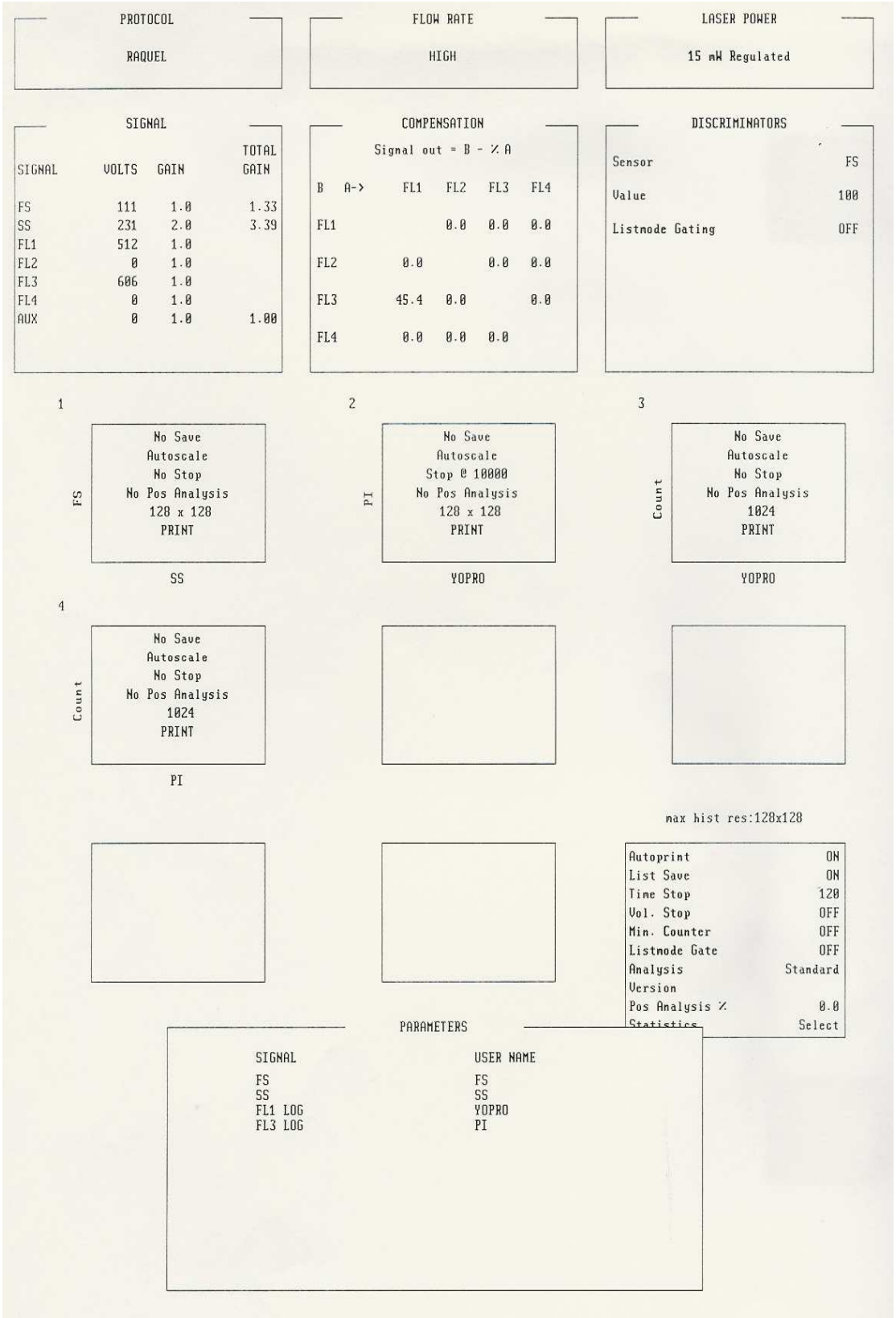


**Figure 23a**. Flow cytometer protocol settings.

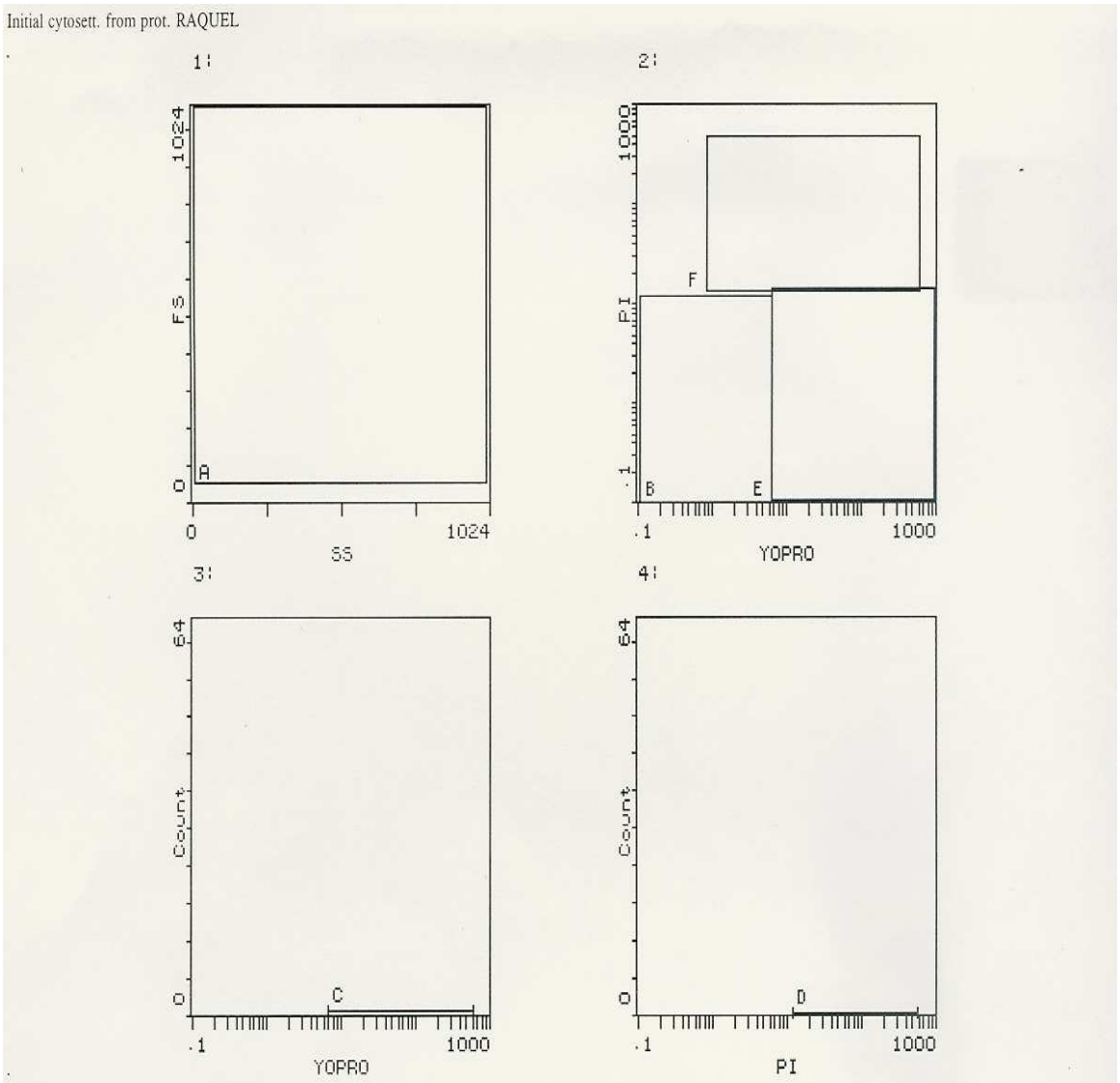


Stats: Normalized, Listgating: Disabled

| Hist | Region | ID | % | Count | Mn X | Mn Y | Md X | Md Y |
|---|---|---|---|---|---|---|---|---|
| 1 | A | A | ** | ** | **** | **** | **** | **** |
| 2 | E | E | ** | ** | **** | **** | **** | **** |
| | F | F | ** | ** | **** | **** | **** | **** |
| | B | B | ** | ** | **** | **** | **** | **** |

| Hist | Region | ID | % | Count | Mn X | Md X | Min | Max |
|---|---|---|---|---|---|---|---|---|
| 3 | C | C | ** | ** | **** | **** | 6.89 | 613.3 |
| 4 | D | D | ** | ** | **** | **** | 12.7 | 591.6 |

**Figure 23b.** Flow cytometric data analysis settings. 1) Forward (FS) and side (SS) scatter discriminate cells according to their size. All sized cells were included in this study. 2) PI (propidium iodide) against YOPRO (YO-PRO®-1) divided the cells into: live (quadrant B), apoptotic (quadrant E) or late apoptotic/necrotic (quadrant F). 3) YOPRO against cell count displays the amount of apoptotic cells according to the fluorescence emitted from the cells. 4) PI against cell count displays the amount of late apoptotic/necrotic cells according to the fluorescence emitted from the cells.

# APPENDIX C - FLOW CYTOMETRY RESULTS

## *C1) DATA SET 1*

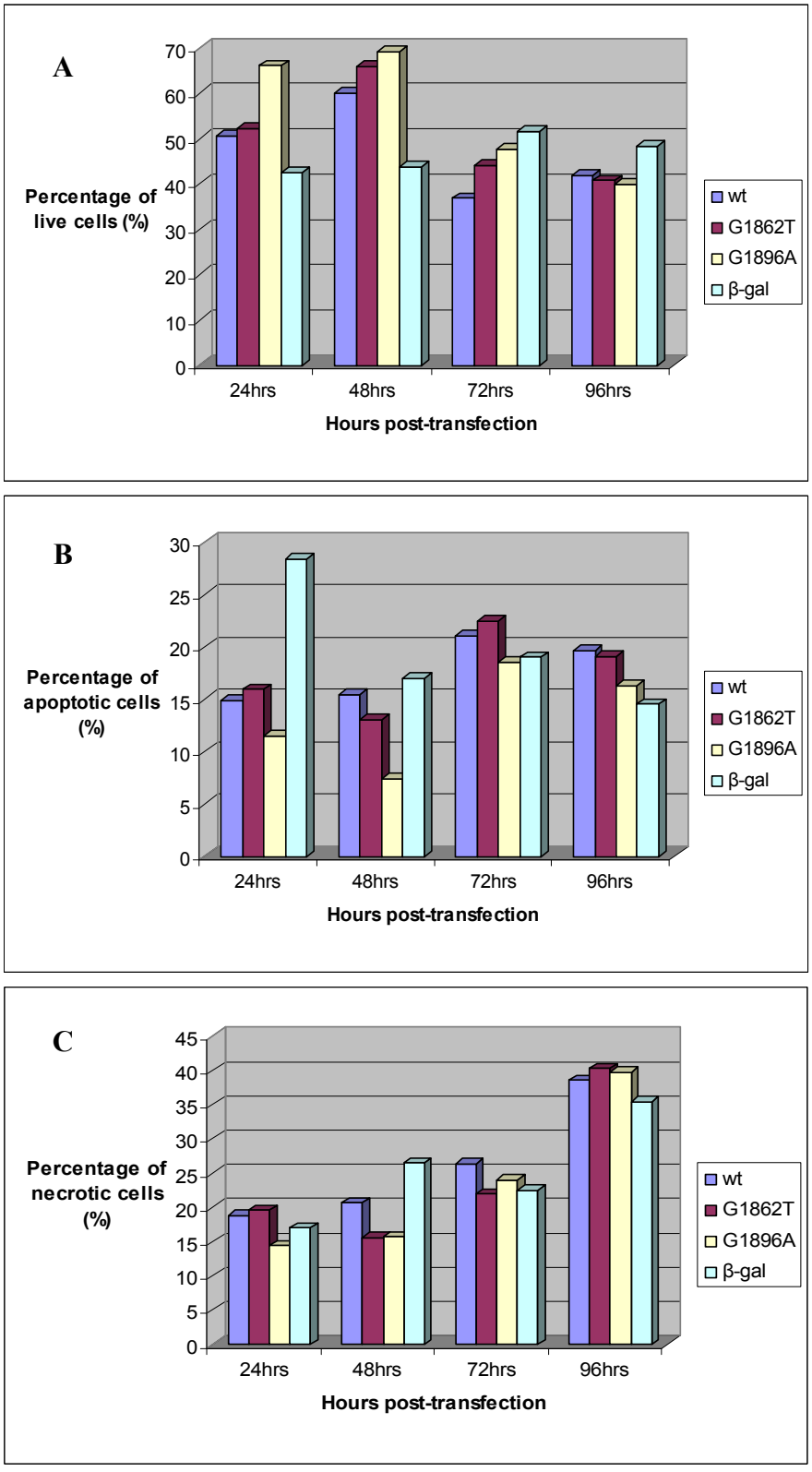


**Figure 24.** Comparison of the amount of live (A), apoptotic (B) and necrotic (C) cells present 24, 48, 72 and 96 hours post-transfection in data set one.

*C2) DATA SET 2*

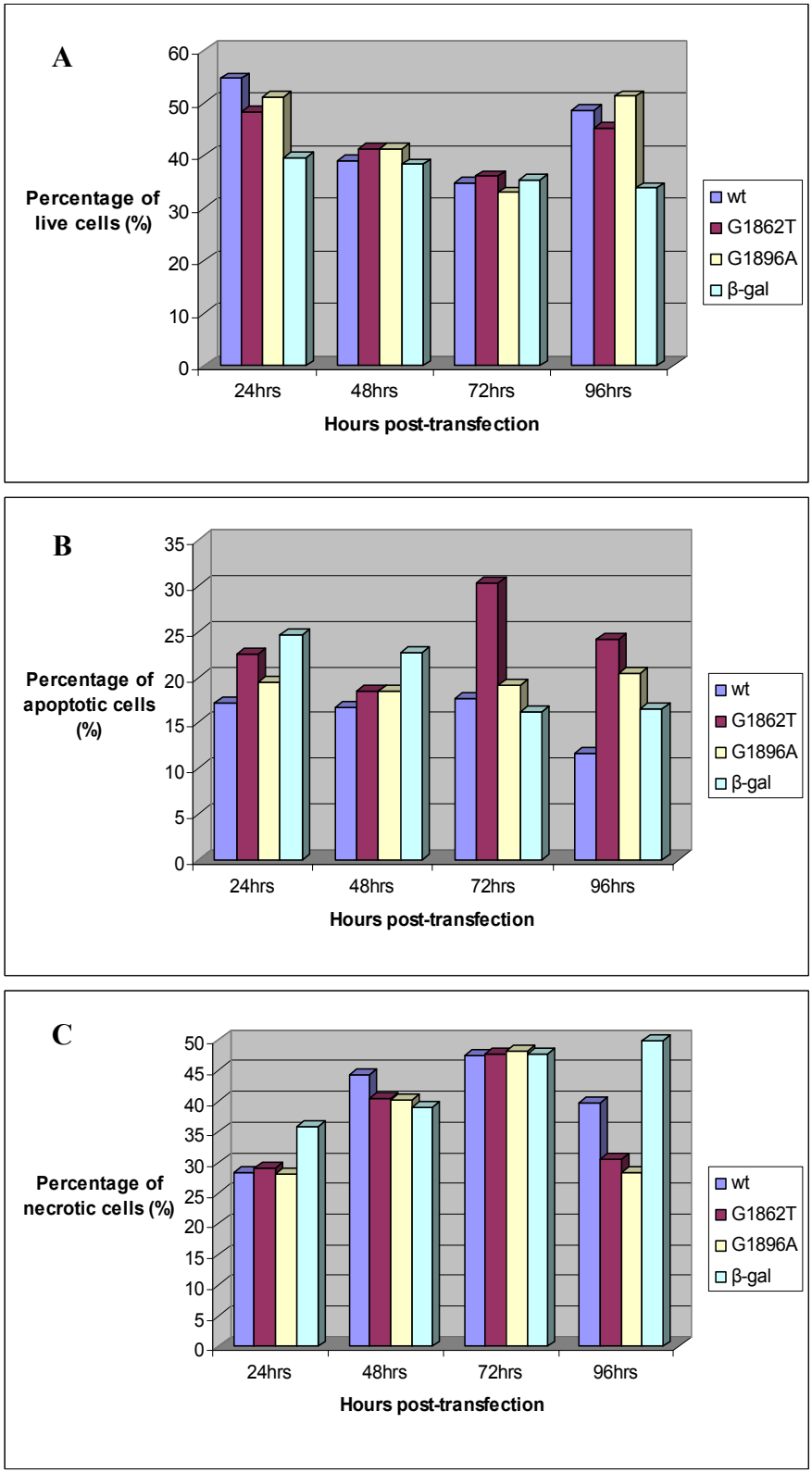


**Figure 25.** Comparison of the amount of live (A), apoptotic (B) and necrotic (C) cells present 24, 48, 72 and 96 hours post-transfection in data set two.

### *C3) DATA SET 3*

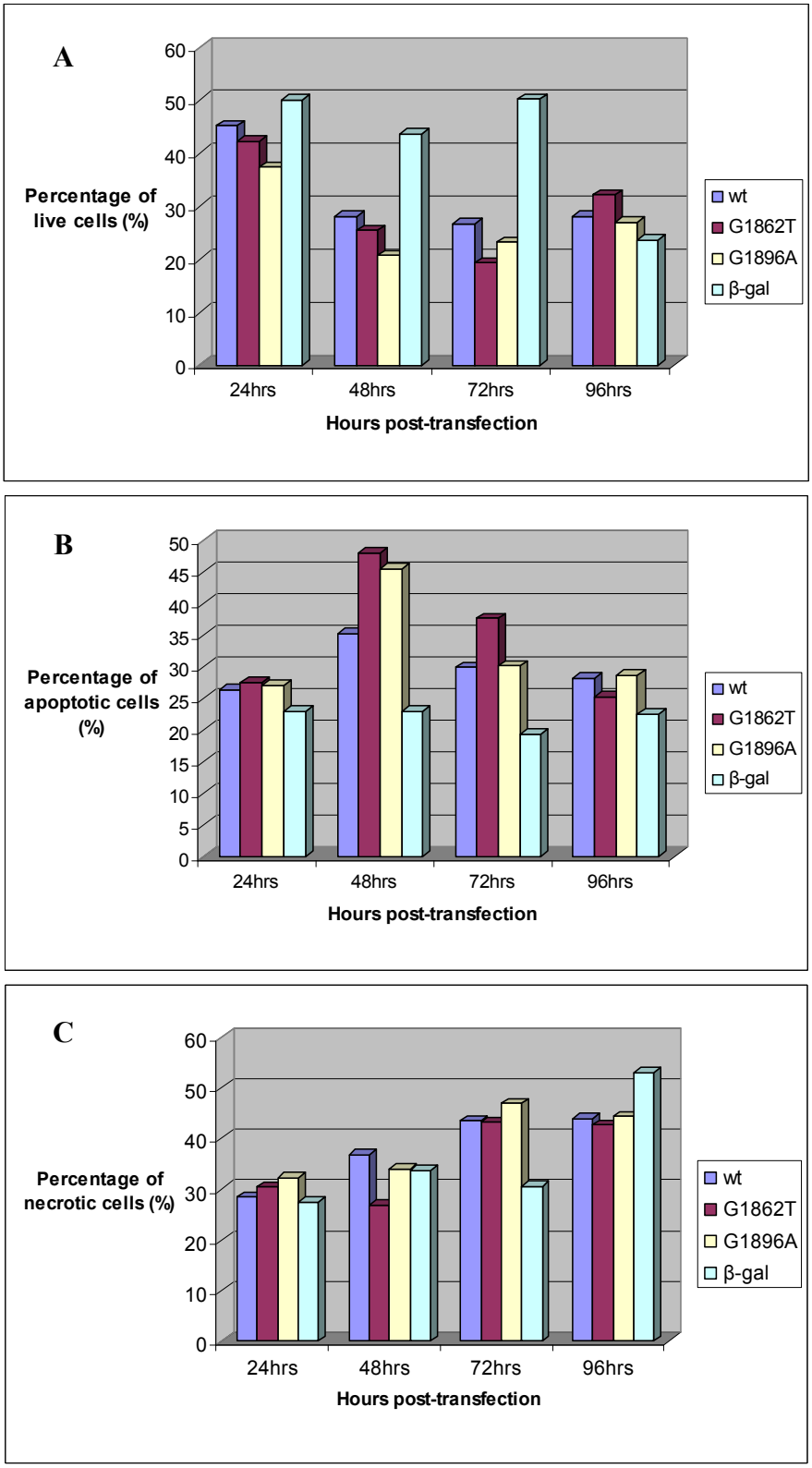


**Figure 26.** Comparison of the amount of live (A), apoptotic (B) and necrotic (C) cells present 24, 48, 72 and 96 hours post-transfection in data set three.

# APPENDIX D - FLOW CYTOMETRY STATISTICS

## *D1) DATA SET 1*

### *D1.1) Live cells*

| Table 3a. t-value for live cells in data set #1 | | | | |
|---|---|---|---|---|
| | Hours post-transfection | | | |
| Transfection Comparison | 24 | 48 | 72 | 96 |
| wt vs G1862T | -0.26 | -0.42 | -2.23 | 0.57 |
| wt vs G1896A | -8.2 | -5.83 | -4.92 | 1.7 |
| wt vs β-gal | 6.18 | 15.47 | -3.15 | -0.81 |
| G1862T vs G1896A | -2.15 | -0.22 | -1.06 | 0.34 |
| G1862T vs β-gal | 1.6 | 1.58 | -1.38 | -0.93 |
| G1896A vs β-gal | 15.13 | 13.51 | -0.77 | -0.103 |

| Table 3b. p-value for live cells in data set #1 | | | | |
|---|---|---|---|---|
| | Hours post-transfection | | | |
| Transfection Comparison | 24 | 48 | 72 | 96 |
| wt vs G1862T | 0.4065 | 0.3562 | 0.0777 | 0.3109 |
| wt vs G1896A | 0.0072 | 0.014 | 0.0194 | 0.115 |
| wt vs β-gal | 0.0125 | 0.002 | 0.0436 | 0.2505 |
| G1862T vs G1896A | 0.0817 | 0.4213 | 0.1994 | 0.3815 |
| G1862T vs β-gal | 0.1248 | 0.1265 | 0.1499 | 0.2245 |
| G1896A vs β-gal | 0.0021 | 0.0027 | 0.2607 | 0.2049 |

All figures highlighted in blue were found to be less than 0.05 and therefore significant.

*D1.2) Apoptotic cells*

| Table 4a. t-value for apoptotic cells in data set #1 | | | | |
|---|---|---|---|---|
| | Hours post-transfection | | | |
| Transfection Comparison | 24 | 48 | 72 | 96 |
| wt vs G1862T | -1.44 | 0.31 | -0.74 | 0.07 |
| wt vs G1896A | 7.48 | 2.75 | 2.32 | 0.52 |
| wt vs β-gal | -11.65 | -0.53 | 1.41 | 0.59 |
| G1862T vs G1896A | 5.56 | 0.84 | 2.37 | 2.07 |
| G1862T vs β-gal | -9.46 | -0.57 | 1.8 | 0.77 |
| G1896A vs β-gal | -13.68 | -22.31 | -0.5 | 0.3 |

| Table 4b. p-value for apoptotic cells in data set #1 | | | | |
|---|---|---|---|---|
| | Hours post-transfection | | | |
| Transfection Comparison | 24 | 48 | 72 | 96 |
| wt vs G1862T | 0.1427 | 0.3896 | 0.2676 | 0.4751 |
| wt vs G1896A | 0.0086 | 0.0551 | 0.0727 | 0.3255 |
| wt vs β-gal | 0.0036 | 0.3238 | 0.1464 | 0.3058 |
| G1862T vs G1896A | 0.0154 | 0.2439 | 0.0703 | 0.087 |
| G1862T vs β-gal | 0.0054 | 0.311 | 0.1066 | 0.2594 |
| G1896A vs β-gal | 0.0026 | 0.001 | 0.3328 | 0.394 |

*D1.3) Necrotic cells*

| Table 5a. t-value for necrotic cells in data set #1 | | | | |
|---|---|---|---|---|
| | Hours post-transfection | | | |
| Transfection Comparison | 24 | 48 | 72 | 96 |
| wt vs G1862T | -0.6 | 0.83 | 2.3 | -0.31 |
| wt vs G1896A | 1.94 | 1.48 | 1.18 | -0.19 |
| wt vs β-gal | 1.36 | -1.37 | 1.77 | 0.59 |
| G1862T vs G1896A | 2.49 | -0.009 | -1.08 | 0.16 |
| G1862T vs β-gal | 2.57 | -1.93 | -0.34 | 6.92 |
| G1896A vs β-gal | -1.26 | -4.21 | 0.64 | 1.44 |

| Table 5b. p-value for necrotic cells in data set #1 | | | | |
|---|---|---|---|---|
| | Hours post-transfection | | | |
| Transfection Comparison | 24 | 48 | 72 | 96 |
| wt vs G1862T | 0.3028 | 0.2448 | 0.0736 | 0.3917 |
| wt vs G1896A | 0.0957 | 0.1375 | 0.1795 | 0.4319 |
| wt vs β-gal | 0.153 | 0.1511 | 0.1086 | 0.3074 |
| G1862T vs G1896A | 0.0651 | 0.4964 | 0.1964 | 0.4422 |
| G1862T vs β-gal | 0.0619 | 0.0964 | 0.3818 | 0.01 |
| G1896A vs β-gal | 0.1666 | 0.0259 | 0.2919 | 0.1424 |

## *D2) DATA SET 2*

### *D2.1) Live cells*

| Table 6a. t-value for live cells in data set #2 | | | | |
|---|---|---|---|---|
| | Hours post-transfection | | | |
| Transfection Comparison | 24 | 48 | 72 | 96 |
| wt vs G1862T | 2.56 | -1.28 | -2.21 | 2.61 |
| wt vs G1896A | 0.51 | -1.92 | 0.69 | -0.75 |
| wt vs β-gal | 4.91 | 0.58 | -1.02 | 10.24 |
| G1862T vs G1896A | -0.41 | -0.12 | 1.25 | -1.59 |
| G1862T vs β-gal | 4.74 | 2.03 | 1.62 | 5.87 |
| G1896A vs β-gal | 1.68 | 3.51 | -0.95 | 4.52 |

| Table 6b. p-value for live cells in data set #2 | | | | |
|---|---|---|---|---|
| | Hours post-transfection | | | |
| Transfection Comparison | 24 | 48 | 72 | 96 |
| wt vs G1862T | 0.062 | 0.1633 | 0.0787 | 0.0601 |
| wt vs G1896A | 0.3289 | 0.0967 | 0.2782 | 0.2657 |
| wt vs β-gal | 0.0194 | 0.3079 | 0.2082 | 0.0047 |
| G1862T vs G1896A | 0.3601 | 0.4555 | 0.1684 | 0.126 |
| G1862T vs β-gal | 0.0208 | 0.089 | 0.1226 | 0.0138 |
| G1896A vs β-gal | 0.1165 | 0.0362 | 0.2207 | 0.0227 |

*D2.2) Apoptotic cells*

| Table 7a. t-value for apoptotic cells in data set #2 | | | | |
|---|---|---|---|---|
| | Hours post-transfection | | | |
| Transfection Comparison | 24 | 48 | 72 | 96 |
| wt vs G1862T | -2.7 | -5.09 | -2.1 | -1.27 |
| wt vs G1896A | -0.34 | -0.67 | -0.34 | -0.66 |
| wt vs β-gal | -2.69 | -1.2 | 0.54 | -1.35 |
| G1862T vs G1896A | 0.43 | -1.30E-15 | 1.79 | 0.22 |
| G1862T vs β-gal | -0.57 | -0.84 | 2.6 | 0.74 |
| G1896A vs β-gal | -0.68 | -0.74 | 0.9 | 0.29 |

| Table 7b. p-value for apoptotic cells in data set #2 | | | | |
|---|---|---|---|---|
| | Hours post-transfection | | | |
| Transfection Comparison | 24 | 48 | 72 | 96 |
| wt vs G1862T | 0.0568 | 0.0182 | 0.085 | 0.1657 |
| wt vs G1896A | 0.3816 | 0.285 | 0.383 | 0.2862 |
| wt vs β-gal | 0.0573 | 0.175 | 0.3188 | 0.1545 |
| G1862T vs G1896A | 0.3528 | 0.5 | 0.1068 | 0.4201 |
| G1862T vs β-gal | 0.3121 | 0.2427 | 0.0607 | 0.267 |
| G1896A vs β-gal | 0.2827 | 0.2662 | 0.2312 | 0.3991 |

*D2.3) Necrotic cells*

| Table 8a. t-value for necrotic cells in data set #2 | | | | |
|---|---|---|---|---|
| | Hours post-transfection | | | |
| Transfection Comparison | 24 | 48 | 72 | 96 |
| wt vs G1862T | -0.24 | 2.72 | 0.52 | 0.82 |
| wt vs G1896A | -0.09 | 1.62 | -0.12 | 0.67 |
| wt vs β-gal | -2.5 | 1.23 | -0.01 | -2 |
| G1862T vs G1896A | 0.24 | 0.05 | -0.67 | 0.11 |
| G1862T vs β-gal | -2.81 | 0.31 | -0.61 | -1.59 |
| G1896A vs β-gal | -5.42 | 0.25 | 0.41 | -1.22 |

| Table 8b. p-value for necrotic cells in data set #2 | | | | |
|---|---|---|---|---|
| | Hours post-transfection | | | |
| Transfection Comparison | 24 | 48 | 72 | 96 |
| wt vs G1862T | 0.4138 | 0.0563 | 0.3249 | 0.2481 |
| wt vs G1896A | 0.4655 | 0.1231 | 0.4564 | 0.2834 |
| wt vs β-gal | 0.0646 | 0.1714 | 0.4944 | 0.0916 |
| G1862T vs G1896A | 0.4135 | 0.4799 | 0.2844 | 0.4597 |
| G1862T vs β-gal | 0.053 | 0.3921 | 0.3001 | 0.1257 |
| G1896A vs β-gal | 0.0161 | 0.4124 | 0.3602 | 0.1721 |

### *D3) DATA SET 3*

#### *D3.1) Live cells*

| Table 9a. t-value for live cells in data set #3 | | | | |
|---|---|---|---|---|
| | Hours post-transfection | | | |
| Transfection Comparison | 24 | 48 | 72 | 96 |
| wt vs G1862T | 1.11 | 2.2 | 2.06 | -1.07 |
| wt vs G1896A | 1.49 | 5.91 | 0.81 | 0.22 |
| wt vs β-gal | -1.61 | -5.33 | -16.6 | 1.1 |
| G1862T vs G1896A | 0.83 | 10.3 | -0.72 | 2.18 |
| G1862T vs β-gal | -2.03 | -6.73 | -8.54 | 7.52 |
| G1896A vs β-gal | -2.13 | -8.38 | -6.3 | 1.32 |

| Table 9b. p-value for live cells in data set #3 | | | | |
|---|---|---|---|---|
| | Hours post-transfection | | | |
| Transfection Comparison | 24 | 48 | 72 | 96 |
| wt vs G1862T | 0.1902 | 0.0789 | 0.0876 | 0.1977 |
| wt vs G1896A | 0.1363 | 0.0137 | 0.2509 | 0.4213 |
| wt vs β-gal | 0.1236 | 0.0167 | 0.0018 | 0.1924 |
| G1862T vs G1896A | 0.2462 | 0.0046 | 0.2724 | 0.08 |
| G1862T vs β-gal | 0.0891 | 0.0106 | 0.0067 | 0.0086 |
| G1896A vs β-gal | 0.0833 | 0.0069 | 0.0121 | 0.1581 |

*D3.2) Apoptotic cells*

| Table 10a. t-value for apoptotic cells in data set #3 | | | | |
|---|---|---|---|---|
| | Hours post-transfection | | | |
| Transfection Comparison | 24 | 48 | 72 | 96 |
| wt vs G1862T | -1.9 | -5.56 | -9 | 0.53 |
| wt vs G1896A | -0.23 | -5.18 | -0.1 | -0.12 |
| wt vs β-gal | 1.88 | 4.72 | 1.94 | 1.17 |
| G1862T vs G1896A | 0.11 | 0.8 | 4.46 | -0.97 |
| G1862T vs β-gal | 2.8 | 7.25 | 3.32 | 0.79 |
| G1896A vs β-gal | 1.06 | 6.93 | 1.9 | 2.42 |

| Table 10b. p-value for apoptotic cells in data set #3 | | | | |
|---|---|---|---|---|
| | Hours post-transfection | | | |
| Transfection Comparison | 24 | 48 | 72 | 96 |
| wt vs G1862T | 0.0988 | 0.0153 | 0.006 | 0.3227 |
| wt vs G1896A | 0.4167 | 0.0176 | 0.4635 | 0.457 |
| wt vs β-gal | 0.1002 | 0.0209 | 0.0956 | 0.1808 |
| G1862T vs G1896A | 0.4597 | 0.2524 | 0.0233 | 0.217 |
| G1862T vs β-gal | 0.0534 | 0.0092 | 0.0399 | 0.2551 |
| G1896A vs β-gal | 0.1991 | 0.01 | 0.098 | 0.0682 |

*D3.3) Necrotic cells*

| Table 11a. t-value for necrotic cells in data set #3 | | | | |
|---|---|---|---|---|
| | Hours post-transfection | | | |
| Transfection Comparison | 24 | 48 | 72 | 96 |
| wt vs G1862T | -0.72 | 4.02 | 0.06 | 0.44 |
| wt vs G1896A | -0.77 | 1.07 | -1.2 | 2.33 |
| wt vs β-gal | 0.93 | 2.44 | 1.96 | 13.11 |
| G1862T vs G1896A | -0.33 | -2.26 | -0.73 | -0.63 |
| G1862T vs β-gal | 1.05 | -3.21 | 1.62 | -3.9 |
| G1896A vs β-gal | 0.96 | 0.17 | 2.32 | -19.99 |

| Table 11b. p-value for necrotic cells in data set #3 | | | | |
|---|---|---|---|---|
| | Hours post-transfection | | | |
| Transfection Comparison | 24 | 48 | 72 | 96 |
| wt vs G1862T | 0.2712 | 0.0282 | 0.4756 | 0.3497 |
| wt vs G1896A | 0.2596 | 0.1983 | 0.1752 | 0.0725 |
| wt vs β-gal | 0.2243 | 0.0672 | 0.0942 | 0.0028 |
| G1862T vs G1896A | 0.3836 | 0.0756 | 0.2684 | 0.296 |
| G1862T vs β-gal | 0.2014 | 0.0423 | 0.1226 | 0.0298 |
| G1896A vs β-gal | 0.2175 | 0.4402 | 0.073 | 0.0012 |

# APPENDIX E - CASPASE PROFILING RESULTS

## *E1) CASPASE 2*

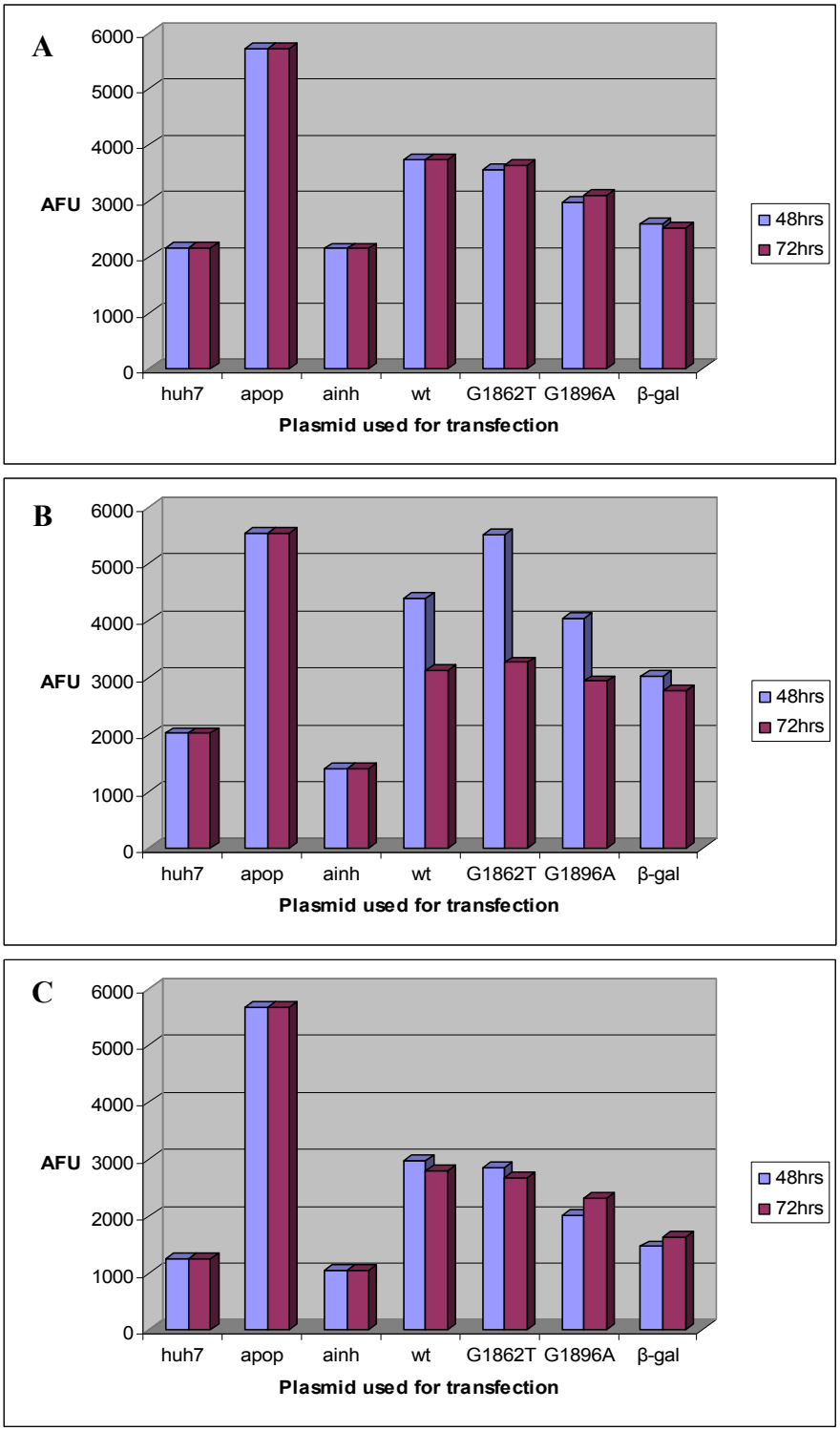


**Figure 27.** Comparison of the amount of activated caspase 2 present 48 and 72 hours post-transfection from data set one (A), two (B) and three (C).

*E2) CASPASE 8*

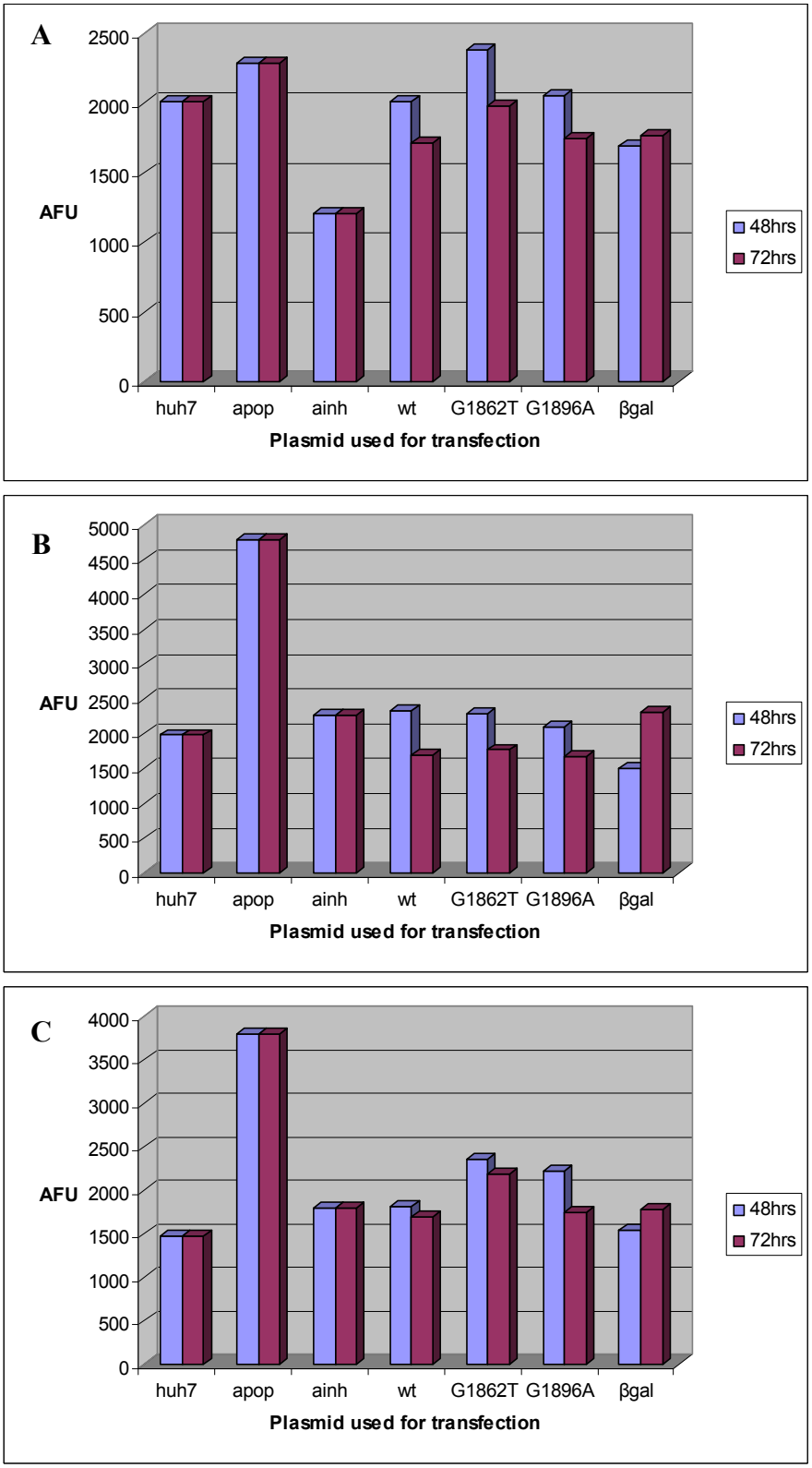


**Figure 28.** Comparison of the amount of activated caspase 8 present 48 and 72 hours post-transfection from data set one (A), two (B) and three (C).

*E3) CASPASE 9*

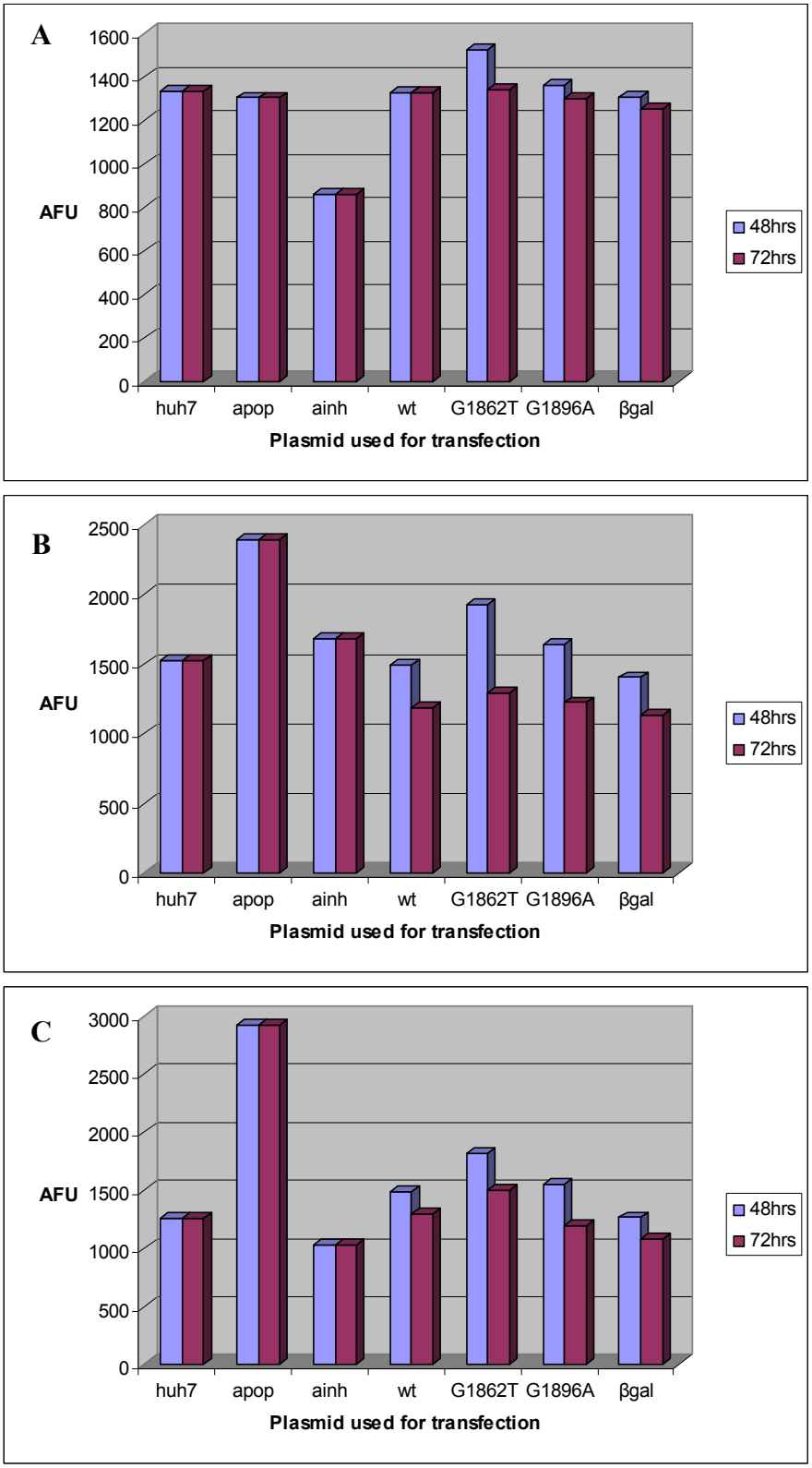


**Figure 29.** Comparison of the amount of activated caspase 9 present 48 and 72 hours post-transfection from data set one (A), two (B) and three (C).

### *E4) CASPASE 3*

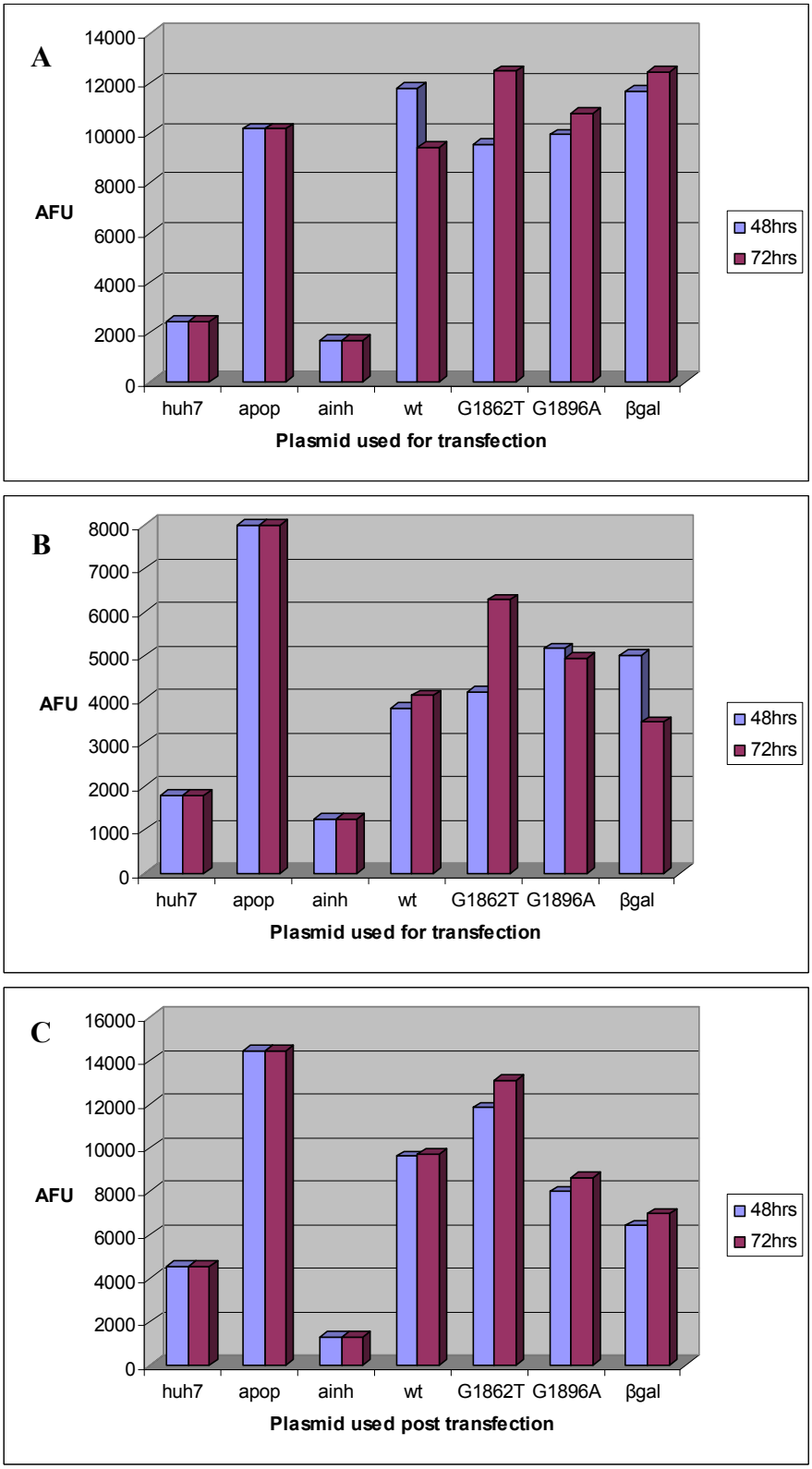


**Figure 30.** Comparison of the amount of activated caspase 3 present 48 and 72 hours post-transfection from data set one (A), two (B) and three (C).

# APPENDIX F - CASPASE PROFILING STATISTICS

## *F1) CASPASE 2*

### *F1.1) Data Set 1*

| Table 12a. t- and p- values for caspase 2 data set #1 | | | | |
|---|---|---|---|---|
| Test of difference within post-transfection hour | | | | |
| | t-values | | p -values | |
| Transfection Comparison | Hours | | Hours | |
| | 48 | 72 | 48 | 72 |
| wt vs G1862T | 1.04 | -15.79 | 0.2026 | 0.0019 |
| wt vs G1896A | 3.12 | -2.58 | 0.0444 | 0.0611 |
| wt vs β-gal | 7.31 | 0.0697 | 0.009 | 0.4753 |
| G1862TvsG1896A | 2.68 | 2.391 | 0.0574 | 0.0696 |
| G1862T vs β-gal | 9 | 22.24 | 0.006 | 0.001 |
| G1896A vs β-gal | 1.9 | 2.671 | 0.0981 | 0.0578 |
| huh7 vs apop | -19.67 | -19.67 | 0.0012 | 0.0012 |
| huh7 vs apop+inh | 0.26 | 0.26 | 0.4065 | 0.4065 |
| apop vs apop+inh | 20.29 | 20.29 | 0.0012 | 0.0012 |
| wt vs huh7 | 10.19 | 4.51 | 0.0047 | 0.0228 |
| G1862T vs huh7 | 13.31 | 27.55 | 0.0027 | 0.0006 |
| G1896A vs huh7 | 4.11 | 4.31 | 0.0271 | 0.0248 |
| B-gal vs huh7 | 6.2 | 5.54 | 0.0125 | 0.0155 |
| wt vs apop | -8.67 | -17.13 | 0.0065 | 0.0016 |
| G1862T vs apop | -10.93 | -11.92 | 0.0041 | 0.0034 |
| G1896A vs apop | -10.52 | -9.44 | 0.0044 | 0.0055 |
| B-gal vs apop | -17.16 | -17.77 | 0.0016 | 0.0015 |
| wt vs apop+inh | 10.67 | 5.44 | 0.0043 | 0.016 |
| G1862T vs apop+inh | 14.64 | 44.34 | 0.0023 | 0.0002 |
| G1896A vs apop+inh | 4.27 | 4.45 | 0.0252 | 0.0233 |
| B-gal vs apop+inh | 7.9 | 7.45 | 0.0078 | 0.0087 |

All figures highlighted in blue were found to be less than 0.05 and therefore significant.

*F1.2) Data Set 2*

| Table 12b. t- and p- values for caspase 2 data set #2 | | | | |
|---|---|---|---|---|
| Test of difference within post-transfection hour | | | | |
| | t-values | | p -values | |
| Transfection | Hours | | Hours | |
| Comparison | 48 | 72 | 48 | 72 |
| wt vs G1862T | -4.35 | -0.69 | 0.0243 | 0.2807 |
| wt vs G1896A | 1.33 | 0.9 | 0.1573 | 0.2303 |
| wt vs β-gal | 5.63 | 1.55 | 0.015 | 0.1298 |
| G1862TvsG1896A | 10.81 | 2.72 | 0.0042 | 0.0563 |
| G1862T vs β-gal | 33.71 | 3.2 | 0.0004 | 0.0426 |
| G1896A vs β-gal | 8.78 | 1.01 | 0.0063 | 0.2077 |
| huh7 vs apop | -89.69 | -89.69 | 6.21E-05 | 6.21E-05 |
| huh7 vs apop+inh | 30.6 | 30.6 | 0.0005 | 0.0005 |
| apop vs apop+inh | 119.91 | 119.91 | 3.48E-05 | 3.48E-05 |
| wt vs huh7 | 9.76 | 5.85 | 0.0051 | 0.0139 |
| G1862T vs huh7 | 46.72 | 16.3 | 0.0002 | 0.0018 |
| G1896A vs huh7 | 17.41 | 9.27 | 0.0016 | 0.0057 |
| β-gal vs huh7 | 41.52 | 5.29 | 0.0002 | 0.0169 |
| wt vs apop | -4.62 | -12.65 | 0.0218 | 0.003 |
| G1862T vs apop | -0.37 | -28.06 | 0.3712 | 0.0006 |
| G1896A vs apop | -12.49 | -25.43 | 0.0031 | 0.0007 |
| β-gal vs apop | -67.81 | -19.45 | 0.0001 | 0.0013 |
| wt vs apop+inh | 12.36 | 9.21 | 0.0032 | 0.0057 |
| G1862T vs apop+inh | 56.88 | 25.32 | 0.0001 | 0.0007 |
| G1896A vs apop+inh | 23.09 | 15.9 | 0.0009 | 0.0019 |
| β-gal vs apop+inh | 104.09 | 9.84 | 4.61E-05 | 0.005 |

*F1.3) Data Set 3*

| Table 12c. t- and p- values for caspase 2 data set #3 | | | | |
|---|---|---|---|---|
| Test of difference within post-transfection hour | | | | |
| | t-values | | p -values | |
| Transfection Comparison | Hours | | Hours | |
| | 48 | 72 | 48 | 72 |
| wt vs G1862T | 0.59 | 2.29 | 0.3065 | 0.0741 |
| wt vs G1896A | 5.54 | 6.3 | 0.0154 | 0.0121 |
| wt vs β-gal | 11.38 | 20.94 | 0.0038 | 0.0011 |
| G1862TvsG1896A | 4.48 | 6.08 | 0.231 | 0.0129 |
| G1862T vs β-gal | 9.16 | 38.03 | 0.0058 | 0.0003 |
| G1896A vs β-gal | 4.77 | 11.19 | 0.0205 | 0.0039 |
| huh7 vs apop | -14.98 | -14.98 | 0.0022 | 0.0022 |
| huh7 vs apop+inh | 4.65 | 4.65 | 0.0215 | 0.0215 |
| apop vs apop+inh | 15.71 | 15.71 | 0.002 | 0.002 |
| wt vs huh7 | 12.58 | 25.63 | 0.0031 | 0.0007 |
| G1862T vs huh7 | 10.3 | 39.34 | 0.0046 | 0.0003 |
| G1896A vs huh7 | 6.34 | 16.3 | 0.0119 | 0.0018 |
| β-gal vs huh7 | 6.3 | 9.61 | 0.0121 | 0.0053 |
| wt vs apop | -8.38 | -9.69 | 0.0069 | 0.0052 |
| G1862T vs apop | -8.53 | -10.23 | 0.0067 | 0.0047 |
| G1896A vs apop | -11.67 | -11.25 | 0.0036 | 0.0039 |
| β-gal vs apop | -14.36 | -13.73 | 0.0024 | 0.0026 |
| wt vs apop+inh | 14.15 | 29.32 | 0.0024 | 0.0005 |
| G1862T vs apop+inh | 11.68 | 45.86 | 0.0036 | 0.0002 |
| G1896A vs apop+inh | 8.16 | 19.65 | 0.0073 | 0.0012 |
| β-gal vs apop+inh | 12.99 | 15.14 | 0.0029 | 0.0021 |

## *F2) CASPASE 8*

### *F2.1) Data Set 1*

| Table 13a. t- and p- values for caspase 8 data set #1 | | | | |
|---|---|---|---|---|
| Test of difference within post-transfection hour | | | | |
| | t-values | | p -values | |
| Transfection | Hours | | Hours | |
| Comparison | 48 | 72 | 48 | 72 |
| wt vs G1862T | -9.82 | -2.18 | 0.0051 | 0.0804 |
| wt vs G1896A | -0.81 | -0.33 | 0.2511 | 0.3858 |
| wt vs β-gal | 8.69 | -0.58 | 0.0064 | 0.3096 |
| G1862TvsG1896A | 7.35 | 2.42 | 0.009 | 0.0682 |
| G1862T vs β-gal | 24.64 | 2.74 | 0.0008 | 0.0555 |
| G1896A vs β-gal | 8.24 | -0.31 | 0.0072 | 0.3898 |
| huh7 vs apop | -14.23 | -14.23 | 0.0024 | 0.0024 |
| huh7 vs apop+inh | -9.19 | -9.19 | 0.0058 | 0.0058 |
| apop vs apop+inh | 9.06 | 9.06 | 0.0059 | 0.0059 |
| wt vs huh7 | 0.06 | -3.08 | 0.4785 | 0.0455 |
| G1862T vs huh7 | 16.64 | -0.51 | 0.0017 | 0.3295 |
| G1896A vs huh7 | 1.05 | -4.37 | 0.2004 | 0.0242 |
| β-gal vs huh7 | -14.75 | -10.47 | 0.0022 | 0.0044 |
| wt vs apop | -7.56 | -5.82 | 0.0085 | 0.0141 |
| G1862T vs apop | 3.76 | -4.19 | 0.032 | 0.0261 |
| G1896A vs apop | -5.32 | -8.69 | 0.0167 | 0.0064 |
| β-gal vs apop | -23.13 | -19.18 | 0.0009 | 0.0013 |
| wt vs apop+inh | -3.3 | -4.21 | 0.0404 | 0.026 |
| G1862T vs apop+inh | 12.27 | -2.02 | 0.0032 | 0.09 |
| G1896A vs apop+inh | -1.63 | -6.22 | 0.122 | 0.0124 |
| β-gal vs apop+inh | -20.68 | -15.81 | 0.0011 | 0.0019 |

*F2.2) Data Set 2*

| Table 13b. t- and p- values for caspase 8 data set #2 | | | | |
|---|---|---|---|---|
| Test of difference within post-transfection hour | | | | |
| | t-values | | p -values | |
| Transfection Comparison | Hours | | Hours | |
| | 48 | 72 | 48 | 72 |
| wt vs G1862T | 0.31 | -0.71 | 0.3896 | 0.2737 |
| wt vs G1896A | 1.6 | 0.26 | 0.1246 | 0.4071 |
| wt vs β-gal | 0.2 | 1.91 | 0.4266 | 0.0981 |
| G1862TvsG1896A | 1.84 | 2.01 | 0.1032 | 0.0905 |
| G1862T vs β-gal | -0.21 | 3.76 | 0.4235 | 0.0319 |
| G1896A vs β-gal | -2.71 | 3.22 | 0.0563 | 0.0421 |
| huh7 vs apop | -6.78 | -6.78 | 0.0105 | 0.0105 |
| huh7 vs apop+inh | -3.37 | -3.37 | 0.0389 | 0.0389 |
| apop vs apop+inh | 6.03 | 6.03 | 0.0131 | 0.0131 |
| wt vs huh7 | 2.63 | -3.05 | 0.0595 | 0.0461 |
| G1862T vs huh7 | 3.55 | -3.7 | 0.0353 | 0.0329 |
| G1896A vs huh7 | 1.83 | -8.7 | 0.1043 | 0.0064 |
| β-gal vs huh7 | 5.72 | -7.55 | 0.0145 | 0.0085 |
| wt vs apop | -5.68 | -7.33 | 0.0147 | 0.009 |
| G1862T vs apop | -5.96 | -7.28 | 0.0134 | 0.0091 |
| G1896A vs apop | -6.44 | -7.55 | 0.0116 | 0.0085 |
| β-gal vs apop | -5.99 | -7.9 | 0.0133 | 0.0078 |
| wt vs apop+inh | 0.49 | -4.93 | 0.3358 | 0.0193 |
| G1862T vs apop+inh | 0.23 | -5.61 | 0.4188 | 0.0151 |
| G1896A vs apop+inh | -1.62 | -7.83 | 0.1227 | 0.0079 |
| β-gal vs apop+inh | 0.51 | -8.27 | 0.51 | 0.0071 |

*F2.3) Data Set 3*

| Table 13c. t- and p- values for caspase 8 data set #3 | | | | |
|---|---|---|---|---|
| Test of difference within post-transfection hour | | | | |
| | t-values | | p -values | |
| Transfection | Hours | | Hours | |
| Comparison | 48 | 72 | 48 | 72 |
| wt vs G1862T | -6.01 | -6.35 | 0.0132 | 0.0119 |
| wt vs G1896A | -9.09 | -5.28 | 0.0059 | 0.0169 |
| wt vs β-gal | 0.42 | 9.31 | 0.3566 | 0.0056 |
| G1862TvsG1896A | 0.78 | 5.75 | 0.2574 | 0.0144 |
| G1862T vs β-gal | 4.84 | 8.05 | 0.02 | 0.0075 |
| G1896A vs β-gal | 5.35 | 16.47 | 0.0166 | 0.0018 |
| huh7 vs apop | -57.58 | -57.58 | 0.0001 | 0.0001 |
| huh7 vs apop+inh | -10.45 | -10.45 | 0.0045 | 0.0045 |
| apop vs apop+inh | 65.01 | 65.01 | 0.0001 | 0.0001 |
| wt vs huh7 | 11.92 | 7.62 | 0.0034 | 0.0083 |
| G1862T vs huh7 | 9.87 | 8.69 | 0.005 | 0.0064 |
| G1896A vs huh7 | 14.22 | 9.89 | 0.0024 | 0.005 |
| β-gal vs huh7 | 4.46 | 2.85 | 0.0233 | 0.052 |
| wt vs apop | -73.27 | -72.47 | 9.31E-05 | 9.52E-05 |
| G1862T vs apop | -17.76 | -16.81 | 0.0015 | 0.0017 |
| G1896A vs apop | -29.95 | -75.45 | 0.0005 | 8.78E-05 |
| β-gal vs apop | -27.3 | -75.67 | 0.0006 | 8.73E-05 |
| wt vs apop+inh | 0.75 | -5.97 | 0.2646 | 0.0134 |
| G1862T vs apop+inh | 6.05 | 5.1 | 0.013 | 0.0181 |
| G1896A vs apop+inh | 8.89 | -3.45 | 0.0062 | 0.0373 |
| β-gal vs apop+inh | -0.25 | -13.52 | 0.4105 | 0.0027 |

## *F3) CASPASE 9*

### *F3.1) Data Set 1*

| Table 14a. t- and p- values for caspase 9 data set #1 | | | | |
|---|---|---|---|---|
| Test of difference within post-transfection hour | | | | |
| | t-values | | p -values | |
| Transfection | Hours | | Hours | |
| Comparison | 48 | 72 | 48 | 72 |
| wt vs G1862T | -3.09 | -0.24 | 0.0452 | 0.4156 |
| wt vs G1896A | -0.6 | 0.57 | 0.3029 | 0.3111 |
| wt vs β-gal | 0.68 | 2.44 | 0.2818 | 0.0669 |
| G1862TvsG1896A | 1.9 | 0.61 | 0.0983 | 0.3 |
| G1862T vs β-gal | 3.14 | 1.56 | 0.0439 | 0.129 |
| G1896A vs β-gal | 0.87 | 1.37 | 0.2378 | 0.152 |
| huh7 vs apop | 0.77 | 0.77 | 0.2586 | 0.2586 |
| huh7 vs apop+inh | 15.7 | 15.7 | 0.002 | 0.002 |
| apop vs apop+inh | 2.86 | 2.86 | 0.0517 | 0.0517 |
| wt vs huh7 | -0.86 | -0.38 | 0.2385 | 0.3699 |
| G1862T vs huh7 | 2.99 | 0.081 | 0.0477 | 0.4713 |
| G1896A vs huh7 | 0.47 | -1.05 | 0.3412 | 0.2005 |
| β-gal vs huh7 | -0.99 | -6.67 | 0.2117 | 0.0108 |
| wt vs apop | 0.57 | 0.43 | 0.3125 | 0.3528 |
| G1862T vs apop | 2.94 | 0.52 | 0.0494 | 0.3248 |
| G1896A vs apop | 0.84 | -0.06 | 0.2445 | 0.4766 |
| β-gal vs apop | 0.07 | -1.22 | 0.4752 | 0.1726 |
| wt vs apop+inh | 11.04 | 4.88 | 0.004 | 0.0197 |
| G1862T vs apop+inh | 5.36 | 2.78 | 0.0165 | 0.054 |
| G1896A vs apop+inh | 3.1 | 3.36 | 0.0449 | 0.0391 |
| β-gal vs apop+inh | 4.12 | 4.33 | 0.0269 | 0.0246 |

*F3.2) Data Set 2*

| Table 14b. t- and p- values for caspase 9 data set #2 | | | | |
|---|---|---|---|---|
| Test of difference within post-transfection hour | | | | |
| | t-values | | p -values | |
| Transfection Comparison | Hours | | Hours | |
| | 48 | 72 | 48 | 72 |
| wt vs G1862T | -5.9 | -3.25 | 0.0137 | 0.0414 |
| wt vs G1896A | -2.3 | -0.46 | 0.0739 | 0.3447 |
| wt vs β-gal | 3.2 | 0.89 | 0.0424 | 0.2333 |
| G1862TvsG1896A | 3 | 1.02 | 0.0476 | 0.2056 |
| G1862T vs β-gal | 7 | 2.89 | 0.0098 | 0.0508 |
| G1896A vs β-gal | 3.61 | 1.04 | 0.0343 | 0.2021 |
| huh7 vs apop | -7.13 | -7.13 | 0.0095 | 0.0095 |
| huh7 vs apop+inh | -4.7 | -4.7 | 0.0211 | 0.0211 |
| apop vs apop+inh | 5.79 | 5.79 | 0.0142 | 0.0142 |
| wt vs huh7 | -1.14 | -9.43 | 0.1464 | 0.0055 |
| G1862T vs huh7 | 5.42 | -13.54 | 0.0161 | 0.0027 |
| G1896A vs huh7 | 1.76 | -4.45 | 0.11 | 0.0234 |
| β-gal vs huh7 | -4.38 | -6.86 | 0.0241 | 0.0102 |
| wt vs apop | -7.42 | -9.73 | 0.0088 | 0.0051 |
| G1862T vs apop | -3.33 | -9.2 | 0.0396 | 0.0057 |
| G1896A vs apop | -5.55 | -8.54 | 0.0154 | 0.0067 |
| β-gal vs apop | -8.12 | -9.57 | 0.0074 | 0.0053 |
| wt vs apop+inh | -5.82 | -11.84 | 0.014 | 0.0035 |
| G1862T vs apop+inh | 3.22 | -14.39 | 0.042 | 0.0023 |
| G1896A vs apop+inh | -0.56 | -6.37 | 0.3153 | 0.0118 |
| β-gal vs apop+inh | -7.86 | -8.94 | 0.0078 | 0.0061 |

*F3.3) Data Set 3*

| Table 14c. t- and p- values for caspase 9 data set #3 | | | | |
|---|---|---|---|---|
| Test of difference within post-transfection hour | | | | |
| | t-values | | p -values | |
| Transfection | Hours | | Hours | |
| Comparison | 48 | 72 | 48 | 72 |
| wt vs G1862T | -4.24 | -6.23 | 0.0256 | 0.0124 |
| wt vs G1896A | -1.66 | 3.83 | 0.1187 | 0.0308 |
| wt vs β-gal | 6.63 | 8.1 | 0.0109 | 0.0074 |
| G1862TvsG1896A | 3.47 | 15.07 | 0.0368 | 0.0021 |
| G1862T vs β-gal | 7.71 | 20.86 | 0.0081 | 0.0011 |
| G1896A vs β-gal | 11.08 | 10.07 | 0.004 | 0.0048 |
| huh7 vs apop | -10.05 | -10.05 | 0.0048 | 0.0048 |
| huh7 vs apop+inh | 2.27 | 2.27 | 0.0754 | 0.0754 |
| apop vs apop+inh | 14.31 | 14.31 | 0.0024 | 0.0024 |
| wt vs huh7 | 2.17 | 0.42 | 0.0808 | 0.3571 |
| G1862T vs huh7 | 4.58 | 2.34 | 0.0222 | 0.0719 |
| G1896A vs huh7 | 2.89 | -0.58 | 0.0507 | 0.308 |
| β-gal vs huh7 | 0.08 | -1.72 | 0.4682 | 0.1133 |
| wt vs apop | -10.55 | -12.06 | 0.0044 | 0.0034 |
| G1862T vs apop | -7.31 | -10.71 | 0.009 | 0.0043 |
| G1896A vs apop | -10.15 | -13.03 | 0.0047 | 0.0029 |
| β-gal vs apop | -12.54 | -13.89 | 0.0031 | 0.0025 |
| wt vs apop+inh | 13.45 | 10.15 | 0.0027 | 0.0047 |
| G1862T vs apop+inh | 10.94 | 23.65 | 0.0041 | 0.0008 |
| G1896A vs apop+inh | 19.37 | 14.93 | 0.0013 | 0.0022 |
| β-gal vs apop+inh | 27.73 | 4.86 | 0.0006 | 0.0199 |

## *F4) CASPASE 3*

### *F4.1) Data Set 1*

| Table 15a. t- and p- values for caspase 3 data set #1 | | | | |
|---|---|---|---|---|
| Test of difference within post-transfection hour | | | | |
| | t-values | | p -values | |
| Transfection Comparison | Hours | | Hours | |
| | 48 | 72 | 48 | 72 |
| wt vs G1862T | 3.13 | -5.74 | 0.0442 | 0.0144 |
| wt vs G1896A | 4.04 | -2.47 | 0.028 | 0.0659 |
| wt vs β-gal | 0.36 | -5.75 | 0.3752 | 0.0144 |
| G1862TvsG1896A | -0.5 | 7.02 | 0.3322 | 0.0098 |
| G1862T vs β-gal | -3.25 | 0.22 | 0.0414 | 0.4208 |
| G1896A vs β-gal | -4.84 | -7.4 | 0.02 | 0.0088 |
| huh7 vs apop | -121.6 | -121.6 | 3.38E-05 | 3.38E-05 |
| huh7 vs apop+inh | 12.35 | 12.35 | 0.0032 | 0.0032 |
| apop vs apop+inh | 3006.3 | 3006.3 | 5.53E-08 | 5.53E-08 |
| wt vs huh7 | 32.46 | 13.38 | 0.0004 | 0.0027 |
| G1862T vs huh7 | 10.86 | 64.44 | 0.0041 | 0.0001 |
| G1896A vs huh7 | 20.45 | 40.18 | 0.0011 | 0.0003 |
| β-gal vs huh7 | 145.11 | 79.41 | 2.37E-05 | 7.93E-05 |
| wt vs apop | 5.72 | -1.48 | 0.0145 | 0.1377 |
| G1862T vs apop | -0.94 | 16.23 | 0.2216 | 0.0018 |
| G1896A vs apop | -0.67 | 3.04 | 0.2853 | 0.0466 |
| β-gal vs apop | 530.68 | 20.87 | 1.78E-06 | 0.0011 |
| wt vs apop+inh | 36.09 | 15 | 0.0003 | 0.0022 |
| G1862T vs apop+inh | 12.12 | 76.11 | 0.0033 | 8.63E-05 |
| G1896A vs apop+inh | 2294 | 46.2 | 0.0009 | 0.0002 |
| β-gal vs apop+inh | 3536.9 | 99.23 | 4.00E-08 | 5.08E-05 |

*F4.2) Data Set 2*

| Table 15b. t- and p- values for caspase 3 data set #2 | | | | |
|---|---|---|---|---|
| Test of difference within post-transfection hour | | | | |
| | t-values | | p -values | |
| Transfection | Hours | | Hours | |
| Comparison | 48 | 72 | 48 | 72 |
| wt vs G1862T | -1.33 | -12.66 | 0.1573 | 0.003 |
| wt vs G1896A | -5.2 | -1.8 | 0.0174 | 0.1062 |
| wt vs β-gal | -4.1 | 2.58 | 0.0272 | 0.0612 |
| G1862TvsG1896A | -6.62 | 2.73 | 0.011 | 0.0557 |
| G1862T vs β-gal | -4.11 | 11.19 | 0.0271 | 0.0039 |
| G1896A vs β-gal | 0.78 | 2.87 | 0.2577 | 0.051 |
| huh7 vs apop | -11.35 | -11.35 | 0.0038 | 0.0038 |
| huh7 vs apop+inh | 10.99 | 10.99 | 0.004 | 0.004 |
| apop vs apop+inh | 12.31 | 12.31 | 0.0032 | 0.0032 |
| wt vs huh7 | 7.8 | 21.1 | 0.008 | 0.0011 |
| G1862T vs huh7 | 17.74 | 32.02 | 0.0015 | 0.0004 |
| G1896A vs huh7 | 45.14 | 6.71 | 0.0002 | 0.01 |
| β-gal vs huh7 | 19.86 | 7.91 | 0.0012 | 0.0077 |
| wt vs apop | -6.99 | -7.05 | 0.0099 | 0.0097 |
| G1862T vs apop | -6.81 | -3.04 | 0.0104 | 0.0465 |
| G1896A vs apop | -5.15 | -4.24 | 0.0178 | 0.0256 |
| β-gal vs apop | -5.22 | -7.74 | 0.0173 | 0.0081 |
| wt vs apop+inh | 9.81 | 24.63 | 0.0051 | 0.0008 |
| G1862T vs apop+inh | 20.96 | 34.63 | 0.0011 | 0.0004 |
| G1896A vs apop+inh | 46.65 | 7.84 | 0.0002 | 0.0079 |
| β-gal vs apop+inh | 22.59 | 10.31 | 0.0009 | 0.0046 |

*F4.3) Data Set 3*

| Table 15c. t- and p- values for caspase 3 data set #3 | | | | |
|---|---|---|---|---|
| Test of difference within post-transfection hour | | | | |
| | t-values | | p -values | |
| Transfection | Hours | | Hours | |
| Comparison | 48 | 72 | 48 | 72 |
| wt vs G1862T | -6.62 | -15.97 | 0.011 | 0.0019 |
| wt vs G1896A | 1.96 | 25.93 | 0.0941 | 0.0007 |
| wt vs β-gal | 3.99 | 10.1 | 0.0286 | 0.0048 |
| G1862TvsG1896A | 11.94 | 28.68 | 0.0034 | 0.0006 |
| G1862T vs β-gal | 11.17 | 16.05 | 0.0039 | 0.0019 |
| G1896A vs β-gal | 2.79 | 4.97 | 0.0537 | 0.019 |
| huh7 vs apop | -24.31 | -24.31 | 0.0008 | 0.0008 |
| huh7 vs apop+inh | 14.42 | 14.42 | 0.0023 | 0.0023 |
| apop vs apop+inh | 38.08 | 38.08 | 0.0003 | 0.0003 |
| wt vs huh7 | 9.97 | 22.2 | 0.0049 | 0.001 |
| G1862T vs huh7 | 27.24 | 28.37 | 0.0006 | 0.0006 |
| G1896A vs huh7 | 10.73 | 15.21 | 0.0042 | 0.0021 |
| β-gal vs huh7 | 4.36 | 4.82 | 0.0243 | 0.0202 |
| wt vs apop | -8.28 | -14.03 | 0.0071 | 0.0025 |
| G1862T vs apop | -3.36 | -7.15 | 0.039 | 0.0094 |
| G1896A vs apop | -12.81 | -18.87 | 0.003 | 0.0013 |
| β-gal vs apop | -12.35 | -17.38 | 0.0032 | 0.0016 |
| wt vs apop+inh | 18.03 | 107.74 | 0.0015 | 4.31E-05 |
| G1862T vs apop+inh | 51.71 | 74.4 | 0.0001 | 9.03E-05 |
| G1896A vs apop+inh | 23.7 | 98.57 | 0.0008 | 5.14E-05 |
| β-gal vs apop+inh | 11.26 | 16.18 | 0.0038 | 0.0018 |

# REFERENCES


1. Aiba, N., M.J. McGarvey, J. Waters, S.J. Hadziyannis, H.C. Thomas, P. Karayiannis, *The precore sequence of hepatitis B virus is required for nuclear localization of the core protein.* Hepatology,1997. **26**: p. 1311-7.

2. Alnemri, E.S., *Mammalian cell death proteases: a family of highly conserved aspartate specific cysteine proteases.* J Cell Biochem,1997. **64**: p. 33-42.

3. Arends, M.J., R.G. Morris, A.H. Wyllie, *Apoptosis: the role of the endonuclease.* Am J Pathol,1990. **136**: p. 593-608.

4. Arsura, M., G.R. Panta, J.D. Bilyeu, L.G. Cavin, M.A. Soyak, A.A. Oliver, V. Factor, R. Heuchel, F. Mercurio, S.S. Thorgeirsson, G.E. Sonenshein, *Transient activation of NF-kappaB through a TAK1/IKK kinase pathway by TGF-beta1 inhibits AP-1/SMAD signaling and apoptosis: implications in liver tumor formation*. Oncogene, 2003. **22**: p. 412-25.

5. Atlas of Genetics and Cytogenetics in Oncology and Haematology, *The Fas - Fas Ligand apoptotic pathway.* 2005 <http://www.infobiogen.fr/services/chromcancer/Deep/Fas-FasLigandID20039.html> [Accessed 10.01.2005]

6. Barrett, A.J., *Nomenclature Committee of the International Union of Biochemistry and Molecular Biology (NC-IUBMB). Enzyme Nomenclature. Recommendations 1992. Supplement 4: corrections and additions (1997).* Eur J Biochem, 1997. **250**: p. 1-6.

7. Bergeron, L., G.I. Perez, G. Macdonald G, L. Shi, Y. Sun, A. Jurisicova, S. Varmuza, K.E. Latham, J.A. Flaws, J.C. Salter, H. Hara, M.A. Moskowitz, E. Li, A. Greenberg, J.L. Tilly, J. Yuan, *Defects in regulation of apoptosis in caspase-2-deficient mice*. Genes Dev, 1998. **12**: p. 1304-14.

8. Bernardi, P., *Modulation of the mitochondrial cyclosporin A-sensitive permeability transition pore by the proton electrochemical gradient. Evidence that the pore can be opened by the membrane depolarization.* J Biol Chem, 1992. **267**: p. 8834-39.

9. Blobel, G., B. Dobberstein, *Transfer of proteins across membranes. I. Presence of proteolytically processed and unprocessed nascent immunoglobulin light chains on membrane-bound ribosomes of murine myeloma.* J Cell Biol, 1975. **67**: p. 835-51.

10. Braakman, I., H. Hoover-Litty, K.R. Wagner, A. Helenius, *Folding of influenza hemagglutinin in the endoplasmic reticulum.* J Cell Biol, 1991. **114**: p. 401-11.

11. Bradham, C.A., T. Qian, K. Streetz, C. Trautwein, D.A. Brenner, J.J. Lemasters, *The mitochondrial permeability transition is required for tumor necrosis factor alpha-mediated apoptosis and cytochrome c release.* Mol Cell Biol, 1998. **18**: p. 6353-64.

12. Breckenridge, D.G., M. Nguyen, S. Kupping, M. Reth, G.C. Shore, *The procaspase-8 isoform, procaspase-8L, recruited to the BAP31 complex at the endoplasmic reticulum*. Proc. Natl. Acad. Sci. USA, 2002. **99**: p. 4331-36.

13. Bruss, V., W.H. Gerlich, *Formation of transmembraneous hepatitis B e-antigen by cotranslational in vitro processing of the viral precore protein.* Virology, 1988. **163**: p. 268-75.

14. Callea, F., M. Brisigotti, G. Fabbretti, F. Bonino, V.J. Desmet, *Hepatic endoplasmic reticulum storage diseases.* Liver, 1992. **12**: p. 357-62.

15. Carman, W.F., M.R. Jacyna, S. Hadziyannis, P. Karayiannis, M.J. McGarvey, A. Makris, H.C. Thomas, *Mutation preventing formation of hepatitis B e antigen in patients with chronic hepatitis B infection.* Lancet, 1989. **2**: p. 588-90.

16. Carman, W.F., M. Thursz, S. Hadziyannis, G. McIntyre, K. Colman, A. Gioustoz, G. Fattovich, A. Alberti, H.C. Thomas, *Hepatitis B e antigen negative chronic active hepatitis: hepatitis B virus core mutations occur predominantly in known antigenic determinants.* J Viral Hepat, 1995. **2**: p. 77-84.

17. Cavin, L.G., R. Romieu-Mourez, G.R. Panta, J. Sun, V.M. Factor, S.S. Thorgeirsson, G.E. Sonenshein, M. Arsura. *Inhibition of CK2 activity by TGF-beta1 promotes IkappaB-alpha protein stabilization and apoptosis of immortalized hepatocytes*. Hepatology, 2003. **38**: p. 1540-51.

18. Chinese Medical Journal, *ER stress pathways*. 2004 < http://www.cmj.org/2wl/ yuanchangqing2.htm> [Accessed 16.02.2004]

19. Ciechanover, A., A.L. Schwartz, *The ubiquitin-proteasome pathway: the complexity and myriad functions of proteins death.* Proc Natl Acad Sci U S A, 1998. **95**: p. 2727-30.

20. Clement, M.V., I. Stamenkovic, *Fas and tumour necrosis factor receptor-mediated cell death: similarities and distinctions.* J Exp Med, 1994. **180**: p. 557-67.

21. Constantini, P., B.V. Chernyak, V. Petronilli, P. Bernardi, *Modulation of the mitochondrial permeability transition pore by pyridine nucleotides and dithiol oxidation at two separate sites.* J. Biol. Chem, 1996. **271**: p. 6746-51.

22. Dusheiko, G.M., S.M. Bowyer, M.H. Sjogren, M.J. Ritchie, A.P. Santos, M.C. Kew, *Replication of hepatitis B virus in adult carriers in an endemic area.* J Infect Dis, 1985. **152**: p. 566-71.

23. Dusheiko, G.M., B.A. Brink, J.D. Conradie, T. Marimuthu, R. Sher, *Regional prevalence of hepatitis B, delta, and human immunodeficiency virus infection in southern Africa: a large population survey.* Am J Epidemiol, 1989. **129**: p. 138-45.

24. Dusheiko, G.M., J.D. Conradie, B.A. Brink, T. Marimuthu, R. Sher, *Differences in the regional prevalence of chronic hepatitis B in southern Africa--implications for vaccination.* S Afr Med J, 1989. **75**: p. 473-78.

25. Eguchi, Y., S. Shimizu, Y. Tsujimoto, *Intracellular ATP levels determine cell death fate by apoptosis or necrosis.* Cancer Res, 1997. **57**: p. 1835-40.

26. Ellis, R.J., S.M. van der Vies, S.M. Hemmingsen, *The molecular chaperone concept.* Biochem Soc Symp, 1989. **55**: p. 145-53.

27. Fagioli, C., A. Mezghrani, R. Sitia, *Reduction of interchain disulfide bonds precedes the dislocation of Ig-mu chains from the endoplasmic reticulum to the cytosol for proteasomal degradation.* J Biol Chem, 2001. **276**: p. 40962-7.

28. Fallows, D.A., S.P. Goff, *Mutations in the epsilon sequences of human hepatitis B virus affect both RNA encapsidation and reverse transcription*. J Virol, 1995. **69**: 3067-3073.

29. Galle, P.R., P.H. Krammer, *CD95-induced apoptosis in human liver disease.* Semin Liver Dis, 1998. **18**: p. 141-51.

30. Ganem, D., A.M. Prince, *Hepatitis B virus infection--natural history and clinical consequences.* N Engl J Med, 2004. **350**: p. 1118-29.

31. Ganem, D., H.E. Varmus, *The molecular biology of the hepatitis B viruses.* Annu Rev Biochem, 1987. **56**: p. 651-93.

32. Garcia-Ruiz, C., A. Colell, M. Mari, A. Morales, J.C. Fernandez-Checa, *Direct effect of ceramide on the mitochondrial electron transport chain leads to generation of reactive oxygen species. Role of mitochondrial glutathione.* J Biol Chem, 1997. **272**: p. 11369-77.

33. Garcia-Ruiz, C., A. Colell, R. Paris, J.C. Fernandez-Checa, *Direct interaction of GD3 ganglioside with mitochondria generates reactive oxygen species followed by mitochondrial permeability transition, cytochrome c release, and caspase activation.* Faseb J, 2000. **14**: p. 847-58.

34. Gonzales-Amaro, R., C. Garcia-Monzon, L. Garcia-Buey, R. Moreno-Otero, J.L. Alonso, E. Yague, J.P. Pivel, M. Lopez-Cabrera, E Fernandez-Ruiz, F. Sanchez-Madrid, *Induction of tumour necrosis factor alpha by human hepatocytes in chronic viral hepatitis.* J Exp Med, 1994. **179**: p. 841-48.

35. Grutter, M.G., *Caspases: key players in programmed cell death.* Curr Opin Struct Biol, 2000. **10** (6): p. 649-55.

36. Guicciardi, M.E., J. Deussing, H. Miyoshi, S.F. Bronk, P.A. Svingen, C. Peters, S.H. Kaufmann, G.J. Gores, *Cathepsin B contributes to TNF-alpha-mediated hepatocyte apoptosis by promoting mitochondrial release of cytochrome c.* J Clin Invest, 2000. **106**: p. 1127-37.

37. Gunter, T.E., D.R. Pfeiffer, *Mechanisms by which mitochondria transport calcium* . Am J Physiol, 1990. **258**: p. C755-86.

38. Hammond, C., A. Helenius, *Quality control in the secretory pathway.* Curr Opin Cell Biol, 1995. **7**: p. 523-9.

39. Hartl, F.U., *Molecular chaperones in cellular protein folding.* Nature, 1996. **381**: p. 571-9.

40. Hatano, E., C.A. Bradham, A. Stark, Y. Iimuro, J.J. Lemasters, D.A. Brenner, *The mitochondrial permeability transition augments Fas-induced apoptosis in mouse hepatocytes.* J Biol Chem, 2000. **275**: p. 11814-23.

41. Helenius, A., T. Marquardt, I. Braakman, *The endoplasmic reticulum as a protein-folding compartment.* Trends Cell Biol, 1992. **2**: p. 227-31.

42. Hentze, H., M. Latta, G. Kunstle, S. Dhakshinamoorthy, P.Y. Ng, A.G. Porter, A. Wendel, *Topoisomerase inhibitor camptothecin sensitizes mouse hepatocytes in vitro and in vivo to TNF-mediated apoptosis.* Hepatology, 2004. **39**: p.1311-20.

43. Herr, I., K.M. Debatin, *Cellular stress response and apoptosis in cancer therapy*. Blood, 2001. **98**: p. 2603-14.

44. Hershko, A., A. Ciechanover, A. Varshavsky, *Basic Medical Research Award. The ubiquitin system.* Nat Med, 2000. **6**: p. 1073-81.

45. Hoofnagle, J.H., G.M. Dusheiko, L.B. Seeff, E.A. Jones, J.G. Waggoner, Z.B. Bales, *Seroconversion from hepatitis B e antigen to antibody in chronic type B hepatitis*. Ann Intern Med, 1981. **94**: p. 744-48.

46. Horikita, M., S. Itoh, K. Yamamoto, T. Shibayama, F. Tsuda, H. Okamoto, *Differences in the entire nucleotide sequence between hepatitis B virus genomes from carriers positive for antibody to hepatitis B e antigen with and without active disease.* J Med Virol, 1994. **44**: p. 96-103.

47. Horst Ibelgaufts' COPE: Cytokines Online Pathfinder Encyclopaedia, *Apoptosis.* 2003 <http://www.copewithcytokines.de/cope.cgi?000607> [Accessed 15.11.2004]

48. Hou, J., Y. Lin, J. Waters, Z. Wang, J. Min, H. Liao, J. Jiang, J. Chen, K. Luo, P. Karayiannis, *Detection and significance of a G1862T variant of hepatitis B virus in Chinese patients with fulminant hepatitis.* J Gen Virol, 2002. **83**: p. 2291-8.

49. Hung, J.H., I.J. Su, H.Y. Lei, H.C. Wang, W.C. Lin, W.T. Chang, W. Huang, W.C. Chang, Y.S. Chang, C.C. Chen, M.D. Lai, *Endoplasmic reticulum stress stimulates the expression of cyclooxygenase-2 through activation of NF-kappaB and pp38 mitogen-activated protein kinase*. J. Biol Chem, 2004. **279**: p. 46384-92.

50. Jacobson, M.D., M. Weil, M.C. Raff, *Programmed cell deathin animal development.* Cell, 1997. **88**: p. 347-54.

51. Jean-Jean, O., M. Levrero, H. Will, M. Perricaudet, J.M. Rossignol, *Expression mechanism of the hepatitis B virus (HBV) C gene and biosynthesis of HBe antigen*. Virology, 1989. **170**: p. 99-106.

52. Jimbo, A., E. Fujita, Y. Kouroku, J. Ohnishi, N. Inohara, K. Sakamaki, S. Yonehara, T. Momoi, *ER stress induces caspase-8 activation, stimulating cytochrome c release and caspase-9 activation*. Exp Cell Res, 2003. **283**: p. 156-66.

53. Johnson, A.E., M.A. van Waes, *The translocon: a dynamic gateway at the ER membrane.* Annu Rev Cell Dev Biol, 1999. **15**: p. 799-842.

54. Jordan, R., L. Wang, T.M. Graczyk, T.M. Block, P.R. Romano, *Replication of a cytopathic strain of bovine viral diarrhea virus activates PERK and induces endoplasmic reticulum stress-mediated apoptosis of MDBK cells*. J Virol, 2002. **76**: p. 9588-99.

55. Junker-Niepmann, M., R. Bartenschlager, H. Schaller, *A short cis-acting sequence is required for hepatitis B virus pregenome encapsidation and sufficient for packaging of foreign RNA.* EMBO, 1998. **9**: p. 3389-96.

56. Kerr, J.F.R., A.H. Wyllie, A.R. Currie, *Apoptosis: a basic biological phenomenon with wide-ranging implications in tissue kinetics.* Br J Cancer, 1972. **26**: p. 239-57.

57. Kim, P.S., P. Arvan, *Endocrinopathies in the family of endoplasmic reticulum (ER) storage diseases: disorders of protein trafficking and the role of ER molecular chaperones.* Endocr Rev, 1998. **19**: p. 173-202.

58. Kopito, R.R., *ER quality control: the cytoplasmic connection.* Cell, 1997. **88**: p. 427-30.

59. Kozutsumi, Y., M. Segal, K. Normington, M.J. Gething, J. Sambrook, *The presence of malfolded proteins in the endoplasmic reticulum signals the induction of glucose-regulated proteins.* Nature, 1988. **332**: p. 462-4.

60. Kramvis, A., S. Bukofzer, M.C. Kew, E. Song, *Nucleic acid sequence analysis of the precore region of hepatitis B virus from sera of southern African black adult carriers of the virus.* Hepatology, 1997. **25**: p. 235-40.

61. Kramvis, A., M.C. Kew, *Structure and function of the encapsidation signal of hepadnaviridae.* J Viral Hepat, 1998. **5**: p. 357-67.

62. Kramvis, A., M.C. Kew, S. Bukofzer, *Hepatitis B virus precore mutants in serum and liver of Southern African Blacks with hepatocellular carcinoma.* J Hepatol, 1998. **28**: p. 132-41.

63. Kronke, M., *Involvement of sphingomyelinases in TNF signaling pathways.* Chem Phys Lipids, 1999. **102**: p. 157-66.

64. Laboissiere, M.C.A., S.L. Sturley, R.T. Raines, *The essential function of protein-disulphide isomerase is to unscramble non-native disulphide bonds.* J Biol Chem, 1995. **270**: p. 28006-9.

65. Lam, M., G. Dubyak, L. Chen, G. Nunez, R.L. Miesfeld, C.W. Distelhorst CW, *Evidence that BCL-2 represses apoptosis by regulating endoplasmic reticulum-associated Ca2+ fluxes.* Proc Natl Acad Sci U S A, 1994. **91**: p. 6569-73.

66. Laskus, T., D.H. Persing, M.J. Nowicki, J.W. Mosley, J. Rakela J, *Nucleotide sequence analysis of the precore region in patients with fulminant hepatitis B in the United States.* Gastroenterology, 1993. **105**: p. 1173-8.

67. Lee, A.S., *The glucose-regulated proteins: stress induction and clinical applications.* Trends Biochem Sci, 2001. **26**: p. 504-10.

68. Leist, M., B. Single, A.F. Castoldi, S. Kuhnle, P. Nicotera, *Intracellular adenosine triphosphate (ATP) concentration: a switch in the decision between apoptosis and necrosis.* J Exp Med, 1997. **185**: p. 1481-6.

69. Lemasters, J.J., *Mechanisms of Hepatic Toxicity V. Necrapoptosis and the mitochondrial permeability transition: shared pathways to necrosis and apoptosis.* Am J Physiol, 1999. **276**: p. G1-6.

70. Li, H., H. Zhu, C.J. Xu, J. Yuan, *Cleavage of BID by caspase 8 mediates the mitochondrial damage in the Fas pathway of apoptosist*. Cell, 1998. **94**: p. 491-501.

71. Lin, Y., L.K. Ong, S.H. Chan, *Differential in situ hybridization for determination of mutational specific expression of the p53 gene in human hepatoma cell lines.* Pathology, 1995. **27**: p. 191-6.

72. Liu, C.H., S.H. Chang, K. Narko, O.C. Trifan, M.T. Wu, E. Smith, C. Haudenschild, T.F. Lane, T. Hla, *Overexpression of cyclooxygenase-2 is sufficient to induce tumorigenesis in transgenic mice*. J Biol Chem, 2001. **276**: p. 18563-9.

73. Loriot, M.A., P. Marcellin, N. Talbodec, V. Guigonis, M. Gigou, N. Boyer, A. Bezeaud, S. Erlinger, J.P. Benhamou, *Low frequency of precore hepatitis B virus mutants in anti-hepatitis B e-positive reactivation after loss of hepatitis B e antigen in patients with chronic hepatitis B.* Hepatology, 1995. **21**: p. 627-31.

74. Luo, X., I. Budihardjo, H. Zou, C. Slaughter, X. Wang, *Bid, a Bcl2 interacting protein, mediates cytochrome c release from mitochondria in response to activation of cell surface death receptors*. Cell, 1998. **94**: p. 481-90.

75. Mach, L., K. Stuwe, A. Hagen, C. Ballaun, J. Glossl, *Proteolytic processing and glycosylation of cathepsin B. The role of the primary structure of the latent precursor and of the carbohydrate moiety for cell-type-specific molecular forms of the enzyme.* Biochem J, 1992. **282**: p. 577-82.

76. Meyer, M., W.H. Caselmann, V. Schluter, R. Schreck, P.H. Hofschneider, P.A. Baeuerle, *Hepatitis B virus transactivator MHBst: activation of NF-kappa B, selective inhibition by antioxidants and integral membrane localization.* Embo J, 1992. **11**: p. 2991-3001.

77. Morishima, N., K. Nakanishi, H. Takenouchi, T. Shibata, Y. Yasuhiko, *Cytochrome c-independent activation of caspase-9 by caspase-12*. J Biol Chem, 2002. **277**: p. 34287-94.

78. Munro, S., H.R. Pelham, *An Hsp70-like protein in the ER: identity with the 78 kd glucose-regulated protein and immunoglobin heavy chain binding protein.* Cell, 1986. **46**: p. 291-300.

79. Nassal, M., H Schaller, *Hepatitis B virus replication--an update.* J Viral Hepat, 1996. **3**: p. 217-26.

80. Netherton, C.L., J.C. Parsley, T. Wileman, *African swine fever virus inhibits induction of the stress-induced proapoptotic transcription factor CHOP/GADD153.* J Virol, 2004. **78**: p. 10825-8.

81. Neuman, M.G., *Apoptosis in diseases of the liver.* Crit Rev Clin Lab Sci, 2001. **38**: p. 109-66.

82. Nieminen, A.L., A.K. Saylor, B. Herman, J.J. Lemasters, *ATP depletion rather than mitochondrial depolarization mediates hepatocyte killing after metabolic inhibition* . Am J Physiol, 1994. **267**: p. C67-C74.

83. Nicholson, D.W., N.A. Thornberry, *Caspases: killer proteases.* Trends Biochem Sci, 1997. **22** (8): p. 299-306.

84. Okamoto, H., S. Yotsumoto, Y. Akahane, T. Yamanaka, Y. Miyazaki, Y. Sugai, F. Tsuda, T. Tanaka, Y. Miyakawa, M. Mayumi, *Hepatitis B viruses with precore region defects prevail in persistently infected hosts along with seroconversion to the antibody against e antigen.* J Virol, 1990. **64**: p. 1298-303.

85. Ou, J.H., O. Laub, and W.J. Rutter, *Hepatitis B virus gene function: the precore region targets the core antigen to cellular membranes and causes the secretion of the e antigen.* Proc Natl Acad Sci U S A, 1986. **83**: p. 1578-82.

86. Pahl, H.L., *Signal transduction from the endoplasmic reticulum to the cell nucleus.* Physiol Rev, 1999. **79**: p. 683-701.

87. Pahl, H.L., P.A. Baeuerle, *Expression of influenza virus hemagglutinin activates transcription factor NF-kappa B.* J Virol, 1995. **69**: p. 1480-4.

88. Pahl, H.L., P.A. Baeuerle, *The ER-overload response: activation of NF-kappa B.* Trends Biochem Sci, 1997. **22**: p. 63-7.

89. Pahl, H.L., M. Sester, H.G. Burgert, P.A. Baeuerle, *Activation of transcription factor NF-kappaB by the adenovirus E3/19K protein requires its ER retention.* J Cell Biol, 1996. **132**: p. 511-22.

90. Pilon, M., R. Schekman, K. Romisch, *Sec61p mediates export of a misfolded secretory protein from the endoplasmic reticulum to the cytosol for degradation.* Embo J, 1997. **16**: p. 4540-8.

91. Plemper, R.K., D.H. Wolf, *Retrograde protein translocation: ERADication of secretory proteins in health and disease.* Trends Biochem Sci, 1999. **24**: p. 266-70.

92. Rao, R.V., E. Hermel, S. Castro-Obregon, G. de Rio, L.M. Ellerby, D.E. Bredesen, *Coupling endoplasmic reticulum stress to the cell death program. Mechanism of caspase activation.* J Biol Chem, 2001. **276**: p. 33869-74.

93. Ron, D., *Translational control in the endoplasmic reticulum stress response.* J Clin Invest, 2002. **110**: p. 1383-88.

94. Rutishauser, J., M. Spiess, *Endoplasmic reticulum storage diseases.* Swiss Med Wkly, 2002. **132**: p. 211-22.

95. Salveson, G.S., V.M. Dixit, *Caspases: intracellular signalling by proteolysis.* Cell, 1997. **91** (4): p. 443-6.

96. Santantonio, T., M.C. Jung, S. Miska, G. Pastore, G.R. Pape, H. Will, *Prevalence and type of pre-C HBV mutants in anti-HBe positive carriers with chronic liver disease in a highly endemic area.* Virology, 1991. **183**: p. 840-4.

97. Scaffidi, C., S. Fulda, A. Srinivasan, C. Friesen, F. Li, K.J. Tomaselli, K.M. Debatin, P.H. Krammer, M.E. Peter, *Two CD95 (APO-1/Fas) signaling pathways.* EMBO J, 1998. **17**: p. 1675-87.

98. Schultz, L., K. Smaira, S. Daniel, J. Heath, N. Chang, *TIAF1 and p53 functionally interact in mediating apoptosis and silencing of TIAF1: abolishes nuclear translocation of serine 15-phosphorylated p53*. DNA and Cell Biology, 2004. **23**: p. 67-74.

99. Shimizu, S., Y. Eguchi, W. Kamiike, Y. Funahashi, A. Mignon, V. Lacronique, H. Matsuda, Y. Tsujimoto, *Bcl-2 prevents apoptotic mitochondrial dysfunction by regulating proton flux.* Proc Natl Acad Sci U S A, 1998. **95**: p. 1455-9.

100. Shimizu, S., Y. Eguchi, W. Kamiike, Y. Itoh, J. Hasegawa, K. Yamabe, Y. Otsuki, H. Matsuda, Y. Tsujimoto Y, *Induction of apoptosis as well as necrosis by hypoxia and predominant prevention of apoptosis by Bcl-2 and Bcl-XL.* Cancer Res, 1996. **56**: p. 2161-6.

101. Song, E., G.M. Dusheiko, S. Bowyer, M.C. Kew, *Hepatitis B virus replication in southern Africa blacks with HBsAg-positive hepatocellular carcinoma.* Hepatology, 1984. **4**: p. 608-10.

102. Stennicke, H.R., G.S. Salvesen, *Properties of the caspases.* Biochim Biophys Acta, 1998. **1387** (1-2): p. 17-31.

103. Stevens, C., W. Szmuness, *Vertical transmission of hepatitis B and neonatal hepatitis B. In: G Stalder, G StalderG Stalders*. Virus and Liver Disease. Lancaster: MTP Press, 1980. p. 285 - 292.

104. Su, H.L., C.L. Liao, Y.L. Lin, *Japanese encephalitis virus infection initiates endoplasmic reticulum stress and an unfolded protein response.* J Virol, 2002. **76**: p. 4162-71.

105. Sugauchi, F., H. Kumada, S. A. Acharya, S. M. Shrestha, M. T. A. Gamutan, M. Khan, R. G. Gish, Y. Tanaka, T. Kato, E. Orito, R. Ueda, Y. Miyakawa, M. Mizokami, *Epidemiological and sequence differences between two subtypes (Ae and Aa) of hepatitis B virus genotype A*. J Gen Virol, 2004. **85**: p. 811-820.

106. Tardif, K.D., K. Mori, A. Siddiqui, *Hepatitis C virus subgenomic replicons induce endoplasmic reticulum stress activating an intracellular signaling pathway.* J Virol, 2002. **76**: p. 7453-9.

107. Teckman, J.H. and D.H. Perlmutter, *The endoplasmic reticulum degradation pathway for mutant secretory proteins alpha1-antitrypsin Z and S is distinct from that for an unassembled membrane protein.* J Biol Chem, 1996. **271**: p. 13215-20.

108. Thompson, C.B., *Apoptosis in the pathogenesis and treatment of disease.* Science, 1995. **267**: p. 1456-62.

109. Thornberry, N.A., Y. Lazebnik, *Caspases: enemies within.* Science, 1998. **281**: p. 1312-16.

110. Tiollais, P., C. Pourcel, A. Dejean, *The hepatitis B virus.* Nature, 1985. **317**: p. 489-95.

111. Tong, S.P., J.S. Li, L. Vitvitski, C. Trepo, *Replication capacities of natural and artificial precore stop codon mutants of hepatitis B virus: relevance of pregenome encapsidation signal.* Virology, 1992. **191**: p. 237-45.

112. Tran, A., D. Kremsdorf, F. Capel, C. Housset, C. Dauguet, M.A. Petit, C. Brechot, *Emergence of and takeover by hepatitis B virus (HBV) with rearrangements in the pre-S/S and pre-C/C genes during chronic HBV infection.* J Virol, 1991. **65**: p. 3566-74.

113. Trombetta, E.S., A. Helenius, *Conformational requirements for glycoprotein reglucosylation in the endoplasmic reticulum.* J Cell Biol, 2000. **148**: p. 1123-9.

114. Valliammai, T., S.P. Thyagarajan, A.J. Zuckerman, T.J. Harrison, *Precore and core mutations in HBV from individuals in India with chronic infection.* J Med Virol, 1995. **45**: p. 321-5.

115. Vander Heiden, M.G., N.S. Chandel, E.K. Williamson, P.T. Schumacker, C.B. Thompson, *Bcl-xL regulates the membrane potential and volume homeostasis of mitochondria.* Cell, 1997. **91**(5): p. 627-37.

116. von Heijne, G., *How signal sequences maintain cleavage specificity.* J Mol Biol, 1984. **173**: p. 243-51.

117. Wallach, D., M. Boldin, E.Varfolomeev, R. Beyaert, P. Vandenabeele. W. Fiers, *Cell death induction by receptors of the TNF family: towards a molecular understanding.* FEBS Lett, 1997. **410**: p. 96-106.

118. Wang, X.Z., M. Kuroda, J. Sok, N. Batchvarova, R. Kimmel, P. Chung, H. Zinszner, D. Ron, *Identification of novel stress-induced genes downstream of chop.* EMBO J, 1998. **17**: p. 3619-30.

119. Wang, K., X.M. Yin, D.T. Chao, C.L. Milliman, S.J. Korsmeyer, *BID: a novel BH3 domain-only death agonist*. Genes Dev, 1996. **10**: p. 2859-69.

120. WHO., *Hepatitis B.* World Health Organization Department of Communicable Diseases Surveillance Response, 2002.WHO/CDS/CRS/LYO/2002. 2: Hepatitis B. <http://www.who.int/emcdocuments/hepatitis/docs/whocdscsrlyo20022.pdf.2004> [Accessed 03.01.2004].

121. Wiertz, E.J., D. Tortorella, M. Bogyo, J. Yu, W. Mothes, T.R. Jones, T.A. Rapoport, H.L. Ploegh, *Sec61-mediated transfer of a membrane protein from the endoplasmic reticulum to the proteasome for destruction.* Nature, 1996. **384**: p. 432-8.

122. Wyllie, A.H., *Glucocorticoid-induced thymocyte apoptosis is associated with endogenous endonuclease activation.* Nature, 1980. **284**: p. 555-6.

123. Wyllie, A.H., *Apoptosis: cell death in tissue regulation.* J Pathol, 1987. **153**: p. 313-16.

124. Wyllie, A.H., J.F.R. Kerr, A.R. Currie, *Cell death: the significance of apoptosis.* Int Rev Cytol, 1980. **68**: p. 251-306.

125. Wyllie, A.H., R.G. Morris, A.L. Smith, D. Dunlop, *Chromatin cleavage in apoptosis: association with condensed chromatin morphology and dependence on macromolecular synthesis.* J Pathol, 1984. **142**: p. 67-77.

126. Xu, Y., S. Bialik, B.E. Jones, Y. Iimuro, R.N. Kitsis, A. Srinivasan, D.A. Brenner, M.J. Czaja, *NF-kappaB inactivation converts a hepatocyte cell line TNF-alpha response from proliferation to apoptosis.* Am J Physiol, 1998. **275**: p. C1058-66.

127. Zhou, M., R. Schekman, *The engagement of Sec61p in the ER dislocation process.* Mol Cell, 1999. **4**: p. 925-34.

128. Zinszner, H., M. Kuroda, X. Wang, N. Batchvarova, R.T. Lightfoot, H. Remotti, J.L. Stevens, D. Ron, *CHOP is implicated in programmed cell death in response to impaired function of the endoplasmic reticulum.* Genes Dev, 1998. **12**: p. 982-95.

129. Zoratti, M., I. Szabo, *The mitochondrial permeability transition.* Biochim Biophys Acta, 1995. **1241** : p. 139-176.